This is to certify that the

thesis entitled

FINITE ELEMENT FORMULATION OF THE
THERMO-HYDRO STRESS PROBLEM
IN SOYBEANS

presented by

Kamyar Haghighi

has been accepted towards fulfillment
of the requirements for

Ph.D. degree in Agricultural Engineering
and Metallurgy, Mechanics
and Material Science

Larry Segerlind

Dr. Larry J. Segerlind

Major professor

Date March 8, 1979

FINITE ELEMENT FORMULATION OF THE THERMO-HYDRO STRESS PROBLEM IN SOYBEANS

by

Kamyar Haghighi

A DISSERTATION

Submitted to
Michigan State University
in partial fulfillment of the requirements
for the degree of

DOCTOR OF PHILOSOPHY

Department of Agricultural Engineering
Department of Metallurgy, Mechanics
and
Material Science

1979

ABSTRACT

FINITE ELEMENT FORMULATION OF THE THERMO-HYDRO STRESS PROBLEM IN SOYBEANS

By

Kamyar Haghighi

The objective of this study was the formulation of a finite element model that could be used to analyze the stress crack formation in soybean kernels resulting from temperature and moisture gradients during the drying process. The soybean kernel was taken as an isotropic sphere, symmetrical with respect to its center and a two dimensional axisymmetric grid was used to model the temperature and moisture gradients.

The finite element method was used to obtain numerical solutions to the simultaneous moisture and heat diffusion equations describing moisture removal and heat intake process for the soybean model. All material parameters of the soybean were assumed to be independent of temperature and moisture content. The distribution and gradients of temperature and moisture developed inside the kernel during the drying process were established. The simulated drying curve for the soybean model was obtained and compared

favorably with the experimental results reported in the literature.

The calculated temperature and moisture gradients were used in a finite element analysis of the thermo-hydro viscoelastic boundary value problem to simulate the stresses in soybeans under the thermo-hydro loads. The kernel was assumed to have no initial stress and free expansion and contraction of the kernel was allowed. Due to lack of information on viscoelastic properties of the soybean, the simulated results reduced to an elastic stress analysis. Tangential stress was shown to change from compressive to tensile stress as it approaches the surface. It reaches its peak value at the surface in one hour and then decays slowly. The effect of different drying conditions on the stresses was studied and the results were discussed. It was found that the magnitude of peak tangential stress is directly proportional to the step increases in temperature and the time to reach its peak value is independent of the change in drying temperature.

This study concludes with suggestions regarding the need for additional investigations on viscoelastic properties of the soybean and the master curves to represent these properties over the entire drying period. This information will improve the soybean model and allow the establishment of specific guidelines for crack free drying of soybeans.

Approved: __________________________
Major Professor

____
Department Chairman

To Iranian Workers
And
Peasants

ACKNOWLEDGMENTS

The author sincerely appreciates the guidance and close cooperation of his major professor, Dr. Larry J. Segerlind. Equally, his gratitude is extended to Dr. W.A. Bradley, Dr. G.E. Mase, Dr. G.E. Merva, and Dr. C. Cress for their time and counseling.

Thanks are due to his wife Atossa and his parents for their patience and encouragement throughout this study.

The author is particularly indebted to the Iranian masses from which, through a scholarship, this graduate program was made possible.

TABLE OF CONTENTS

Page

Page

LIST OF FIGURES

Figure		Page

LIST OF TABLES

1. INTRODUCTION

The field harvesting of soybeans at a higher than optimal moisture content necessitates the artificial drying of this product. During drying, temperature and moisture gradients are superimposed within the soybean kernel, both resulting in volumetric change. Expansion occurs in heating and shrinkage or contraction occurs because of moisture removal. The stress states arising throughout the thermal and hydro-loaded material often results in the initiation of cracks.

Stress crack phenomena is one of the most important problems in grain drying. The cracks lead to splits, decreased storage life and lower germination. Thompson and Foster (1963) reported that stress cracks develop on heating or cooling of corn kernel when the thermal and hydro stresses exceed the failure strength of the material. Overhults et al. (1973) noted severe physical damage to soybeans during their drying tests. They believed these cracks occured because the seed coat shrank before the endosperm had begun to dry. Milner and Shellenberger (1953) has studied the formation of stress cracks in wheat through the use of radiography. High moisture content or high drying temperature gave visible fissures.

Soybeans initially damaged during harvest are likely to be more susceptible to damage from subsequent handling and processing. Mechanically damaged beans, including those which are split or have seed coat checks, are of less commercial value because of reduced canning and cooking quality. Mechanical damage not only affects market value of the bean but also impairs germination vigor.

Increased concern has been shown by bean growers, processors, and shippers, to minimize the mechanical damage to beans caused by artificial drying and impact loading during harvesting and handling.

The stress crack phenomenon is a function of rheoloical properties of the material like bulk, shear and tension moduli, Poisson's ratio, failure stress and time-temperature and time-moisture shift factors. In order to apply the theories of engineering mechanics to the solution of stress field equations, it is necessary to know the rheological properties of the stressed material as affected by time, temperature and moisture content.

It is apparent that physical properties and more importantly viscoelastic properties of the soybean kernel are required with respect to the important variables such as temperature and moisture content. There is a physical basis for assuming that the soybean kernel behaves in a similar manner as other viscoelastic materials and that similar mathematical techniques may be employed to define the behavior of the soybean kernel under the influence of external loads.

The basic unit of a kernel is the living cell. The cell consists of wall and protoplasm. The cell walls are composed of cellulose microfibrils embedded in an amorphous matrix. The cell walls exhibit a high degree of elasticity. Inside the cell, protoplasm consists of cytoplasm, nucleus and vacuoles. The cytoplasm shows both elastic and viscous properties. Vacuoles are made up of droplets of solution called cell sap. While the elasticity of the cell walls is the main factor responsible for the elasticity of the kernel, the cell sap is responsible for exerting a hydrostatic pressure called turgor pressure on the cell walls. The combined effects with the elastic cell walls determine the viscoelastic properties of soybean kernel.

Based on experimental evidences due to Zoerb and Hall (1960), Mohsenin (1968), Timbers (1964) and Morrow (1965), agricultural products are viscoelastic.

The soybean is processed in large quantities. Besides its oil which is used for different kinds of oil products and protein rich livestock feed, the soybean has been used in the production of synthetic food in recent years.

Stress cracks, in fact, account for increased breakage during storage, handling and processing. Such damage contributes to susceptibility to molds and insect damage and to the production of low quality and high cost soybean grains and soybean products.

It is hardly possible to give a dollar value to the damage resulting from thermo-hydro stress cracks. Martin and Stephens (1976) reported that corn initially consisting of 2% breakage had 15.7% breakage after 21 handling operations.

If the stress state arising from both temperature and moisture gradients could be determined, and if the necessary material properties are known or could be evaluated, a failure criterion could be established which would define the critical temperature and moisture gradients. This would enable drying facilities to adjust ambient temperatures and relative humidities to soybean moisture content in order to minimize stress crack formation in soybean kernel.

The objective of this work was to develop a numerical technique that could be used to analyze the stress crack formation in the soybean kernel resulting from temperature and moisture gradients during the drying process. The specific objectives were:

(1) To numerically study the phenomenon of coupled moisture and heat diffusion within the soybean kernel by use of finite element method.

(2) To determine the stress state due to the temperature and moisture gradients inside the soybean kernel, using computer simulation.

The basic assumption of isotropy, continuity and homogeneity which is a good macroscopic approximation was made in order to solve the theoretical stress analysis problem.

2. REVIEW OF LITERATURE

The cracking phenomena is of great concern to soybean industry. Cracked kernels are objectionable because they are quite susceptible to breakage during handling and cause problems in storage, manufacturing processes, grading and shipping.

Over much of the moisture content range encountered in grain drying, a kernel will shrink as heat is applied and water is removed. In this process, a moisture gradient and a temperature gradient are established with the outermost layers of the kernel. The outer layer thus tends to skrink more causing tensile stresses tangent to the surface. These stresses in the outer layers increase as the moisture and temperature gradients increase. Kernel breakage results if the magnitude of the moisture and temperature gradients are such that the outer layers are stressed beyound their ultimate strength (Hammerle, 1970).

2.1 Development of Stress Cracks

Under favorable weather conditions, soybeans dry in the field to moisture levels safe for storage. Soybeans require lower moisture content than corn or other cereal grains to store safely under similar conditions (Hall, 1961).

However, the soybean stalks and pods become brittle at a moisture content of 11 per cent, resulting in high harvest losses. Byg and Johnson (1970) reported 8 per cent shattering losses when soybeans were harvested at a moisture content of 10 percent as compared with only a 2 percent loss when harvested at 17 percent. Harvesting soybeans at moisture contents much above 11 percent would require conditioning the beans to a lower moisture for safe storage (Alam and Shove, 1972).

The actual mechanisms for mechanical breakdown of seed coat and loss of seed viability during drying are complicated and frequently involve the previous history of the seed including any mechanical damage and disease infection.

Seed coat cracking induced by drying is associated with the drying rate imposed upon the seed and with the corresponding rate of shrinkage as well as the level of moisture content. Thus the high percentage of cracking associated with the conventional drying method is essentially due to the high percentage of the overdried seed. Sabbah, et al. (1976) achieved a great reduction in percentage of the overdried seeds by reversing the air flow. The use of the reversed-direction drying method also resulted in more uniform final bed moisture contents, with less seed coat cracking and germination loss than with the conventional (one-direction-air-flow) method.

Overhults et al. (1973) determined thin-layer drying characteristics of soybeans as affected by harvest moisture content and drying air conditions.

In a study by Ekstrom (1965) certain physical properties of corn kernels related to stress cracking were investigated and an attempt was made to determine whether or not stress cracks can be caused by temperature gradients alone.

Zoerb (1958) concluded that moisture content has the greatest influence on the mechanical properties of grain and that all of the strength properties generally decrease in magnitude as the moisture increases. He further concluded that initial rate of deformation has more effect on the rate of stress relaxation than moisture content or the initial amount of deformation.

Goncharova (1962) studied the dependence of structural strength characteristics of grain on humidity, temperature, and the speed of loading. His results were in agreement with the conclusions from the the work of Zoerb (1958) and Chizhikov (1960).

Extensive studies of the causes of stress cracks and breakage in artifically dried corn were made by Thompson and Foster (1963), who found that drying speed, expressed in percentage points of moisture removed per hour, was the most significant factor in stress crack development. The amount of drying, as well as the rate, also appeared to affect stress crack development.

According to Chizhikov (1960) stress crack formation in corn can be blamed on the compact construction of the shells of the kernels. This structure makes evaporation difficult since the main channel through which moisture can leave during the drying process is located around the germ. He further observed that when the drying temperature was increased, the structural strength decreased.

Henderson (1954) observed that the cracking in rice standing in the field began at the center of the kernel and progressed toward the minor circumference. He concluded that stress cracks resulted from an increase in either temperature or moisture.

Kunze and Hall (1965) investigated the effects of relative humidity and moisture gradient on stress cracking in brown rice. They found that a thermal gradient of 17°C did not produce fissures in rice as long as the grain were maintained at a constant moisture content.

In a study of the penetration of wheat grains by water, Grosh and Milner (1959) concluded that the forces which produced cracking as a result of tempering might have two causes: a residual stress set up within the wheat endosperm during the maturing stage of kernel development, and a gradient of swelling forces produced when the moisture is absorbed into the wheat kernel.

Ekstrom et al. (1966) and Mannapperuma (1975) concluded that stress cracks in shelled corn and brown rice, respectively, probably are not caused exclusively by temperature gradients alone in the kernel. Therefore moisture gradients or a combination of moisture gradients and temperature gradients appear to produce greater stresses than those caused by thermal gradients alone. Arora et al. (1973) also found the temperature gradient in the rice kernel is dependent upon the moisture gradient.

Milner and Shellenberger (1953) detected an increased number of fissures in weathered wheat under increased initial moisture content and elevated temperature. The cracking was primarily due to stresses arising from unequal moisture gradients.

Wang (1956) used intermittent application of dry air in a test to dry pea beans. He was interested in seed coat cracking as well as splitting.

Perry (1959) noted in examining the checked beans that the cracks "seemed to radiate from the hilum" creating a common check pattern.

The analysis of navy bean seed coat strength and maximum shear stress acting on the bean was studied by Hoki (1973) based upon the thin ring theory and Hertz's contact theory, respectively. He concluded that Young's moduli and ultimate stresses increased with decreasing moisture content for both the seed coat and cotyledon.

2.2 Process of Moisture Movement

Sarvacos and Charm (1962) and Chirife (1971) have studies the diffusion process in fruits and vegetables and have indicated that the linear diffusion equation does not apply over the entire period of drying.

Chen and Johnson (1969) gave a mathematical analysis of moisture diffusion assuming thermal diffusion to be negligible.

The removal of moisture from grains has been the subject of considerable research. However, most of this research has been devoted to a study of bulk or batch drying in which only the average effect on a relatively large quantity of material has been considered. In order to understand better the effects of certain drying and curing practices, it is important that more emphasis be placed on moisture movement within individual kernels. Therefore, the drying rate of the whole bed, as well as that of each layer, depends upon the accurate description of moisture movement from a single kernel which is fully exposed to drying air of a changing temperature and relative humidity.

Moisture movement has been described reasonably well with the diffusion equation when the kernel temperature does not change substantially. Becker and Sallans (1955), Hustrulid and Flikke (1959), Henderson and Perry (1967), and others treated a grain kernel as an isotropic sphere, symmetrical with respect to its center and used the diffusion equation to describe moisture movement, without regard to the kernel temperature. Chittenden and Hustrulid (1966) and many others found that the diffusion coefficient varied with the initial moisture content of corn and concluded that diffusion coefficient must depend on moisture concentration. Whitaker, et al., (1969) solved the equation for a non-homogeneous sphere with a moisture and position dependent diffusion coefficient and a non-uniform initial moisture concentration drying under changing air conditions. They concluded that the diffusion coefficient was dependent more on temperature than on moisture and that the moisture diffusion equation alone is inadequate for describing the process completely.

Wang and Hall (1961) used the diffusion equation to characterize heat and moisture transfer in a corn kernel assuming constant boundary conditions. They pointed out that the effect of temperature changes due to moisture vaporization within the kernel is important and has a profound influence on the rate of moisture diffusion.

Whitaker and Young (1972) evaluated the diffusion equation, characterizing moisture movement in a homogeneous body, as a model to describe the drying rate of peanut kernel and further studies are needed to evaluate the diffusion equation characterizing moisture movement in a composite body as a method of predicting the drying rate of peanut pods.

Young and Whitaker (1971) listed the solutions of the diffusion equation characterizing moisture transfer in plane sheets, infinite cylinders, finite cylinders and spheres, for the constant boundary conditions.

The influence of a temperature gradient as a moisture-driving potential was investigated by Whitney and Porterfield (1968) as a means of controlling the moisture gradient during the drying process. The investigations revealed a net moisture transfer in the direction of decreasing temperature. They further concluded that after a given amount of water has been removed, the moisture gradients are similar whether or not a temperature gradient (resulting from internal heating) exists in the same direction as the moisture gradient and this can be used to decrease the total drying time, without increasing the shrinkage stresses in the solid due to the moisture gradient.

Absorption or evolution of water by solid results in evolution or absorption of heat, respectively. This heat diffuses through the solid, causing changes in temperature, which affects the ability of solid to absorb or evolve water (Whitney and Porterfield, 1968). Thus the transfer of moisture and heat are coupled together and in general, should be considered simultaneously.

Young (1969) described a mathematical model for a drying porous sphere using the diffusion equation for both moisture and heat transfer assuming that moisture diffusivity is linearly function of moisture. He defined a modified Lewis number and suggested that the moisture diffusion equation alone is sufficient if the number is greater than 60 (negligible temperature gradient).

Singh, et al. (1972) solved the simultaneous heat and moisture diffusion equations under continuously changing boundary conditions. This study improved the kernel model by using a more accurate heat conduction equation, but did not account for the temperature dependence of the moisture diffusion coefficient.

2.3 Properties of the Soybean Kernel

Swelling and shrinkage are natural occurring phenomena as biomaterials are heated, cooled, or absorb and deabsorb moisture. This movement of the material results in internal strains causing formation of stress cracks which reduce the quality of the product, permit excessive loss of moisture and provide accessability for disease.

The differential expansion of a composite body experiencing a thermal gradient has been known for a long time. The stresses which result from a thermal gradient are called thermal stresses and their calculation is discussed by several authors including Timoshenko and Goodier (1970). The mass transfer due to moisture loss (or addition) also produces stresses in composite bodies. These stresses are called hydro stresses. The combined existence of thermal and hydro (thermo-hydro) stresses requires a modification of the theory for thermal stresses as outlined by Timoshenko and Goodier (1970). This modification was performed by Hammerle (1972) who expanded the basic theory to include the viscoelastic nature of agricultural products and the expansion or contraction resulting from a change in moisture content. The solution of this theory will give the stresses in the endosperm and seed coat or hull. An analysis of stresses would indicate what temperature and moisture conditions give rise to stresses that are likely to crack the seed coat or hull. A knowledge of failure stresses of the hull or seed coat must also be known in order to make this decision.

An important contribution of Hammerle's work is the indication of which material constants must be determined before an analysis can be performed. Several are required and they include the viscoelastic modulus and the coefficients of thermal and hydro expansion of each material component. If there are temperature and moisture gradients within the kernel, then the theories governing the temperature and moisture distributions must also be considered. These theories require a knowledge of the thermal conductivity and specific heat of each material as well as the moisture diffusion coefficient.

Several of the required constants have been determined but some such as the moisture diffusion coefficient and thermal properties of the individual material coponents have not been determined and no specific standard or procedure exists for their determination.

Alam and Shove (1972) obtained a linear relationship between specific heat and moisture content of soybean which is in agreement with the results obtained by Bellinger (1964) and Watts and Bilanski (1970). Jasansky and Bilanski (1973) found a linear relationship between soybean thermal conductivity and kernel temperature at 11.2% moisture content (wet bulb) using transient heat flow measurement method. They further indicated that the thermal conductivity of soybean is dependent upon its particle size, moisture content and temperature. Their results for whole soybean thermal conductivity compare favorably with those of Watts (1967), even though his conductivity evaluation was calculated from measurement of density, specific heat and thermal diffusivity. Using the method of transient heat conduction, Watts and Bilanski (1973) found an average value for soybean thermal diffusivity. A small interaction between temperature and moisture content was noted but was not considered. The coefficient of linear thermal expansion of soybean was found by Bacchus (1971). He further studied the effect of moisture on this property and concluded that this property is linearly related to kernel moisture content. Paulsen and Brusewitz (1976) determined the coefficient of thermal expansion for spanish peanut kernels (α_k) and skin (α_s) and as drying occurs, α_s decreases with moisture loss more than does α_k. As further drying continues there would be a greater tendency for the kernel to expand more than the skin causing an increased stress on the skin. It also appeared from their work that peanuts and possibly other oilseed grains would have expansion coefficients larger than those of grains containing relatively low amount of oil.

The values of the different properties of soybean which are available in the literature are tabulated in Table 2.1.

2.4 Structure of the Soybean Kernel

2.4.1 Description

According to the botanical classification, soybean is a member of the family Leguminosae, subfamily Papilionoideae and its genus is Glycine (L.). Wilson (1955) mentions the correct botanical name as Glycine Max (L.) Merrill.

Classification relating to the life of the plant and its response to its environment i.e. on the basis of its growth habit describe the plant as a summer annual with a maturity requirement of approximately 75 days for the early varities to 200 days or more for the very late varities.

According to the market classification, there are five market classes of soybeans based on the color of seed: yellow, green, brown, black and mixed soybeans.

The chemical composition of the soybean kernel is, protein 33.98 percent, fat 16.85 percent, nitrogen free extract 28.89 percent, fiber 4.79 percent, ash 4.69 percent and water 10.80 percent (Saxena, 1972).

Table 2.1. Properties of the Soybean Kernel.

Property	Value	Moisture content range(%W.b.)	Temperature range (°C)	Reference
Sphericity	91%	6.8-17	-	Bacchus (1971)
Specific Heat (C)	1884.0, J/kg.°C	7.4	30.2-127.8	Watts and Bilanski (1970)
	2051.5, J/kg.°C	21	23-88	Bellinger (1964)
Density (ρ)	1180, kg/m^3	-	-	Bellinger (1964)
	1204, kg/m^3	7-17	-	Bacchus (1971)
	1230, kg/m^3	6-35	-	Watts (1967)
Thermal Conductivity (K')	.097-.133, Watts/m-°C	11.2	10-65.5	Jasansky and Bilanski (1973)
Thermal Diffusivity (α')	0.00045, cm^2/sec.	-	-	Watts and Bilanski (1973)
Diffusion Coefficient (D)	3.32×10^{-12}-7.38×10^{-11}, m^2/sec.	20-27	8-20(*)	Sabbah et al. (1976)
Coefficient of Thermal expansion (α)	$(28.8\text{-}38.8)10^{-5}$/°C	7-17	25-90	Bacchus (1971)
Coefficient of Hydro expansion (β)	$.2657 \times 10^{-2}$ m/(m-%mc,d.b.)	-	-	Misra (1977)
Poisson's Ratio (μ)	.4	-	-	Bacchus (1971) Misra (1977)
	24.75×10^8 - 2.9×10^8, Pa	6.8-17	-	Misra (1977)
Young's Modulus (E)	30.42×10^7-13.88×10^7, Pa	6.8-20	-	Bacchus (1971)

(*) Indicates the seed temperature

2.4.2 Morphology and Anatomy

Most mature seeds are made up of three basic parts: the seed coat, the embryo, and one or more food storage structures. The soybean seed has only two parts. Its two food storage structures, the cotyledons, are part of the embryo. That is, the embryo of the soybean seed consists of two thick, fleshy cotyledons which account for most of the bulk and weight of the seed (about 90 percent). They contain nearly all the oil and protein in the bean. The seed coat is relatively thin and protects the embryo from fungi and bacteria before and after planting. If this protective coat is cracked, the seed has little chance of developing into a healthy seedling.

A variety of distinct layers can be recognized in the seed coat and cotyledons. The outermost layer, the epidermis, remains uniseriate and develops into the palisade layer characteristic of leguminous seeds. The palisade cells have a definite cuticular layer (Smith and Circle 1976). Two palisade layers and a compact group of tracheids of unknown role occur in the hilum region. The palisade layer has attracted much attention because its structure in certain hard legume seeds such as soybean is assumed to be connected with their high degree of impermeability and thus germinability (Esau, 1960). The column cells are hourglass or I-shaped, similar to those of other beans, but in soybeans they are thicker and longer. They vary from 30 to 70 microns in length and from 16 to 36 microns in width. The spongy parenchyma consist of 6 to 8 layers of thin-walled, somewhat compressed, boxlike, empty cells ranging in width from 20 to 120 microns but mostly 40 to 60 microns. One of the most characteristic features of the soybean seed is the presence of the endosperm. This is represented by a layer of aleurone cells and several layers of thin-walled cells which have been crushed by compression. The aleurone cells are rather thick-walled and are filled with dense protein. The surface of the cotyledons are covered with a typical epidermis made up of small cubical cells filled with grains of aleurone. The remainder of the cotyledon is largely made up of layers of elongated palisadelike cells with thin walls and filled with aleurone and oil.

The hard legume seeds such as soybean achieve and maintain a very low percent moisture which is not affected by fluctuations in moisture content of the surrounding air. The attainment of this high degree of desiccation is ascribed to a combination of intensely impremiable testa with valvular action of the hilum (Hyde 1954). The hilum is said to act like a hygroscopic valve. A fissure occurs along the groove of the hilum. This fissure opens when the seed is surrounded by dry air and closes when the outside air is moist. Thus the entry of moisture is prevented but loss of moisture is permitted. The occurrence of highly impermeable seed coats is one of the important factors in delayed germination of seeds in Leguminosae. In this connection the occurrence of cuticular layers in seeds is of particular interest. Some good pictures of the soybean seed structure are shown by Esau (1960) and Smith and Circle (1976).

2.5 Viscoelastic Characterization as Affected by Temperature and Moisture Gradients

In recent years the subject of viscoelasticity has received considerable attention from both theoreticians and experimentalists, which is evident in the reviews of Hilton (1954), Lee (1964) and Morland and Lee (1960). Within the engineering requirements of accuracy many material have been found to satisfy the assumption of thermorheologically simple behavior. Mōrland and Lee (1960) have shown how this assumption can be used to derive isotropic constitutive equations with transient temperatures. Hilton (1954) has investigated the thermal stresses in thick walled incompressible cylinders exhibiting temperature dependent viscoelastic properties of the Kelvin type.

Sharma (1964) and Rosen (1964) have discussed in detail the time-temperature dependence of linear viscoelastic materials and the Boltzman superpostion theory. Verification of these principles by experimentation has been done by Ferry (1961), where the transient tests described are basically creep and relaxation for various shaped specimen.

The experimental determination of stress relaxation moduli from tensile stress-strain curves at various temperatures has been discussed by Sharma (1964). Hammerle and Mohsenin (1970) determined the stress relaxation modulus of corn at various temperature and moisture levels. Muki and Sternberg (1961) have worked on the theoretical analysis of thermal stress distribution within infinite and finite viscoelastic plates, and viscoelastic spheres. The time dependent yielding for the above problems was investigated by Landau et al. (1960). Bland (1960), Ferry (1961) and Sharma (1964) have arrived at the relaxation integral laws where deviatoric and isotropic stresses are given as a function of strain-time loading. Utilizing the constitutive laws of a continuous Maxwell model and the superposition method, Rao (1971) arrived with the solution of the stress state in a viscoelastic cylinder subjected to transient temperature and moisture gradients. Later on Rao et al. (1975) solved the same problem for a viscoelastic sphere subjected to radially symmetric temperature and moisture gradients. They further concluded that this approach is applicable to approximately spherical seeds or formed foods.

Studying the physical properties of small grains by a triaxial testing method, Stewart (1964) found that an interrelationship exists between their moisture content and their viscoelastic properties.

Bacchus (1971) studied the mechanical properties of soybean by assuming Hookean behavior using the Hertz contact theory for convex bodies. He concluded that yield point, Young's modulus and maximum compressive strength decreased with an increase in moisture content and initial rate of deformation had more effect on the rate of stress relaxation than moisture level or initial amount of deformation. He also found that the coefficient of linear thermal expansion has a linear relation with the kernel moisture content and the assumption that soybean is a sphereholds good for all practical purposes.

Silberstein and Rao (1976) evaluated the uniaxial modulus of elasticity at constant loading rates for Florruhher peanut variety. The time-temperature and time moisture shift factors were evaluated and a three element Maxwell model was found to adequately apprximate the peanut behavior. This information is vital for stress analysis of peanut kernels to determine the stress cracks and shrinkage. Herum et al. (1973) evaluated the time dependent uniaxial moduli of intact soybeans, determined by relaxation tests in parallel plate compression, at four temperatures and four levels of moisture content. They concluded that the time scale shift factors were not constant but were sufficiently similar to permit description of intact soybeans as thermo-rheologically and hydro-rheologically simple. This means that viscoelastic properties such as uniaxial modulus function of the soybean can be described by one master curve. This curve allows the calculation of the viscoelastic modulus over the range of temperatures and moisture contents which would be encountered during the drying process. Further, they found that an increase or decrease of 1% in moisture content, computed on the dry basis, has approximately thirteen times as much effect on the uniaxial modulus in compression as does a 1° Fahrenheit increase or decrease in temperature. Saxena (1972) reported that the soybean kernel behaves as a viscoelastic material in response to the applied forces and is characterized by a generalized Maxwell model having as few as three Maxwell elements and one spring in parallel. He further observed that the orientation of stress cracks depends on the test position of the kernel and also there was no way to ascertain whether seed coat or the cotyledons cracked first.

3. SIMULTANEOUS MOISTURE AND HEAT DIFFUSION

3.1 Governing Equations

Since the temperature distribution within the soybean kernel may not be uniform during the initial stages of drying, simultaneous equations of moisture and heat diffusion are needed to describe moisture movement within the soybean kernel. Crank (1964) gave the mathematical model characterizing moisture and heat diffusion, in a sphere (in cylinderical coordinates) as follows:

$$\frac{\partial M}{\partial t} = \frac{1}{r}\frac{\partial}{\partial r}\left(rD\frac{\partial M}{\partial r}\right) + D\frac{\partial^2 M}{\partial z^2} \qquad (3.1)$$

$$\rho c\frac{\partial T}{\partial t} = \frac{1}{r}\frac{\partial}{\partial r}\left(rK'\frac{\partial T}{\partial r}\right) + K'\frac{\partial^2 T}{\partial z^2} + L\rho\frac{\partial M}{\partial t} \qquad (3.2)$$

where

M = mositure concentration, % dry basis

T = temperature, °C

r = radial coordinate, z = vertical coordinate

t = time, sec.

D = moisture diffusivity, m^2/sec.

K'= thermal conductivity, w/m°C or J/m sec. °C

c = specific heat, J/kg°C

ρ = density, kg/m^3

L = latent heat of vaporization of water, J/kg

Parameters D, K', ρ and c are in general functions of local temperature and moisture values inside the kernel. No analytical solution to this complex problem has been found. Computer solutions would also be extremely hard to obtain, especially when the nature of some of these properties such as D is not known. It is felt that considerable information on the model about temperature and moisture distribution within the kernel could be gained by treating ρ, c, D and K' as constants in a finite element analysis. Therefore this study assumes that ρ, c, D and K' do not change substantially in the temperature and moisture ranges under consideration.

Equations (3.1) and (3.2) now reduce to

$$\frac{\partial M}{\partial t} = D \frac{\partial^2 M}{\partial r^2} + \frac{D}{r} \frac{\partial M}{\partial r} + D \frac{\partial^2 M}{\partial z^2} \tag{3.3}$$

$$\rho c \frac{\partial T}{\partial t} = K' \frac{\partial^2 T}{\partial r^2} + \frac{K'}{r} \frac{\partial T}{\partial r} + K' \frac{\partial^2 T}{\partial z^2} + L\rho \frac{\partial M}{\partial t} \tag{3.4}$$

3.2 Initial and Boundary Conditions

(1) Kernel is at uniform temperature and moisture initially

$$M = M_o \big|_{t=0} \quad , \quad T = T_o \big|_{t=0}$$

(2) for t>o and at thc surface (r=R)

$$D\left(\frac{\partial M}{\partial r} + \frac{\partial M}{\partial z}\right)\Big|_{r=R} + h_m\,(M_{surf.} - M_{eq.}) = 0$$

where h_m = mass transfer coefficient, m/sec.

(3) for t>o and at the surface (r=R)

$$K'\left(\frac{\partial T}{\partial r} + \frac{\partial T}{\partial z}\right)\Big|_{r=R} + h(T_{surf.} - T_{eq.}) = 0$$

where h = heat transfer coefficient, $W/m^2{}^\circ C$ or $J/m^2 sec.{}^\circ C$

3.3 Finite Element Formulation of Coupled Heat and Mass Diffusion

In most problems the integral of a functional is minimized. This functional possesses the property that any function which makes it a minimum also satisfies the governing differential equation and the boundary conditions. As for this case, the functional form of the governing equations (3.3) and (3.4) by use of variational calculus may be written as

$$\chi_1 = \int_V \frac{1}{2}\left[D\left(\frac{\partial\{M\}}{\partial r}\right)^2 + D\left(\frac{\partial\{M\}}{\partial z}\right)^2 + 2\left(\frac{\partial\{M\}}{\partial t}\right)\{M\}\right]dv + \int_S \frac{h_m}{2}\,(M_s - M_\infty)^2 ds \qquad (3.5)$$

$$\chi_2 = \int_V \frac{1}{2}[K'(\frac{\partial\{T\}}{\partial r})^2 + K'(\frac{\partial\{T\}}{\partial z})^2 - 2L\rho(\frac{\partial\{M\}}{\partial t})\{T\}$$

$$+ 2\rho c(\frac{\partial\{T\}}{\partial t})\{T\}]dv + \int_S \frac{h}{2}(T_s - T_\infty)^2 ds \qquad (3.6)$$

where M_∞ and T_∞ denote ambient moisture content and temperature respectively. V is the total volume of the body and S is the boundary. The solution of the boundary value problem stated in (3.3) and (3.4) can be obtained by finding the stationary value of the functionals χ_1 and χ_2 in (3.5) and (3.6) with respect to the set of nodal values {M} and {T}. The finite element method can be used as a numercial technique based on the minimization of these functionals.

Define four matrices:

$$\{g_1\}^T = [\frac{\partial M}{\partial r}, \frac{\partial M}{\partial z}] \qquad (3.7a)$$

$$\{g_2\}^T = [\frac{\partial T}{\partial r}, \frac{\partial T}{\partial z}] \qquad (3.7b)$$

$$[D] = \begin{bmatrix} D & o \\ o & D \end{bmatrix} \qquad (3.8a)$$

$$[k] = \begin{bmatrix} K' & o \\ o & K' \end{bmatrix} \qquad (3.8b)$$

Equations (3.5) and (3.6) can be written as

$$\chi_1 = \int_V \frac{1}{2}[\{g_1\}^T[D]\{g_1\} + 2(\frac{\partial\{M\}}{\partial t})\{M\}]dv$$

$$+ \int_S \frac{h_m}{2}(M_s^2 - 2M_sM_\infty + M_\infty^2)ds \qquad (3.9)$$

$$\chi_2 = \int_V \frac{1}{2}[\{g_2\}^T[k]\{g_2\} - 2L\rho(\frac{\partial\{M\}}{\partial t})\{T\} + 2\rho c(\frac{\partial\{T\}}{\partial t})\{T\}]dv$$

$$+ \int_s \frac{h}{2}(T_s^2 - 2T_sT_\infty + T_\infty^2)ds \tag{3.10}$$

The volume and surface integrals in (3.9) and (3.10) can be expressed as a sum of integrals over a set of sub-regions or elements.

$$\chi_1 = \sum_{e=1}^{E} \int_{v^{(e)}} \frac{1}{2}\{g_1^{(e)}\}^T[D^{(e)}]\{g_1^{(e)}\}dv + \int_{v^{(e)}} \frac{\partial M^{(e)}}{\partial t}\{M^{(e)}\}dv$$

$$+ \int_{s^{(e)}} \frac{h_m^{(e)}}{2}(M_s^{(e)}M_s^{(e)} - 2M_s^{(e)}M_\infty^{(e)} + M_\infty^{(e)}M_\infty^{(e)})ds \tag{3.11}$$

$$\chi_2 = \sum_{e=1}^{E} \int_{v^{(e)}} \frac{1}{2}\{g_2^{(e)}\}^T[k^{(e)}]\{g_2^{(e)}\}dV - L\rho\int_{v^{(e)}} \frac{\partial M^{(e)}}{\partial t}\{T^{(e)}\}dv$$

$$+\rho c\int_{v^{(e)}} \frac{\partial T^{(e)}}{\partial t}\{T^{(e)}\}dV + \int_{s^{(e)}} \frac{h^{(e)}}{2}(T_s^{(e)}T_s^{(e)} -$$

$$2T_s^{(e)}T_\infty^{(e)} + T_\infty^{(e)}T_\infty^{(e)})ds \tag{3.12}$$

where the superscripts e indicate the elements or subregions and E is the total number of elements. These two equations can also be written as

$$\chi_1 = \chi_1^{(1)} + \chi_1^{(2)} + \ldots + \chi_1^{(E)} = \sum_{e=1}^{E} \chi_1^{(e)} \qquad (3.13)$$

$$\chi_2 = \chi_2^{(1)} + \chi_2^{(2)} + \ldots \chi_2^{(E)} = \sum_{e=1}^{E} \chi_2^{(e)} \qquad (3.14)$$

where $\chi_1^{(e)}$ is the contribution of a single element to χ_1 and similarly for $\chi_2^{(e)}$. The minimization of χ_1 and χ_2 occurs when

$$\frac{\partial \chi_1}{\partial \{M\}} = \frac{\partial}{\partial \{M\}} \sum_{e=1}^{E} \chi_1^{(e)} = \sum_{e=1}^{E} \frac{\partial \chi_1^{(e)}}{\partial \{M\}} = 0 \qquad (3.15)$$

$$\frac{\partial \chi_2}{\partial \{T\}} = \frac{\partial}{\partial \{T\}} \sum_{e=1}^{E} \chi_2^{(e)} = \sum_{e=1}^{E} \frac{\partial \chi_2^{(e)}}{\partial \{T\}} = 0 \qquad (3.16)$$

The derivatives $\frac{\partial \chi_1^{(e)}}{\partial \{M\}}$ in (3.15) and $\frac{\partial \chi_2^{(e)}}{\partial \{T\}}$ can not be evaluated until the integrals in (3.11) and (3.12) have been written in terms of nodal moisture contents and temperatures, {M} and {T}. The moistures and temperatures in each subregion or element are approximated by algebraic polynomials relating them to moisutres and temperature of nodal points of that element (Zienkiewicz, 1971) or

$$M^{(e)} = [N^{(e)}] \{M\} \quad (3.17)$$

$$T^{(e)} = [N^{(e)}] \{T\} \quad (3.18)$$

$[N^{(e)}]$ is the matrix of shape functions relating moistures and temperatures in the element, $M^{(e)}$ and $T^{(e)}$, to the nodal moistures and temperatures, $\{M\}$ and $\{T\}$.

The similarity between the axisymmetric and two dimensional problem makes the solution of the axisymmetric problem quite straight forward. An example of an axisymmetric element is given in Figure 3.1. Equations (3.17) and (3.18) can be written as

$$M^{(e)} = N_iM_i + M_jM_j + N_kM_k \quad (3.19)$$

$$T^{(e)} = N_iT_i + N_jT_j + N_kT_k \quad (3.20)$$

where

$$N_i = \frac{1}{2A} (a_i + b_ir + c_iz)$$

$$N_j = \frac{1}{2A} (a_j + b_jr + c_jz)$$

$$N_k = \frac{1}{2A} (a_k + b_kr + c_kz)$$

A is total area of the triangular element and constants a, b and c are defined as

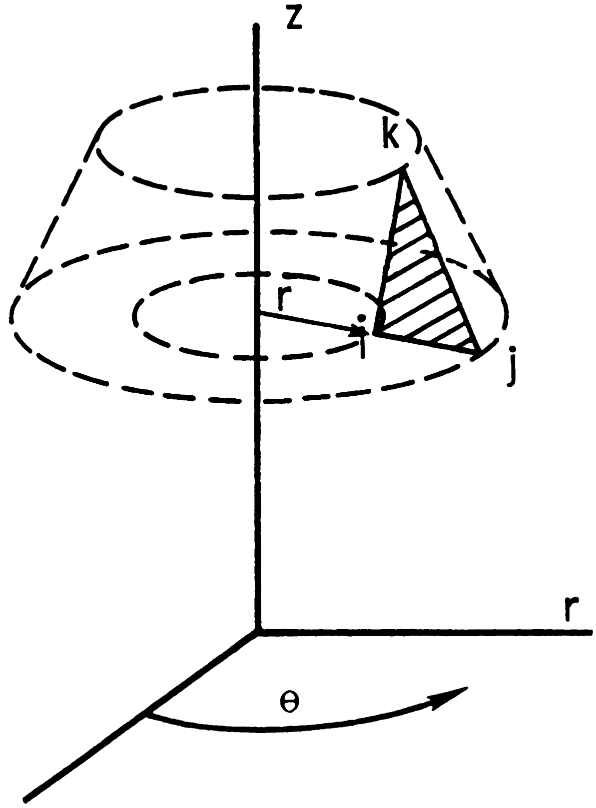

Figure 3.1. Simplex Triangular Axisymmetric Elements

$$a_i = r_j z_k - r_k z_j \qquad a_j = r_k z_i - z_k r_i$$

$$b_i = z_j - z_k \qquad b_j = z_k - z_i$$

$$c_i = r_k - r_j \qquad c_j = r_i - r_k$$

$$a_k = r_i z_j - r_j z_i$$

$$b_k = z_i - z_j$$

$$c_k = r_j - r_i$$

We can now evaluate (3.7a) and (3.7b) which along with (3.19) and (3.20) can be substituted in (3.11) and (3.12).

$$\{g_1^{(e)}\} = \begin{Bmatrix} \dfrac{\partial M^{(e)}}{\partial r} \\ \dfrac{\partial M^{(e)}}{\partial z} \end{Bmatrix} = \begin{bmatrix} \dfrac{\partial N_i^{(e)}}{\partial r} & \dfrac{\partial N_j^{(e)}}{\partial r} & \dfrac{\partial N_k^{(e)}}{\partial r} \\ \dfrac{\partial N_i^{(e)}}{\partial z} & \dfrac{\partial N_j^{(e)}}{\partial z} & \dfrac{\partial N_k^{(e)}}{\partial z} \end{bmatrix} \begin{Bmatrix} M_i \\ M_j \\ M_k \end{Bmatrix}$$

$$= [B^{(e)}] \{M\} \qquad (3.21)$$

and similarly

$$\{g_2^{(e)}\} = [B^{(e)}] \{T\} \qquad (3.22)$$

Element integrals in (3.11) and (3.12) now become

$$\chi_1^{(e)} = \int_{V^{(e)}} \frac{1}{2}\{M\}^T[B^{(e)}]^T[D^{(e)}][B^{(e)}]\{M\}dV + \int_{V^{(e)}} [N^{(e)}]\{M\}$$

$$[N^{(e)}]\frac{\partial\{M\}}{\partial t}\, dV + \int_{S^{(e)}} \frac{h_m}{2}\{M\}^T[N^{(e)}]^T[N^{(e)}]\{M\}ds -$$

$$\int_{S^{(e)}} h_m M_\infty [N^{(e)}]\{M\}ds \qquad (3.23)$$

$$\chi_2^{(e)} = \int_{V^{(e)}} \frac{1}{2}\{T\}^T[B^{(e)}]^T[k^{(e)}][B^{(e)}]\{T\}dV - L\rho\int_{V^{(e)}} [N^{(e)}]$$

$$\{T\}[N^{(e)}]\frac{\partial\{M\}}{\partial t}\, dV + \rho c\int_{V^{(e)}} [N^{(e)}]\{T\}[N^{(e)}]\frac{\partial\{T\}}{\partial t}dV +$$

$$\int_{S^{(e)}} \frac{h}{2}\{T\}^T[N^{(e)}]^T[N^{(e)}]\{T\}ds - \int_{S^{(e)}} hT_\infty[N^{(e)}]\{T\}ds \qquad (3.24)$$

where $[B^{(e)}]^T$ is the transpose of matrix [B] and element superscripts are going to be deleted for clarity from now on. The order of integration can be changed. Performing differentiation in (3.15) and (3.16) for the purpose of minimizing χ_1 and χ_2 in (3.23) and (3.24) yields

$$\frac{\partial \chi_1}{\partial \{M\}} = (\int_v [N]^T[N]dV)\frac{\partial \{M\}}{\partial t} + (\int_v [B]^T[D][B]dV + \int_s h_m[N]^T[N]ds)$$

$$\{M\} - \int_s h_m M_\infty [N]^T ds = 0 \qquad (3.25)$$

$$\frac{\partial \chi_2}{\partial \{T\}} = (\rho c \int_v [N]^T[N]dV)\frac{\partial \{T\}}{\partial t} - (L\rho \int_v [N]^T[N]dV)\frac{\partial \{M\}}{\partial t}$$

$$+ (\int_v [B]^T[k][B]dV + \int_s h[N]^T[N]ds)\{T\} - \int_s hT_\infty [N]^T ds = 0$$

$$(3.26)$$

Evaluating the integrals in (3.25) and (3.26) (Segerlind, 1976) yield

$$(\frac{2\pi A}{60}[c_{ij}])\frac{\partial \{M\}}{\partial t} + (\frac{2\pi \bar{r} D}{4A}\begin{bmatrix} b_i^2+c_i^2 & & \text{sym.} \\ b_ib_j+c_ic_j & b_j^2+c_j^2 & \\ b_ib_k+c_ic_k & b_jb_k+c_jc_k & b_k^2+c_k^2 \end{bmatrix}$$

$$+ \frac{2\pi h_m L_{jk}}{12}\begin{bmatrix} o & o & o \\ o & 3r_j+r_k & r_j+r_k \\ o & r_j+r_k & r_j+3r_k \end{bmatrix})\{M\} - \frac{2\pi h_m L_{jk} M_\infty}{6}$$

$$\begin{bmatrix} o & o & o \\ o & 2 & 1 \\ o & 1 & 2 \end{bmatrix} \begin{Bmatrix} r_i \\ r_j \\ r_k \end{Bmatrix} = 0 \qquad (3.27)$$

$$\left(\rho c \frac{2\pi A}{60} [c_{ij}]\right)\frac{\partial\{T\}}{\partial t} - \left(L\rho\frac{2\pi A}{60} [c_{ij}]\right)\frac{\partial\{M\}}{\partial t} + \left(\frac{2\pi\bar{r}k'}{4A}\right.$$

$$\left.\begin{bmatrix} b_i^2+c_i^2 & & \\ b_ib_j+c_ic_j & b_j^2+c_j^2 & \\ b_ib_k+c_ic_k & b_jb_k+c_jc_k & b_k^2+c_k^2 \end{bmatrix} + \frac{2\pi hL_{jk}}{12}\begin{bmatrix} o & o & o \\ o & 3r_j+r_k & r_j+r_k \\ o & r_j+r_k & r_j+3r_k \end{bmatrix}\right)$$

$$\{T\} - \frac{2\pi hL_{jk}T_\infty}{6}\begin{bmatrix} o & o & o \\ o & 2 & 1 \\ o & 1 & 2 \end{bmatrix}\begin{Bmatrix} r_i \\ r_j \\ r_k \end{Bmatrix} = 0 \qquad (3.28)$$

where $\bar{r} = \dfrac{r_i+r_j+r_k}{3}$

L_{jk} = length between nodes j and k of the triangular element where convection takes place.

and

$$[c_{ij}] = (1 + \delta_{ij})(3\bar{r} + r_i + r_j) \qquad \text{(Brocci, 1969)}$$

where δ_{ij} = Kronecker delta

(3.27) and (3.28) can be written in condensed form

$$[C_{11}]\frac{\partial\{M\}}{\partial t} + [K_{11}]\{M\} - \{f_1\} = 0 \qquad (3.29)$$

$$[C_{21}]\frac{\partial\{M\}}{\partial t} + [C_{22}]\frac{\partial\{T\}}{\partial t} + [K_{22}]\{T\} - \{f_2\} = 0 \qquad (3.30)$$

and in matrix form

$$\begin{bmatrix} C_{11} & o \\ C_{21} & C_{22} \end{bmatrix}\begin{Bmatrix} \dot{M} \\ \dot{T} \end{Bmatrix} + \begin{bmatrix} K_{11} & o \\ o & K_{22} \end{bmatrix}\begin{Bmatrix} M \\ T \end{Bmatrix} - \begin{Bmatrix} f_1 \\ f_2 \end{Bmatrix} = 0 \qquad (3.31)$$

where $[C_{11}]$, $[C_{21}]$, $[C_{22}]$, $[K_{11}]$, $[K_{22}]$, $\{f_1\}$ and $\{f_2\}$ are appropriate coefficients in (3.27) and (3.28) and

$$\{\dot{M}\} = \frac{\partial\{M\}}{\partial t}, \qquad \{\dot{T}\} = \frac{\partial\{M\}}{\partial t}$$

Equation (3.31) can also be written as

$$[C]\begin{Bmatrix}\dot{M}\\ \dot{T}\end{Bmatrix} + [K]\begin{Bmatrix}M\\ T\end{Bmatrix} - \{F\} = 0 \tag{3.32}$$

Note that this equation is for one element and for the whole body a summation over all the elements must be carried out.

We now solve (3.29) for $\frac{\partial\{M\}}{\partial t}$ or

$$\frac{\partial\{M\}}{\partial t} = \frac{1}{[C_{11}]}\left(\{f_1\} - [K_{11}]\{M\}\right)$$

inserting this in (3.30) yields

$$[C_{22}]\{\dot{T}\} + [K_{22}]\{T\} - \{f_2\} = [C_{21}]\left[\frac{1}{[C_{11}]}(\{f_1\} - [K_{11}]\{M\})\right] = 0$$

After simplification and substitution of (3.29) the equations become

$$[C_{11}]\{\dot{M}\} + [K_{11}]\{M\} - \{f_1\} = 0 \tag{3.29}$$

$$[C_{22}]\{\dot{T}\} + [K_{22}]\{T\} - \{f_2\} + L\rho([K_{11}]\{M\} - \{f_1\}) = 0 \tag{3.33}$$

Equation (3.33) indicates that the moisture values $\{M\}$ are needed for every time step in order to obtain the temperature values for the same time step

3.4 Finite Difference Solution in the Time Domain

To solve the linear differential equations (3.29) and (3.33) to obtain the values of $\{M\}$ and $\{T\}$ at each point in time, a central finite difference technique to approximate the time derivatives is used (Segerlind, 1976).

Given two points on a curve (Figure 3.2) an approximation for the first derivative at the midpoint of the increment is

$$\{\dot{M}\} = \frac{d\{M\}}{dt} = \frac{\{M\}_{i+1} - \{M\}_i}{\Delta t} \tag{3.34a}$$

$$\{\dot{T}\} = \frac{d\{T\}}{dt} = \frac{\{T\}_{i+1} - \{T\}_i}{\Delta t} \tag{3.34b}$$

Since $\{\dot{M}\}$ and $\{\dot{T}\}$ are evaluated at the midpoint of the time increment, we should also evaluate $\{M\}$, $\{T\}$, $\{f_1\}$ and $\{f_2\}$ at this point. So we have

$$\{M\}^* = \frac{1}{2}\left(\{M\}_{i+1} + \{M\}_i\right) \tag{3.35a}$$

$$\{T\}^* = \frac{1}{2}\left(\{T\}_{i+1} + \{T\}_i\right) \tag{3.35b}$$

$$\{f_1\}^* = \frac{1}{2}\left(\{f_1\}_{i+1} + \{f_1\}_i\right) = \{f_1\} \tag{3.36a}$$

$$\{f_2\}^* = \frac{1}{2}\left(\{f_2\}_{i+1} + \{f_2\}_i\right) = \{f_2\} \tag{3.36b}$$

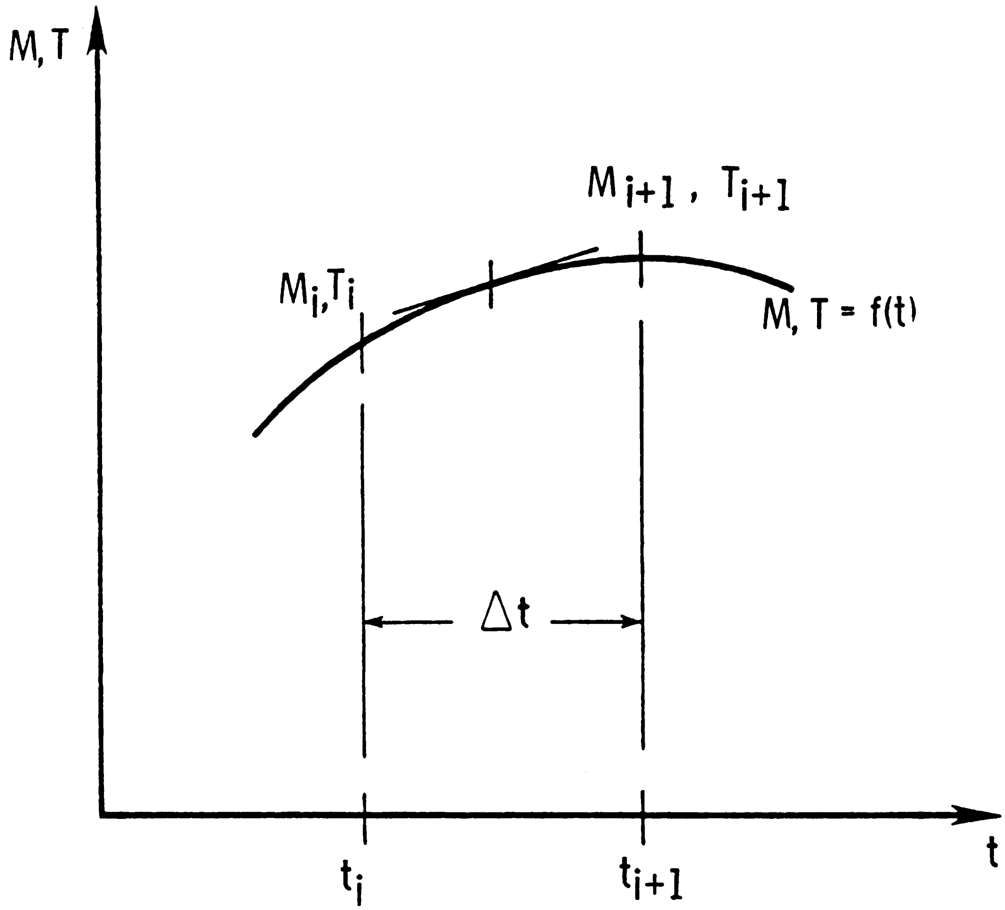

Figure 3.2. Numerical Determination of the First Derivatives of {M} and {T}

since $\{f_1\}$ and $\{f_2\}$ are constant and do not vary with time. Substitution of (3.34a), (3.35a) and (3.36a) into the differential equation (3.29) gives

$$([C_{11}] + \frac{\Delta t}{2}[K_{11}])\{M\}_{i+1} = ([C_{11}] - \frac{\Delta t}{2}[K_{11}])\{M\}_i + \Delta t\ \{f_1\} \tag{3.37}$$

Given the nodal moisture values at time t, equation (3.37) can be solved to yield the nodal moisture values at the time $t+\Delta t$. The column vector $\{f_1\}$ consists of known parameters; hence, its evaluation at t and $t+\Delta t$ can be carried out before (3.37) is solved.

Let us rewrite equation (3.33) as

$$[C_{22}]\{\dot{T}\} + [K_{22}]\{T\} - \{f_2'\} = 0 \tag{3.38}$$

where

$$\{f_2'\} = \{f_2\} - L\rho([K_{11}]\{M\} - \{f_1\}) \tag{3.39}$$

using (3.34b), (3.35b) and (3.36b) equation (3.38) may be written as

$$([C_{22}] + \frac{\Delta t}{2}\ [K_{22}])\{T\}_{i+1} = ([C_{22}] - \frac{\Delta t}{2}[K_{22}]\{T\}_i + \Delta t\ \{f_2'\}^* \tag{3.40}$$

where

$$\{f_2'\}^* = \frac{1}{2}\ (\{f_2'\}_{i+1} + \{f_2'\}_i) \tag{3.41}$$

$$\{f_2'\}_{i+1} = \{f_2\} - L\rho([K_{11}]\{M\}_{i+1} - \{f_1\}) \tag{3.42a}$$

and

$$\{f_2'\}_i = \{f_2\} - L\rho([K_{11}]\{M\}_i - \{f_1\}) \qquad (3.42b)$$

substituting (3.41), (3.42a) and (3.42b) in (3.40) yield

$$([C_{22}] + \frac{\Delta t}{2}[K_{22}])\{T\}_{i+1} = ([C_{22}] - \frac{\Delta t}{2}[K_{22}])\{T\}_i +$$

$$\frac{\Delta t}{2}[(\{f_2\} - L\rho([K_{11}]\{M\}_{i+1} - \{f_1\})) + (\{f_2\} - L\rho([K_{11}]$$

$$\{M\}_i - \{f_1\}))]$$

Simplifications gives

$$([C_{22}] + \frac{\Delta t}{2}[K_{22}])\{T\}_{i+1} = ([C_{22}] - \frac{\Delta t}{t}[K_{22}])\{T\}_i +$$

$$\Delta t[\{f_2\} + L\rho\{f_1\} - \frac{L\rho}{2}[K_{11}](\{M\}_{i+1} + \{M\}_i)] \qquad (3.43)$$

This equation along with equation (3.37) defines the process of coupled heat and mass diffusion inside the soybean kernel.

3.5 Computer Implementation and the Soybean Model

A finite element method for the solution of coupled moisture and heat diffusion within a spherical body was presented in the previous sections. A computer program for two dimensional transient field problem such as the one described by equation (3.37) was written by Segerlind (1976).

This program was modified to incorporate the coupling effect of moisture content and temperature for each time step. Modification also included a change to axially symmertric triangular elements.

The modified program first solves equation (3.37) for a given initial nodal values. For every time step Δt and given $\{M\}_i$ values, a set of nodal moisture values $\{M\}_{i+1}$ will be obtained and stored on a tape. Then the last term of equation (3.43) was evaluated and stored. Finally equation (3.43) was solved for a given initial values of $\{T\}_i$ to yield the new nodal temperature values $\{T\}_{i+1}$. Ninety six iterations were calculated using a time step Δt, of 10 minutes. Total drying time was 16 hours. Nodal moisture and temperature values were printed for one hour intervals for 16 hours.

3.5.1 The Soybean Model

The following assumptions for the soybean model were made:

(1) Soybean kernel was taken as an isotrpic sphere symmetrical with respect to its center. A two dimensional axisymmetric finite element grid as is shown in Figure 3.3 was used. This was due to the fact that no knowledge of temperature variation within the soybean kernel was available.

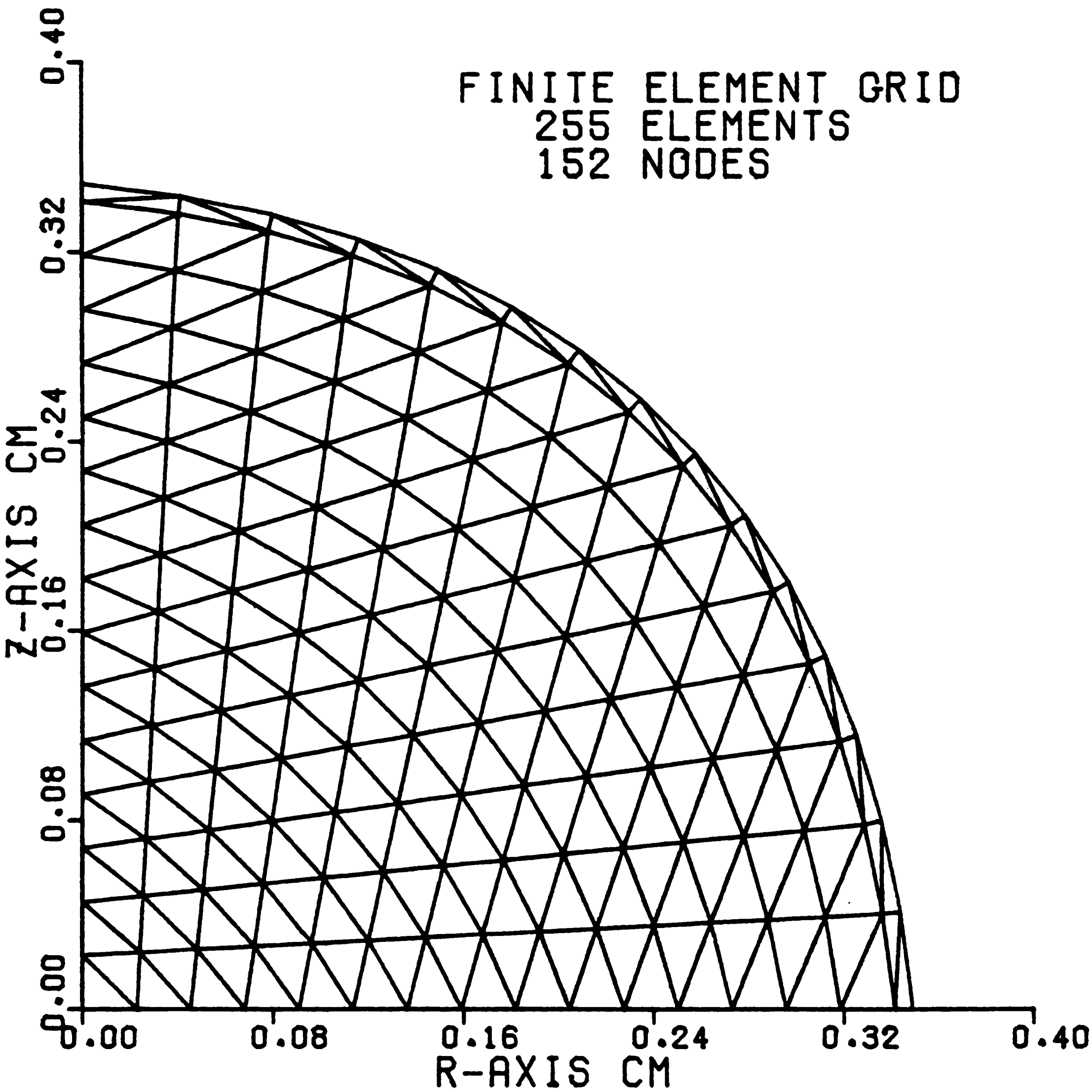

Figure 3.3 The Two-Dimensional Axisymmetric Finite Element Grid with Simplex Triangular Elements

Some researchers such as Whitaker et al. (1969), Misra and Young (1978) assumed a uniform temperature variation, solved only the moisture diffusion equation and used a one dimensional model. The finite element grid that was used in this model consists of 255 elements and 152 nodes. The thickness of the soybean skin is incorporated in the grid and the computer program has the option of having different material properties for the skin and the cotyledones.

(2) Moisture removal and heat intake take place by convection process through the whole surface area of the kernel skin as was shown in section 3.2. It is noteworthy to mention that some unsuccessful attempts were made to incorporate the effect of the hilum in the process of moisture removal. Failure was due to the fact that there was no way to find what percentage of moisture was removed from the kernel through the hilum region even though some preliminary tests proved that more moisture was removed through the hilum than through the skin.

(3) All material parameters of the soybean kernel were assumed to be constant for two reasons: (1) it was felt that considerable information on the model about temperature and moisture

distribution within the kernel could be gained.
(2) There was a lack of information on the material properties of the soybean as most of the properties which where needed for this model are functions of temperature, moisture, time, etc. Some of these properties as are available in the literature are tabulated in Table 2.1. The values of the different material properties which were used in this model are presented in Table 3.1.

Table 3.1 Values of the different material properties of the soybean used in modeling the kernel

Material Property	Value	Dimension
Diffusion coefficient (D)	$7.0\text{X}10^{-11}$	m^2/sec.
Thermal conductivity (K')	0.1	w/m-°C
Specific heat (c)	2000.0	J/kg-°C
Density (ρ)	1200.0	kg/m^3
Heat convection coefficient (h)	60.0	w/m^2-°C
Mass convection coefficient (h_m)	0.05	m/sec.

3.5.2 Mass Average Moisture and Temperature

In order to have a measure of the kernel moisture content and temperature as a whole, rather than the nodal

moisture and temperature values, the concept of mass average moisture and mass average temperature was used. Mass average moisture and temperature of a body are defined by (Segerlind, 1976)

$$\bar{M} = \frac{\int_V M(r,z)\,dm}{\int_V dm} \qquad \text{for every time step} \qquad (3.44)$$

$$\bar{T} = \frac{\int_V T(r,z)\,dm}{\int_V dm} \qquad \text{for every time step} \qquad (3.45)$$

where dm is an element of mass. Using (3.19) and (3.20) and after some simplification (3.44) and (3.45) yield

$$\bar{M} = \frac{\sum_{e=1}^{E} \frac{\pi A^{(e)}}{6} \left[(2r_i+r_j+r_k)M_i+(r_i+2r_j+r_k)M_j+(r_i+r_j+2r_k)M_k\right]}{\sum_{e=1}^{E} \frac{2\pi A^{(e)}}{3} (r_i+r_j+r_k)} \qquad (3.46)$$

and similarly

$$\bar{T} = \frac{\sum_{e=1}^{E} \frac{\pi A^{(e)}}{6} \left[(2r_i+r_j+r_k)T_i+(r_i+2r_j+r_k)T_j+(r_i+r_j+2r_k)T_k\right]}{\sum_{e=1}^{E} \frac{2\pi A^{(e)}}{3} (r_i+r_j+r_k)} \qquad (3.47)$$

Both equations are applicable only for the axisymmetric triangular simplex element.

3.6 Distribution of Moisture and Temperature within the Kernel and Drying Curves

Based on the results for $\bar{M}$, a drying curve was obtained and compared with the experimental results from two different sources, as is shown in Figure 3.4. The simulated drying curve is between the two experimental drying curves and agress very closely with the results given by Overhults et al. (1973). Figure 3.5 shows the variation of the kernel mass average temperature vs. drying time. It is obvious from the figure that there is very sharp increase in simulated mass average temperature of the model in the first hour of drying. Mass average temperature reaches the equilibrium temperature (drying air temperature) in about one hour and then stays constant for the rest of the drying period. Distribution of the nodal moisture content of the soybean model at different radii for the whole drying period is shown in Figure 3.6. It is apparent from the figure that nodes which are located on the skin reach the quilibrium moisture content much faster than the internal nodes. It was also felt that there is a need to monitor the nodal moisture distribution for the first few hours of drying since according to several researchers such as Misra (1977) this is the period in which stress cracking occurs. This is shown in Figure 3.7.

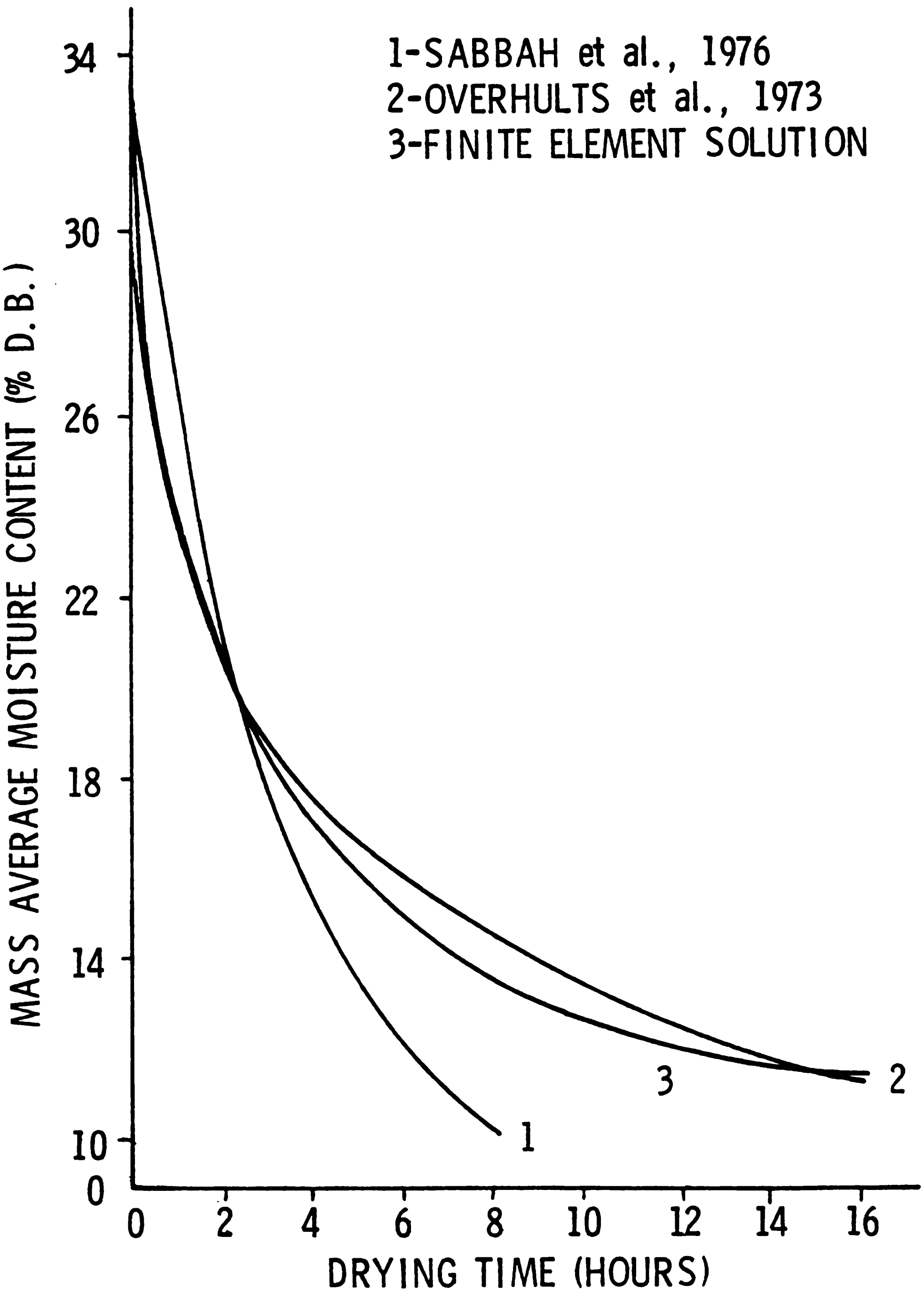

Figure 3.4. Drying Curve for the Soybean Model Compared with Experimental Results

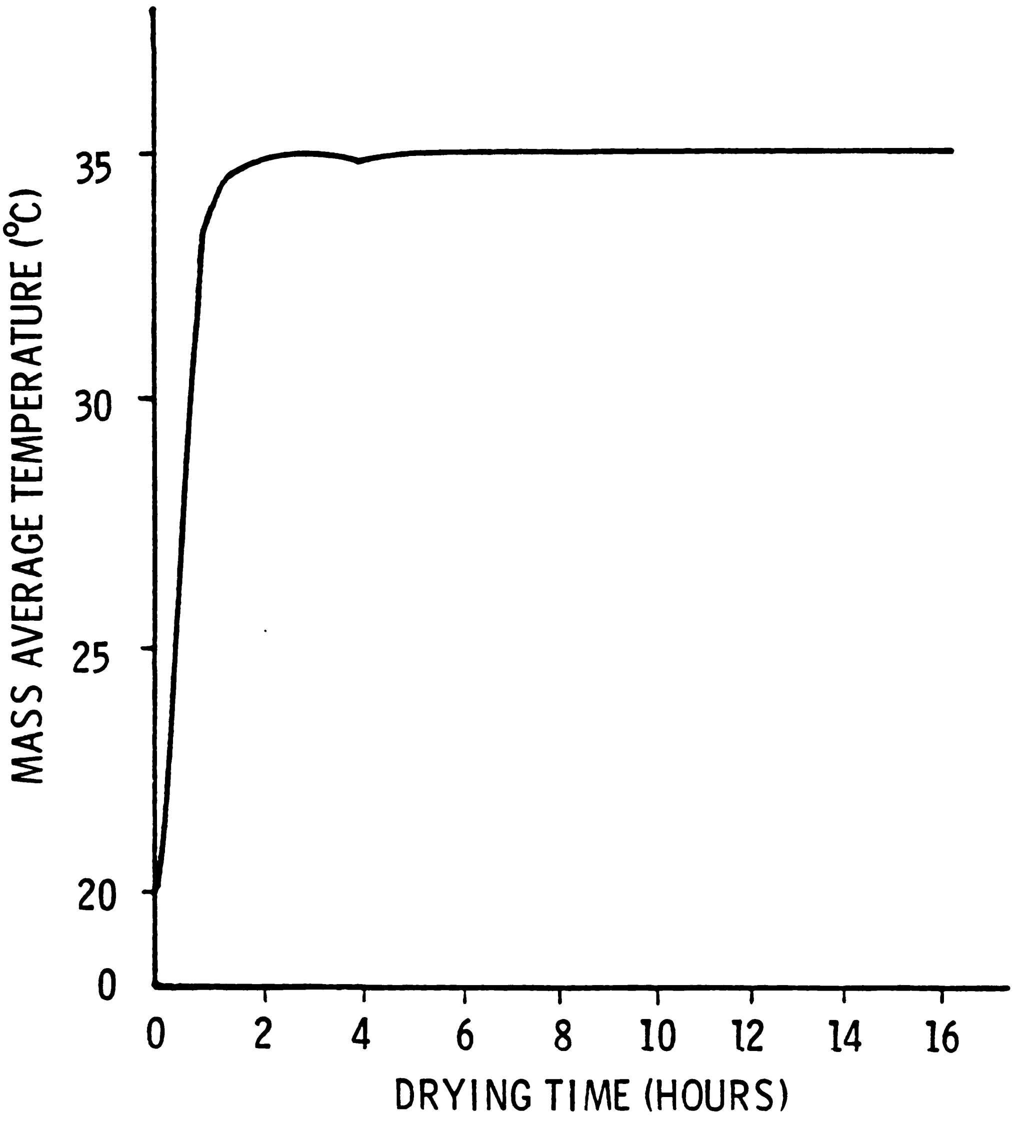

Figure 3.5. Simulated Mass Average Temperature of the Soybean Model vs. Time

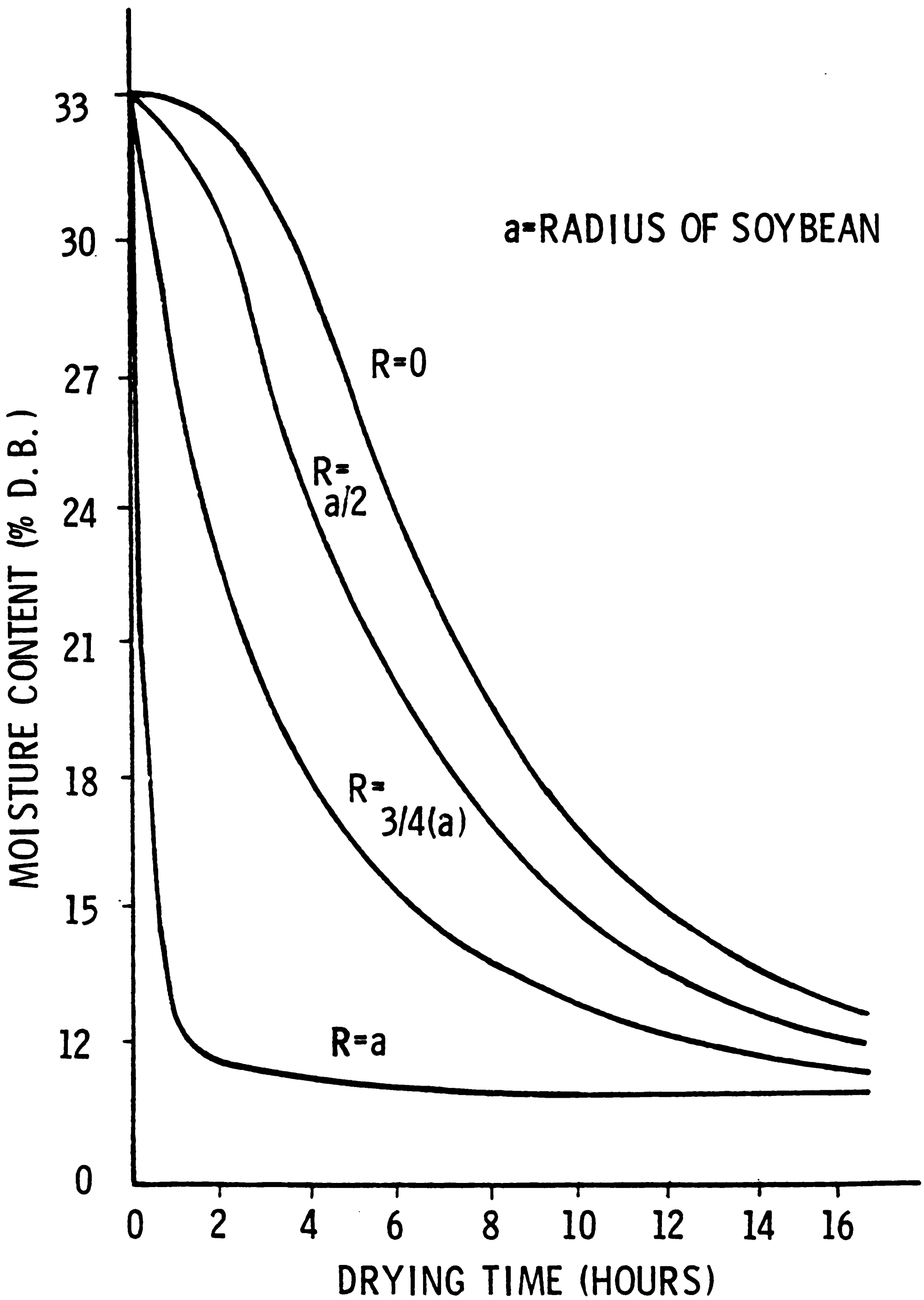

Figure 3.6. Moisture Content Distribution of the Soybean Model at Different Radii for the Whole Drying Period (z=0)

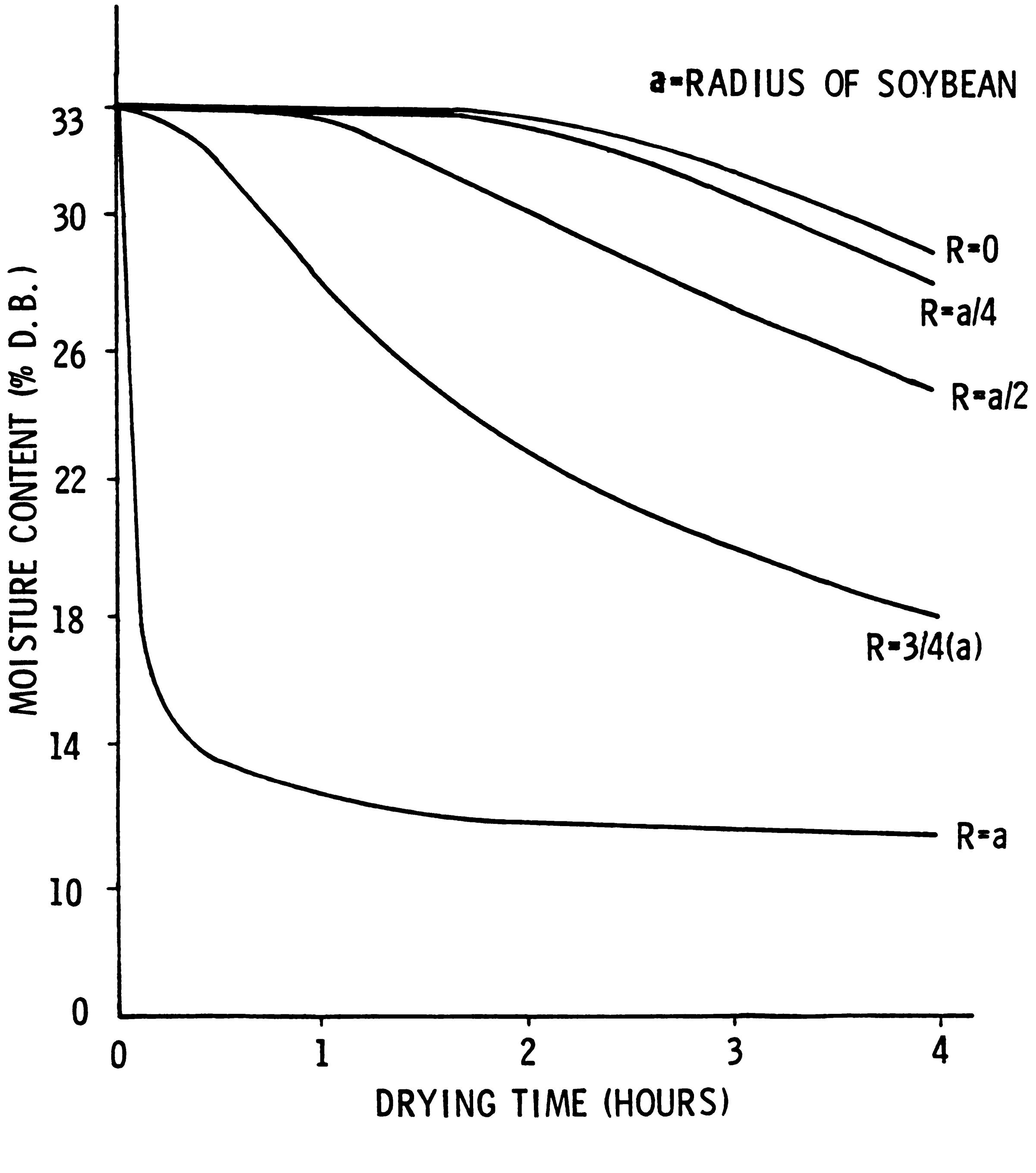

Figure 3.7. Distribution of the Soybean Moisture Content at Different Radii for the First Four Hours of Drying

4. SIMULATION OF THERMO-HYDRO STRESSES

It is assumed that the total stress at a point is some combination of the thermal and hydro stresses superimposed upon whatever stress may exist due to mechanical loading. The thermal and hydro stresses may arise from either tension or compression, and it might be expected that since both high temperature and high moisture content cause swelling or expansion of the soybean kernel and since temperature and moisture gradients are of opposite sign in a heated material undergoing drying, a very complicated tension-compression state may occure within the kernel. This complicated stress state, when it exceeds some critical state at a point, results in internal failure.

4.1 Equations of the Linear Theory of Viscoelasticity

4.1.1 Viscoelastic Constitutive Equations

The theory of viscoelasticity is adequately described by several authors such as Flügge (1975), Christensen (1971), and Ferry (1961). There are several equivalent forms of the constitutive equations of viscoelastic materials: hereditary integral forms, differential operator forms, and complex modulus form. The integral form of the constitutive equations can be written as (Christensen, 1971)[1]

$$S_{ij} = \int_{-\infty}^{t} G_1(t-\tau) \frac{de_{ij}(\tau)}{d\tau} d\tau \tag{4.1}$$

$$\sigma_{kk} = \int_{-\infty}^{t} G_2(t-\tau) \frac{d\varepsilon_{kk}(\tau)}{d\tau} d\tau \tag{4.2}$$

where $G_1(t)$ is a relaxation function appropriate to states of shear and $G_2(t)$ is a relaxation function appropriate to states of dilatation. The deviatoric stress and strain tensors are

$$S_{ij} = \sigma_{ij} - \frac{1}{3} \delta_{ij}\sigma_{kk} \quad , \quad S_{ii} = 0 \tag{4.3}$$

and

$$e_{ij} = \varepsilon_{ij} - \frac{1}{3} \delta_{ij}\varepsilon_{kk} \quad , \quad e_{ii} = 0 \tag{4.4}$$

respectively with σ_{ij} = stress tensor

ε_{ij} = strain tensor

δ_{ij} = Kronecker delta, zero for $i \neq j$ and $\delta_{ii} = \delta_{11} + \delta_{22} + \delta_{33} = 3$

σ_{kk} = first invariant of the stress tensor

ε_{kk} = first invariant of the strain tensor

In order to use the same notation as in elasticity, the relaxation functions in simple shear and dilatation are taken as

---

[1]The standard indicial system for a rectangular Cartesian reference frame is employed whenever applicable: Repeating the subscripts i, j, k or l implies summation, Kronecker's delta is denoted by δ_{ij}, differentiation with respect to space is indicated by subscripts preceded by a comma.

$$G(t) = \frac{G_1(t)}{2} \tag{4.5}$$

$$K(t) = \frac{G_2(t)}{3} \tag{4.6}$$

These relaxation functions are equivalent to the elastic shear and bulk moduli, respectively.

An alternate form of the stress-strain relation is obtained by using creep functions to represent the current strain as determined by current value and past history of stress (Christensen, 1971)

$$e_{ij} = \int_{-\infty}^{t} J_1(t-\tau) \frac{ds_{ij}(\tau)}{d\tau} d\tau \tag{4.7}$$

$$\varepsilon_{kk} = \int_{-\infty}^{t} J_2(t-\tau) \frac{d\sigma_{kk}(\tau)}{d\tau} d\tau \tag{4.8}$$

where $J_1(t)$ and $J_2(t)$ are creep functions for states of shear and dilatation. They can be related to the relaxation functions by use of Laplace Transforms or other interconversion techniques. Shear and bulk modulus are two independent constants characterizing a homogeneous elastic solid, and the relations between these and more commonly used engineering parameters like Young's modulus and Poisson's ratio have been established. Similar relations exist between the Laplace Transforms of the viscoelastic

relaxation functions (Christensen, 1971).

A widely used form of the relaxation function is an exponential series representation known as the generalized Maxwell Model

$$G(t) = \sum_{j=0}^{n} G_j e^{-t/\tau_j} \qquad (4.9)$$

where G_j and τ_j are the shear moduli and relaxation times for each element in the model. In a similar manner the time dependent bulk modulus K(t) could be defined for the dilatational response (or volume change).

Creep functions are sometimes approximated using elastic elements and viscous elements in parallel, as represented by the series (Gradowczyk and Moavenzadeh, 1969)

$$J(t) = \sum_{j=0}^{m} J_j (1-e^{-t/\tau_j}) \qquad (4.10)$$

4.1.2 Laplace Transform of Viscoelastic Equations

The convolution integral form of the viscoelastic constitutive equations was given in the previous section, equations (4.1)-(4.8). The relationship between the different relaxation and creep functions can be established by introducing the Laplace transformation. Let f(t) be a continuous function over $o<t\leq\infty$. The Laplace transform

of this function is

$$\bar{f}(s) = L[f(t)] = \int_0^\infty f(t)e^{-st}\, dt \qquad (4.11)$$

Application of the transformation to the convolution integrals (4.1), (4.2), (4.7) and (4.8) yields (Christensen, 1971)

$$\bar{S}_{ij}(s) = s\, \bar{G}_1(s)\, \bar{e}_{ij}(s) \qquad (4.12)$$

$$\bar{\sigma}_{kk}(s) = s\, \bar{G}_2(s)\, \bar{\varepsilon}_{kk}(s) \qquad (4.13)$$

$$\bar{e}_{ij}(s) = s\, \bar{J}_1(s)\, \bar{S}_{ij}(s) \qquad (4.14)$$

$$\bar{\varepsilon}_{kk}(s) = s\, \bar{J}_2(s)\, \bar{\sigma}_{kk}(s) \qquad (4.15)$$

It follows from (4.12)-(4.15) that

$$\bar{J}_\alpha = (s^2\bar{G}_\alpha)^{-1}\ , \quad \alpha=1,2 \qquad (4.16)$$

The solution in the time domain can be obtained using the inverse transform of a function. This is given by

$$f(t) = L^{-1}[\bar{f}(s)] = \frac{1}{2\pi i} \int_{a-i\infty}^{a+i\infty} \bar{f}(s)\, e^{st} ds \qquad (4.17)$$

The inverse Laplace transform of several common functions can be obtained from a table of Laplace transforms and a partial fraction expansion of $\bar{f}(s)$. An approximate numerical method to evaluate the inverse Laplace transform is discussed by Miller and Guy (1966) and uses an orthogonal polynomial series expansion.

4.1.3 Viscoelastic Boundary Value Problem

A viscoelastic boundary value problem is governed by the following relations which have to be satisfied, and which are similar to the elastic boundary value relations (Christensen, 1971):

(I) Equilibrium equations

$$\sigma_{ij,j} + F_i = 0 \qquad i,j=1,2,3 \tag{4.18}$$

where a comma denotes a differentiation and F_i is a body force vector.

(II) Constitutive equations

$$\sigma_{ij} = \int_0^t G_{ijkl}(t-\tau) \frac{\partial \varepsilon_{k\ell}(\tau)}{\partial \tau} d\tau \tag{4.19}$$

where

$$G_{ijkl} = \frac{1}{3}[G_2(t)-G_1(t)]\delta_{ij}\delta_{kl}+\frac{1}{2}G_1(t)[\delta_{ik}\delta_{jl}+\delta_{il}\delta_{jk}] \tag{4.20}$$

Using convolution notation (4.19) can be written as

$$\sigma_{ij} = G_{ijkl} * \varepsilon_{kl} \tag{4.21}$$

(III) Strain displacement relations

$$\varepsilon_{ij} = \frac{1}{2}(U_{i,j}+U_{j,i}) \tag{4.22}$$

(IV) Prescribed boundary values

$$\sigma_{ij}n_j = S_i \text{ on } B_\sigma \tag{4.23}$$

$$U_i = \Delta_i \quad \text{on } B_u \tag{4.24}$$

B_σ is the part of the bounardy on which the tractions S_i are prescribed and B_u is that part on which the displacements Δ_i are prescribed. n_j denotes the components of the unit normal vector to the boundary.

4.2 Thermo-Hydro Viscoelastic Constitutive Equations

The constitutive laws discussed in the preceeding section rest on the assumption that the entire body is permanently maintained at a uniform temperature and moisture content. Accordingly, the response functions $G_\beta(t)$ and $J_\beta(t)$, as well as the material parameters are to be regarding as having been determined at the relevant fixed "base temperature" and "base moisture content" which are designated by T_o and M_o. Unfortunately, however, such a treatment, which disregards the influence of temperature and moisture upon the basic response characteristics of the material, is remote from physical reality; for it is well known that the rate processes of viscoelasticity are highly sensitive to temperature changes. Such a temperature dependence is schematically shown for relaxation function in Figure 4.1 (Christensen, 1971).

4.2.1 Thermo-Hydro Rheologically Simple Materials and Shift Factors

In general, an increase in temperature increases the rate of creep, that is, the rate of change of the creep function and relaxation modulus with time (Morland and Lee 1960). There is a special class of viscoelastic materials which exhibit approximately a particular simple property with change of temperature. This is a translational shift - no change in shape - of the relaxation modulus plotted against the logarithm of time at different uniform temperature, which leads to an equivalence relation between temperature and ln t. It has also been reported by many researchers that a change in the experimental time scale in viscoelastic small deformation tests at elevated temperatures is equivalent to some corresponding temperature change. That is, data measured over a limited time scale at a series of temperatures can be combined to

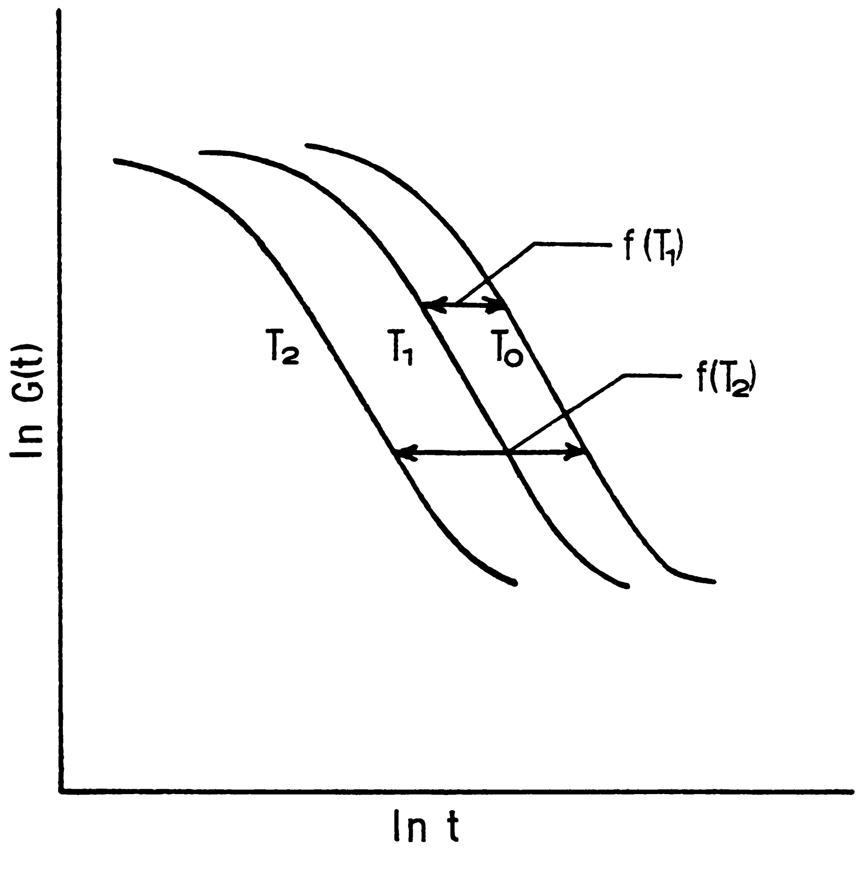

Figure 4.1. Temperature Dependence of Relaxation Function

give a master curve which represents the behavior of the material at some selected temperatures, but over an extended time scale. Use of this concept, to extend the time scale of experimental data was first proposed by Leaderman (1943). Such a material has been classified as "thermorheologically simple" by Schwarzl and Staverman (1952), who show that all the characteristic functions of the material must obey the same property.

To relate time to temperature, a dimensionless time-temperature shift factor, a_T, is defined as (Hammerle, 1968)

$$a_T = \frac{t_T}{t_o} \tag{4.25}$$

where

t_T = time required to observe some phenomenon at temperature T,

t_o = time required to observe the same phenomenon at the reference temperature T_o.

For a biological moisture-sensitive material, an increase in moisture content would yield similar results and, hence, the time-moisture shift factor a_M is defined similar to time-temperature shift factor. Therefore, following a temperature superposition, a corresponding moisture content superpoistion can be made. In this manner a material property which is both temperature and moisture content dependent, can be reduced to simple time dependency over a very long time period.

Since the thermorheological nature of a material indicates that an increase in temperature corresponds to an increase in time, by the same reasoning in a "hydrorheologically simple material" an increase in moisture content would correspond to an increase in either temperature or time.

We now turn to the modifications arising in the stress-strain law if the temperature and moisture fields are variable with position and time. With a view toward the analytical formulation of the time-temperature-moisture equivalence hypothesis we focus our attention at first to the effect of a uniform temperature and moisture change and second to the case of nonconstant temperature and moisture states.

4.2.2 Constant Temperature and Moisture States

The mathematical description of the temperature and moisture dependence of thermo and hydrorheologically simple materials will now be formulated for constant temperature and moisture states. We designate the isotropic relaxation and creep functions at the base temperature $T=T_o$ by

$$G_\alpha(t) \text{ and } J_\alpha(t), \quad T=T_o$$

where $\alpha=1,2$ throughout. Based on the work of Muki and Sternberg (1961), if $g_\alpha(t,T)$ is the relaxation function at constant temperature T, then

$$g_\alpha(t,T_o) = G_\alpha(t) \tag{4.26}$$

We change the independent variable in $G_\alpha(t)$ such that

$$G_\alpha(t) = L_\alpha(\ell nt) \tag{4.27}$$

Since the material is assumed thermorheologically simple, any viscoelastic property, here the relaxation modulus, can be expressed as

$$g_\alpha(t,T) = L_\alpha[\ell nt + f(t)] \tag{4.28}$$

where the "temperature shift function" f(T) obeys the relations

$$f(T_o) = 0, \quad \frac{df(T)}{dT} > 0 \tag{4.29}$$

f(T) is measured relative to some arbitrary temperature T_o. Since the rate of change is increased with increase of temperature, the modulus curve will shift towards shorter times with increase of temperature, as illustrated in Figure 4.1. We introduce a change of variable in shift function by setting

$$f(T) = \ell n\ a_T(T) \tag{4.30}$$

or in another way the "temperature shift factor" $a_T(T)$ is

$$a_T(T) = \exp[f(T)] \tag{4.31}$$

Relation (4.29) now implies that

$$a_T(T_o)=1 \quad , \; a_T(T)> 0 \quad , \quad \frac{da_T(T)}{dT} > 0 \tag{4.32}$$

The temperature shift factor is therefore a positive, monotonically increasing function of T throughout the range of validity of equation (4.28) (Muki and Sternberg, 1961).

Substituting equation (4.30) into (4.28), the relaxation modulus can be expressed as

$$\begin{aligned} g_\alpha(t,T) &= L_\alpha[\ell nt + \ell n\ a_T(T)] \\ &= L_\alpha \ell n[t \cdot a_T(T)] \end{aligned} \tag{4.33}$$

Now, recalling (4.27), (4.33) is written as

$$g_\alpha(t,T) = G_\alpha[t \cdot a_T(T)] = G_\alpha(\xi) \tag{4.34}$$

provided the "reduced time" is defined by

$$\xi = t \cdot a_T(T) \tag{4.35}$$

Thus, the relaxation function $g_\alpha(t,T)$ at any temperature can be obtained directly from the relaxation function $G_\alpha(t)$ at base temperature T_o by replacing t with ξ from (4.35) or once the temperature shift function f(T) is

known for the temperature range considered. The temperature shift function $f(T)$, and hence the temperature shift factor $a_T(T)$, represents an inherent property of the viscoelastic material. Christensen (1971) describes the experimental technique for determining the shift functions and hence, the shift factors. The viscoelastic mechanical property when plotted versus the logarithm of time can be superimposed to form a single curve merely by shifting the various curves at different temperatures along the logarithm of time axis. If the curves do coincide within experimental error, the basic postulate of thermorheologically simple material is verified. He further discusses that there are no general inclusive guidelines that can be given to answer the question as to whether a given material can be expected to exhibit the thermo-rheologically simple type of behavior. The only safe and certain answer lies in experimentally verifying or invalidating the shifting procedure for every material of interest.

Based on temperature shift factor, an analogy is established for the moisture shift factor, a_M. It is also defined as

$$a_M(M) = \exp[f(M)] \tag{4.36}$$

where

$f(M)$ = moisture shift function

From the development of a time-temperature shift factor the relaxation modulus can now be expressed by

$$G_\alpha\ (t,T,M) = f[G_\alpha(t),\ a_T(T),\ a_M(M)] \tag{4.37}$$

where the concept of a time-moisture shift factor is included. Equation (4.37) actually means that, by knowning any material property (here relaxation modulus) at the base temperature and moisture and also knowning temperature and moisture shift factors, one can get the relaxation modulus at any constant temperature and moisture content.

The thermo-hydrorheologically simple postulate is also sometimes referred to as the time-temperature-moisture superpostiion principle, or the method or reduced variables.

Saxena (1972) experimentally verified that the soybean grain is both thermo and hydrorheologically simple. Herum, et al. (1973) found the temperature and moisture shift factors as

$$\ell n\ a_T(T) = -.049(T-32.2) \tag{4.38}$$

$$\ell n\ a_M(M) = 1.61-.63(M-16.5\%) \tag{4.39}$$

where base temperature and moisture content were assumed to be 32.2°C and 16.5% (dry basis) respectively. His results for the mean values of a_T and a_M are tabulated in Table 4.1.

Table 4.1 Mean values of temperature and moisture shift factors for soybean (Herum, et al., 1973).

Temperature (°C)	Mean a_T	Moisture content (%d.b.)	Mean a_M
21.1	88	11	500
32.2	1.0	16.5	1.0
43.3	.38	21.3	.045
54.4	.14	30.2	.0017

Comparing equations (4.30) and (4.38) we see that for soybean

$$f(T) = -\ell n\ a_T(T)$$

or

$$a_T(T) = \exp-[f(T)]$$

this would change the equation (4.33) to

$$g_\alpha(t,T) = L_\alpha[\ell nt - \ell n\ a_T(T)] = L_\alpha \ell n[\frac{t}{a_T(T)}]$$

and relation (4.34) becomes

$$g_\alpha(t,T) = G_\alpha[\frac{t}{a_T(T)}] = G_\alpha(\xi)$$

where now

$$\xi = \frac{t}{a_T(T)}$$

The "shifted time" (which relates the physical time and shift factors) incorporating and summing the time-temperature and time-moisture shift factors (a_T and a_M) which are superimposed can be written as (Rao, et al., 1975)

$$\xi = \frac{t}{a} \qquad (4.40)$$

where

$$a = \frac{a_M a_T}{a_M + a_T}$$

Equations (4.37) and (4.40) enable us to pass from equations (4.1) and (4.2), which hold at the base temperature and moisture to the corresponding relaxation integral law applicable at any constant temperature and moisture. This transition is evidently effected by replacing $G_\alpha(t-\tau)$ in (4.1) and (4.2) with $G_\alpha(\xi-\xi')$, where ξ is given by $\xi=\frac{t}{a}$ and $\xi'=\frac{\tau}{a}$ provided the body (in the absence of loads) is considered to be in the unstrained state at the uniform temperature T.

The preceeding section described the equivalence relation for the body held at different uniform temperatures and moistures, and this must now be extended to cover the case of a general temperature and moisture fields (also dependent on space coordinates), $T(r,t)$ and $M(r,t)$. First consider the temperature and moisture dependent only on the space coordinates, $T(r)$ and $M(r)$, a steady state temperature and moisture fields, then assuming that the shift law applies to each particle independently, the relation (4.35) holds for each particle with a pseudo-time (reduced time) which depends on its position. The stress-strain law again has previous form ($G_\alpha(t-\tau)$ replaced by $G_\alpha(\xi-\xi')$ in equation (4.1) and (4.2) where now $\xi=\frac{t}{a}$). It should be noted that $\sigma_{kk}(r,\xi)$ and similarly for $\varepsilon_{kk}(r,\xi)$, means the mapping of the function $\sigma_{kk}(r,t)$ from (r,t) plane into the (r,ξ) plane, and not the same function with ξ replacing t (Morland and Lee, 1960).

4.2.3 Nonconstant Temperature and Moisture States

It is of interest to extend the results just described for dependence of mechanical properties upon constant temperature and moisture states, to model material behavior under nonconstant, nonuniform temperature and moisture states. The reason for considering this extension would be as an application in solving thermo-hydro-viscoelastic boundary value problems. The effects to be studied here are outside the scope of the first order linear theory, and consequently, a coupled thermo-hydro-viscoelastic theory which includes the nonconstant temperature and moisture dependence of mechanical properties is necessarily nonlinear (Christensen, 1971).

Starting with the general nonlinear theory Morland and Lee (1960) arrive at the stress-strain relations for nonconstant temperature and moisture states with two basic modifications. First to allow for the temperature and moisture dependence of the response functions in the presence of a time-dependent temperature and moisture distributions, the definition (4.35) of the reduced time ξ must be generalized consistant with the assumed time-temperature-moisture equivalence. Second, since constitutive law for bulk response governs the dilatational response (or volume change), it is necessary to incorporate the temperature and moisture induced expansion. The generalized relaxation constitutive equations are

$$S_{ij}(r,t) = \int_{-\infty}^{t} G_1(\xi-\xi') \frac{\partial e_{ij}(r,\tau)}{\partial r} \, d\tau \tag{4.41}$$

$$\sigma_{kk}(r,t) = \int_{-\infty}^{t} G_2(\xi-\xi') \frac{\partial}{\partial \tau} [\varepsilon_{kk}(r,\tau) - 3\alpha\Delta T(r,\tau) - 3\beta\Delta M(r,\tau)] d\tau \tag{4.42}$$

where

α = coefficient of thermal expansion, constant

β = coefficient of hydro expansion, constant

$\Delta T(r,\tau)$ = temperature deviation from the base temperature T_o

$\Delta M(r,\tau)$ = moisture deviation from the base moisture M_o

and according to Hammerle (1972)

$$\xi(r,t) = \int_0^t \frac{dt''}{a_T[T(r,t'')]} + \int_0^t \frac{dt''}{a_M[M(r,t'')]} \qquad (4.43)$$

and

$$\xi'(r,\tau) = \int_0^\tau \frac{dt''}{a_T[T(r,t'')]} + \int_0^\tau \frac{dt''}{a_M[M(r,t'')]} \qquad (4.44)$$

Note that α and β were taken to be constant throughout this study. For a thermo-hydrorheologically simple material (a_T and a_M= constant), relation (4.43) reduces to

$$\xi(t) = \frac{t}{a_T} + \frac{t}{a_M} = \frac{t}{a} \qquad (4.45)$$

where

$$a = \frac{a_T a_M}{a_T + a_M}$$

Relation (4.45) is comparable to relation (4.40). Since both t and ξ are involved in equations (4.41) and (4.42), a reduced form for these stress-strain relations involving only ξ is obtained. Relation (4.43) may be inverted with respect to t, so that

$$t = g(r,\xi) \qquad (4.46)$$

Also by (4.43) and (4.46), using only a temperature gradient,

$$\frac{\partial \xi}{\partial t} = \frac{1}{a_T[T(r,t)]} \quad , \quad \frac{\partial t}{\partial \xi} = \left(\frac{\partial \xi}{\partial t}\right)^{-1} \tag{4.47}$$

Suppose F(r,t) is any function of position and time. Then, to avoid ambiguity, we shall consistently adopt the notation

$$F(r,t) = F(r,g(r,\xi)) = \hat{F}(r,\xi) \tag{4.48}$$

Using (4.46), a different stress, strain, temperature, and moisture functions are defined as

$$\varepsilon_{ij}(r,t) = \varepsilon_{ij}(r,g(r,\xi)) = \hat{\varepsilon}_{ij}(r,\xi) \tag{4.49}$$

$$\sigma_{ij}(r,t) = \sigma_{ij}(r,g(r,\xi)) = \hat{\sigma}_{ij}(r,\xi) \tag{4.50}$$

$$T(r,t) = T(r,g(r,\xi)) = \hat{T}(r,\xi) \tag{4.51}$$

and

$$M(r,t) = M(r,g(r,\xi)) = \hat{M}(r,\xi) \tag{4.52}$$

Through the use of (4.49)-(4.52) and taking into account the relations (4.5) and (4.6), (4.41) and (4.42) become

$$\hat{S}_{ij}(r,\xi) = 2\int_0^{\xi} G(\xi-\xi')\frac{\partial \hat{e}_{ij}(r,\xi')}{\partial \xi'}\, d\xi' \tag{4.53}$$

$$\hat{\sigma}_{kk}(r,\xi) = 3\int_0^{\xi} K(\xi-\xi')\frac{\partial}{\partial \xi'}[\hat{\varepsilon}_{kk}(r,\xi')-3\alpha\Delta\hat{T}(r,\xi') -3\beta\Delta\hat{M}(r,\xi')]\,d\xi' \tag{4.54}$$

where strain history before time zero was neglected for simplicity. Relations (4.53) and (4.54) now involve convolution integrals, and because of this, it would seem that the Laplace transform might conveniently be used to solve boundary value problems involving thermo-hydrorheologically simple materials. Performing the Laplace transforms we have

$$\bar{\hat{S}}_{ij}(r,s) = 2s\bar{G}(s)\bar{\hat{e}}_{ij}(r,s) \tag{4.55a}$$

$$\bar{\hat{\sigma}}_{kk}(r,s) = 3s\bar{K}(s)[\bar{\hat{\varepsilon}}_{kk}(r,s)-3\alpha\Delta\bar{\hat{T}}(r,s)-3\beta\Delta\bar{\hat{M}}(r,s)] \tag{4.55b}$$

or more simply

$$\bar{\hat{S}}_{ij} = 2s\bar{G}\bar{\hat{e}}_{ij} \tag{4.56a}$$

$$\bar{\hat{\sigma}}_{kk} = 3s\bar{K}(\bar{\hat{\varepsilon}}_{kk}-3\alpha\Delta\bar{\hat{T}}-3\beta\Delta\bar{\hat{M}}) \tag{4.56b}$$

In general, by incorporating the temperature and moisture effects, constitutive equatoin (4.19) becomes

$$\sigma_{ij} = \int_{o}^{\xi} G_{ijkl}(\xi-\xi')\frac{\partial}{\partial\xi'}[\varepsilon_{kl}(\xi')-\alpha\Delta T_{kl}(\xi')-\beta\Delta M_{kl}(\xi')]d\xi' \tag{4.57}$$

which by using convolution notation, may be written as

$$\sigma_{ij} = G_{ijkl} * (\varepsilon_{kl}-\alpha\Delta T_{kl}-\beta\Delta M_{kl}) \tag{4.58}$$

4.3 Finite Element Formulation in Thermo-Hydro Viscoelasticity

Constitutive relations governing a viscoelastic boundary value problem were presented in the previous sections. These equations are essential for the analysis of the behavior of these materials under different loading conditions.

A finite element method for solving thermo-hydro loaded viscoelastic boundary value problems in now presented. Finite element methods have already been used by several authors in solving these kind of problems. The following derivations are similar to those by Taylor et al., (1970), Heer and Chen (1969) and De Baerdemaeker (1975).

4.3.1 A Variational Theorem

Let V be a functional defined as (Christensen, 1971)

$$V = \int_V [\tfrac{1}{2} G_{ijkl} * \varepsilon_{ij} * \varepsilon_{kl} - G_{ijkl} * \alpha \Delta T_{ij} * \varepsilon_{kl} -$$

$$G_{ijkl} * \beta \Delta M_{ij} * \varepsilon_{kl} - F_i * U_i] dV - \int_{\beta_\sigma} (S_i * U_i) da \quad (4.59)$$

where it is assumed that the displacement boundary conditions are satisfied. V is the total volume of the solid. It can be shown that the first variation vanishes when the equilibrium equations and boundary conditions are satisfied. In other words, the solution of the boundary value problem stated in (4.18), (4.19), (4.22) and (4.23) can be obtained by finding the stationary value of the functional V in (4.59). The finite element method can be used as a numerical technique based on the minimization of this functional. Note that in equation (4.59) ΔT and ΔM are prescribed functions of time and place associated with a solution of the simultaneous heat and mass diffusion boundary value problem for the body.

4.3.2 Radially Symmetric Viscoelastic Solids

In this section the previous results are specialized for a particular class of problems for isotropic solids. Consider a solid sphere subjected to an arbitrary radially symmetric temperature and moisture distribution. The sphere is assumed to be istropic, continuous and homogenous, and let the origin be at the center of the sphere. Because of symmetry, Figure 4.2, using spherical coordinates, the displacements are

$$U_r = U_r(r,t) \quad ; \quad U_\theta = U_\phi = 0 \tag{4.60}$$

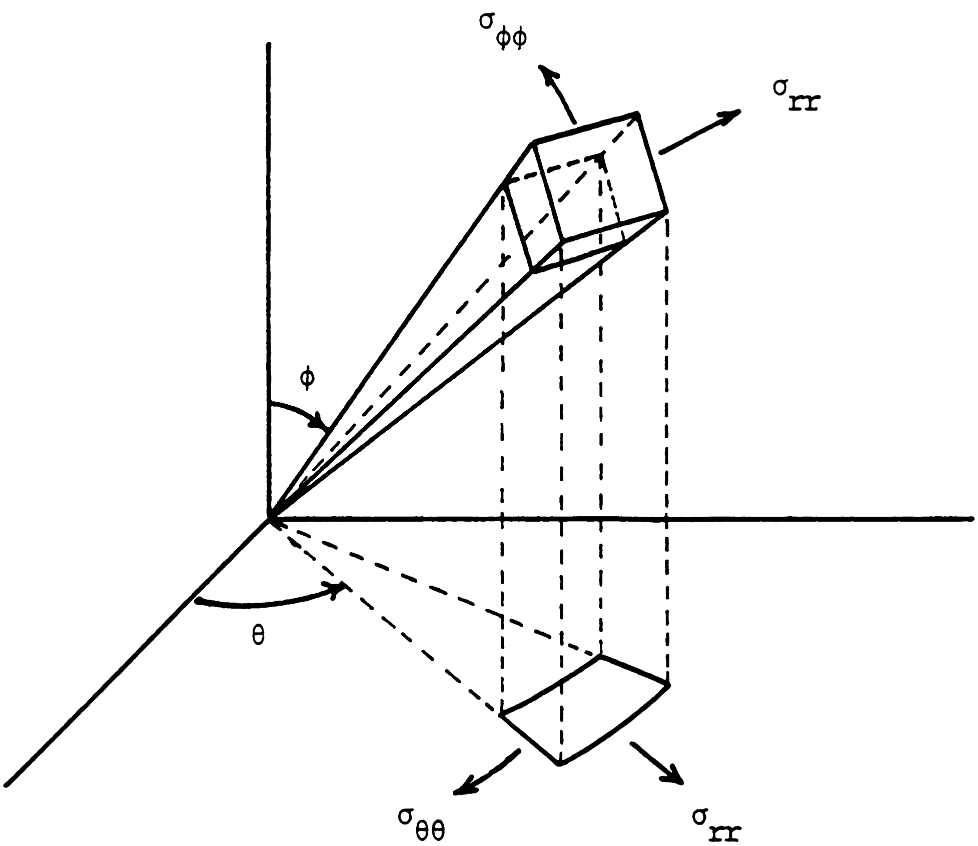

Figure 4.2. Stresses in Radially Symmetric Problems

The strains therefore, are

$$\varepsilon_{rr} = \frac{\partial U_r}{\partial r} \; ; \; \varepsilon_{\theta\theta} = \frac{U_r}{r} = \varepsilon_{\phi\phi} \tag{4.61}$$

$$\varepsilon_{r\theta} = \varepsilon_{\theta\phi} = \varepsilon_{\phi r} = 0 \tag{4.62}$$

The dilatational strain is

$$\varepsilon = \frac{1}{3}(\varepsilon_{rr}+\varepsilon_{\theta\theta}+\varepsilon_{\phi\phi}) \tag{4.63}$$

The deviatoric strains are

$$e_{rr} = \varepsilon_{rr}-\varepsilon = \frac{2r}{3}\frac{\partial}{\partial r}\left(\frac{U_r}{r}\right) \tag{4.64}$$

$$e_{\theta\theta} = e_{\phi\phi} = \frac{-r}{3}\frac{\partial}{\partial r}\left(\frac{U_r}{r}\right) = -\frac{1}{2}e_{rr} \tag{4.65}$$

Again, because of symmetry there will be three non-zero components of the stress tensor, the radial component σ_{rr} and two tangential components $\sigma_{\theta\theta}$ and $\sigma_{\phi\phi}$ such that

$$\sigma_{\theta\theta} = \sigma_{\phi\phi} \tag{4.66}$$

while

$$\sigma_{r\theta} = \sigma_{\theta\phi} = \sigma_{\phi r} = 0 \tag{4.67}$$

Now, decomposing the stress tensor into a uniform normal stress term (spherical or isotropic part) and a pure shear term (deviatoric part), one finds the isotropic stress is

$$\sigma = \frac{1}{3}(\sigma_{rr}+\sigma_{\theta\theta}+\sigma_{\phi\phi}) = \frac{1}{3}(\sigma_{rr}+2\sigma_{\theta\theta}) \tag{4.68}$$

The deviatoric components of the stresses are

$$S_{rr} = \sigma_{rr} - \sigma = \frac{2}{3}(\sigma_{rr}-\sigma_{\theta\theta}) \tag{4.69}$$

$$S_{\theta\theta} = S_{\phi\phi} = -\frac{1}{2}S_{rr} \tag{4.70}$$

and

$$S_{r\theta} = S_{\theta\phi} = S_{\phi r} = 0 \tag{4.71}$$

Combining (4.57) and (4.20) the constitutive equations are

$$\sigma_{rr} = \int_o^{\xi}[\frac{1}{3}(G_2-G_1)\frac{d}{d\xi'}(\varepsilon_{rr}+\varepsilon_{\theta\theta}+\varepsilon_{\phi\phi}) + G_1\frac{d\varepsilon_{rr}}{d\xi'} - G_2\frac{d}{d\xi'}$$

$$(\alpha\Delta T+\beta\Delta M)]d\xi' \tag{4.72}$$

or

$$\sigma_{rr} = \frac{1}{3}[(G_2-G_1)+3G_1]*\varepsilon_{rr}+\frac{1}{3}(G_2-G_1)*(\varepsilon_{\theta\theta}+\varepsilon_{\phi\phi}) - G_2*$$

$$\alpha\Delta T - G_2*\beta\Delta M \tag{4.73}$$

Equation (4.73) can be rewritten as

$$\sigma_{rr} = (K+\frac{4}{3}G)*\varepsilon_{rr}+(K-\frac{2}{3}G)*\varepsilon_{\theta\theta}+(K-\frac{2}{3}G)*\varepsilon_{\phi\phi} -3K*\alpha\Delta T- 3K*\beta\Delta M \quad (4.74)$$

Similar expressions can be derived for the other stress components $\sigma_{\theta\theta}$ and $\sigma_{\phi\phi}$. The expression for the functional (4.59) becomes

$$V = \int_V [\frac{1}{2}A_{ij}*\varepsilon_i*\varepsilon_j-3K*\alpha\Delta T_i*\varepsilon_i-3K*\beta\Delta M_i*\varepsilon_i-F*U]dV - \int_{B_\sigma} (s*U)da \quad (4.75)$$

where

$i,j=1,2,3$

A_{ij} is a 3x3 symmetric array whose components are

$$A_{11}=A_{22}=A_{33}=K+\frac{4}{3}G$$
$$A_{12}=A_{13}=A_{23}=K-\frac{2}{3}G \quad (4.76)$$

4.3.3 Discretization of a Region

A. Nodal Displacements

The volume and surface integrals in (4.75) can be expressed as a sum of integrals over a set of subregions or elements

$$V = \sum_{e=1}^{E} \frac{1}{2} \int_{V^{(e)}} (\varepsilon_i^e * A_{ij} * \varepsilon_j^e) dV - \sum_{e=1}^{E} \int_{V^{(e)}} (\varepsilon_i^e * 3K * \alpha \Delta T_i^e) dV$$

$$- \sum_{e=1}^{E} \int_{V^{(e)}} (\varepsilon_i^e * 3K * \beta \Delta M_i^e) dV - \sum_{e=1}^{E} \int_{V^{(e)}} (U^e * F^e) dV - \sum_{e=1}^{E} \int_{B_\sigma^{(e)}} (U^e * S^e) da \tag{4.77}$$

where the superscript e indicates the element and E is the total number of elements in the body.

The displacement in each element are approximated by algebraic polynomials relating them to displacements of nodal points of that element (Zienkiewicz, 1971) or

$$\{U^e\} = [N^e]\{U\} \tag{4.78}$$

An example of radially symmetric element is given in Figure 4.3, where each line element represents a concentric shell. The shape functions for the one dimensional element, written in terms of the radial coordinate r are (Segerlind, 1976)

$$N_i = \frac{r_j - r}{r_j - r_i} \quad , \quad N_j = \frac{r - r_i}{r_j - r_i} \tag{4.79}$$

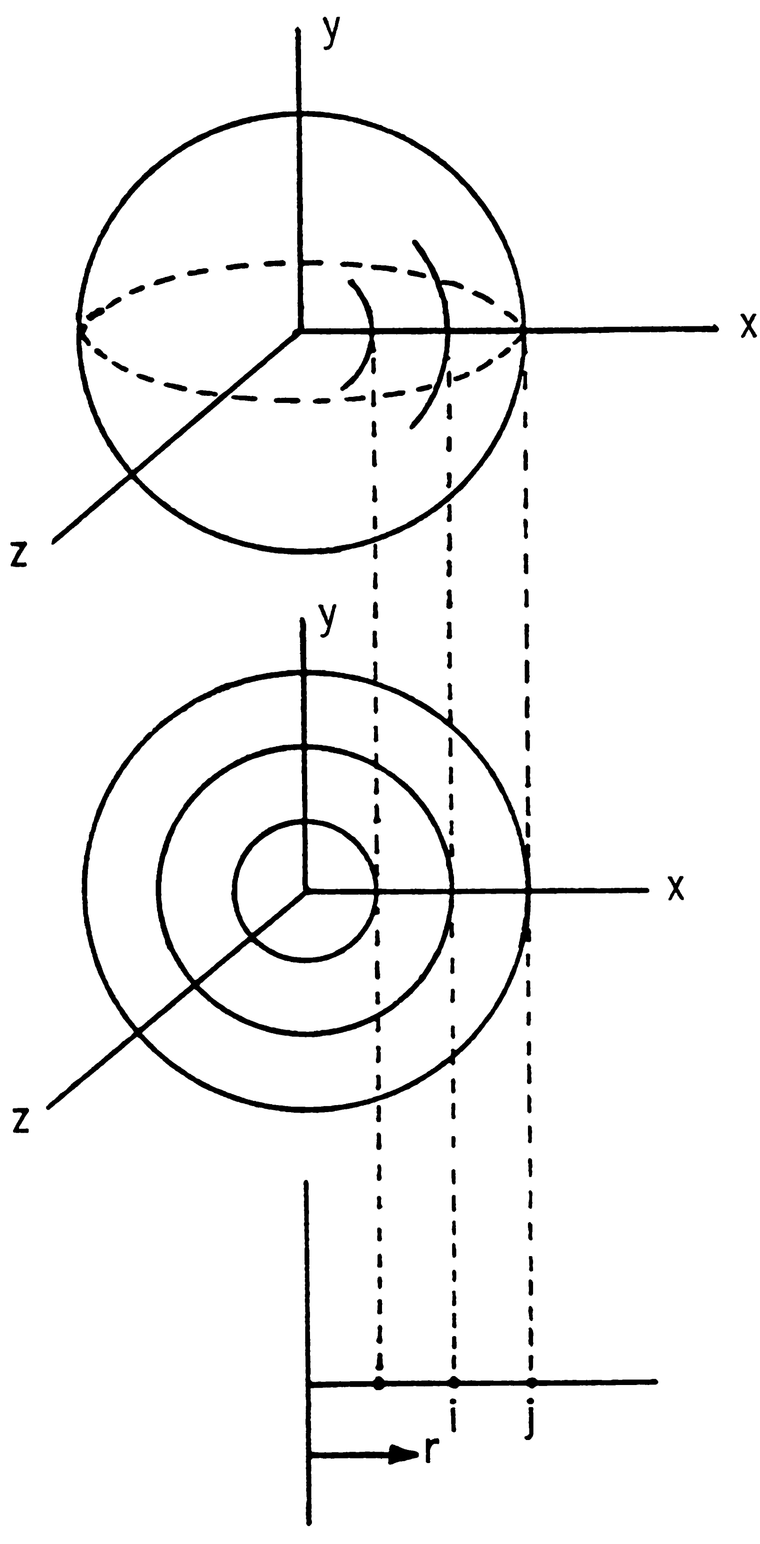

Figure 4.3. Radially Symmetric Line Elements and Corresponding Concentric Shells

The strain vector is obtained by appropriate space differentiation of (4.78)

$$\{\varepsilon^e\} = \begin{bmatrix} \frac{\partial N_i}{\partial r} & \frac{\partial N_j}{\partial r} \\ \frac{N_i}{r} & \frac{N_j}{r} \\ \frac{N_i}{r} & \frac{N_j}{r} \end{bmatrix} \begin{Bmatrix} U_i \\ U_j \end{Bmatrix} = \begin{bmatrix} -\frac{1}{L} & -\frac{1}{L} \\ \frac{N_i}{r} & \frac{N_j}{r} \\ \frac{N_i}{r} & \frac{N_j}{r} \end{bmatrix} \begin{Bmatrix} U_i \\ U_j \end{Bmatrix} = [\bar{B}^e]\{U\} \tag{4.80}$$

where $L=r_j-r_i$ is the length between nodes i and j of the line element. The evaluation of the $[\bar{B}]$ matrix is no longer a simple procedure since $[\bar{B}]$ matrix contains terms that are functions of the coordinate r. One procedure to evaluate the $[\bar{B}]$ matrix is by using the r values at the center of the element.

Also note that in (4.77) terms ΔT and ΔM are

$$\Delta T = [T(r,t)-T(r,o)] = [T(r,t)-T_o] = \{\theta\}$$

and (4.81)

$$\Delta M = [M(r,t)-M(r,o)] = [M(r,t)-M_o] = \{m\}$$

So $\{\theta\}$ and $\{m\}$ are prescribed functions of place and time associated with a solution of the simultaneous heat and mass diffusion boundary value problem for the body, which are already obtained from Chapter 3. Recalling (3.17) and (3.18), we may write

$$\{\Theta^e\} = N_i\Theta_i + N_j\Theta_j = [N^e]\{\Theta\}$$
$$\{m^e\} = N_i m_i + N_j m_j = [N^e]\{m\} \tag{4.82}$$

where the matrix of shape functions $[N^e]$, relates temperatures and moistures in the element to the nodal temperature and moisture values.

Substitution of (4.78), (4.80), (4.81) and (4.82) into (4.77) and the use of matrix notation instead of indicial notation and also taking $\{I\}^T = [1\ 1\ 1]$, yields

$$V = \sum_{e=1}^{E} \frac{1}{2} \int_v (\{U\}^T[\bar{B}]^T * [A] * [\bar{B}]\{U\})dV - \sum_{e=1}^{E} \int_v (\{U\}^T[\bar{B}]^T *$$
$$3K*\alpha\{I\}[N]\{\theta\})dV - \sum_{e=1}^{E} \int_v (\{U\}^T[\bar{B}]^T * 3K*\beta\{I\}[N]\{m\})dV$$
$$- \sum_{e=1}^{E} \int_v (\{U\}^T[N]^T * \{F\})dV - \sum_{e=1}^{E} \int_{B_\sigma} (\{U\}^T[N]^T * \{S\})da \tag{4.83}$$

where the element superscripts are deleted for simplicity. The order of integration can be changed. The integration over space is performed first, then the convolution. Hence,

$$V = \sum_{e=1}^{E} \frac{1}{2}\{U\}^T * [\int_v [\bar{B}]^T [A] [\bar{B}] dV] * \{U\} - \sum_{e=1}^{E} \{U\}^T * [3\alpha \int_v K [\bar{B}]^T \{I\} [N] \{\Theta\} dV] - \sum_{e=1}^{E} \{U\}^T * [3\beta \int_v K [\bar{B}]^T \{I\} [N] \{m\} dV] \tag{4.84}$$

where the last two integerals were dropped since it is our assumption that the body is only under thermal and hydro loads and there are no body and external forces involved. This functional can be written in a simpler form as

$$V = \frac{1}{2}\{U\}^T * [K] * \{U\} - \{U\}^T * \{R\} \tag{4.85}$$

where the stiffness matrix [K], is

$$[K] = \sum_{e=1}^{E} [K^e] = \sum_{e=1}^{E} \int_{v^e} [\bar{B}^e]^T [A] [\bar{B}^e] dV \tag{4.86}$$

and the force vector is

$$\{R\} = \sum_{e=1}^{E} \{r^e\} = \sum_{e=1}^{E} (3\alpha \int_{v^e} K [\bar{B}^e]^T \{I\} [N^e] \{\Theta\} dV + 3\beta \int_{v^e} K [\bar{B}^e]^T \{I\} [N^e] \{m\} dV) \tag{4.87}$$

It should be noted that the displacement vector {U} now contains all the nodal displacements of a region and {R}

is the vector of the nodal thermo and hydro forces.

Taking the first variation of (4.85) and setting it equal to zero yields

$$\delta V = \delta\{U\}^T * [K] * \{U\} - \delta\{U\}^T * \{R\} = 0$$

or

$$[K]*\{U\} - \{R\} = 0 \tag{4.88}$$

Equation (4.88) is very similar to the finite element equations of elasticity. However, the explicit form of (4.88) contains a time integral

$$\int_{\tau=0}^{t} [K(\xi-\xi')]d\{U(\tau)\} = \{R(t)\} \tag{4.89}$$

where, K is an assemblage of element stiffness relaxation functions for the body, and R is an assemblage of thermo-hydro loads. The solution of equation (4.89) yields the nodal point displacements. The strains and stresses can then be computed from equations (4.61) and (4.74).

The integral equations in (4.89) can be solved numerically by the use of time increments (Gupta and Heer, 1974). Rewriting the integral in (4.89) as a summation over time steps, results in

$$\sum_{m=1}^{n} [K(\xi_n-\xi_m)\{\Delta U(t_m)\} = \{R(t_n)\} \tag{4.90}$$

where $\{\Delta U(t_m)\}$ is a vector of displacement increments from time t_m to t_{m+1}, approximated as a displacement at the beginning of the time increment.

The last displacement increment can now be found from the previous displacement increments and a possible initial step displacement $\{U_o\}$ at time t=0. This is done by rearranging the terms in the summation in (4.90)

$$[K(\xi_n-\xi_m)]\{\Delta U(t_n)\} = \{R(t_n)\} - \sum_{m=1}^{n-1} [K(\xi_n-\xi_m)]\{\Delta U(t_m)\} - [K(\xi_n)]\{U_o\} \tag{4.91}$$

Therefore the equation for the first few time steps are

$$[K(o)]\{U_o\} = \{R(t_o)\}$$

$$[K(o)]\{\Delta U(t_1)\} = \{R(t_1)\} - [K(\xi_1)]\{U_o\} \tag{4.92}$$

$$[K(o)]\{\Delta U(t_2)\} = \{R(t_2)\} - [K(\xi_1)]\{\Delta U(t_1)\} - [K(\xi_2)]\{U_o\}$$

A disadvantage of this method is that the number of terms on the right-hand side in (4.92) increases with an increasing number of time steps. If the stiffness matrix for each time interval is stored, an enormous amount of computer storage space is required. An alternate method is to rebuild these stiffness matrices each time they are used. This procedure, however, rapidly increases the required computer time, and, therefore, the cost. The latter method was used in the computer programs written for the study of stresses in viscoelastic materials with constnat temperature (De Baerdemaeker, 1975). The same method with some modification in the computer program to incorporate the temperature and moisture effects on the force vector R, was used in this study. Another approach is the use of logarithmic time increments which can be organized such that only one stiffness matrix has to be stored at each moment (Gupta, 1974). Using Zak's method, White (1968) arrived at a relation where only the immediate past two solutions were required to be saved to account for memory effect. More simplifications could be made in the case of exponential series representation of relaxation functions (Taylor et al., 1970; Heer and Chen, 1969).

B. Element Stresses

In order to derive the stresses in each element, first by combining (4.74), (4.76), and (4.81), we may write

$$\{\sigma^e\} = [A]*\{\varepsilon^e\} - 3K*\{\alpha\theta^e\} - 3K*\{\beta m^e\} \tag{4.93}$$

Substitution of (4.80) yields

$$\{\sigma^e\} = [A]*[\bar{B}^e]\{U^e\} - 3K*\{\alpha\theta^e\} - 3K*\{\beta m^e\}$$

or

$$\{\sigma^e\} = [A][\bar{B}^e]*\{U^e\} - 3K*\{\alpha\theta^e\} - 3K*\{\beta m^e\} \qquad (4.94)$$

Writing (4.94) as a convolution integral and dropping the superscript notation gives

$$\{\sigma(t)\} = \int_0^t [A(\xi-\xi')][\bar{B}]d\{U(\tau)\} - 3\alpha\int_0^t K(\xi-\xi')\{\theta(\tau)\}$$

$$-3\beta \int_0^t K(\xi-\xi')\{m(\tau)\} \qquad (4.95)$$

Replaceing the integral by a summation over discrete time steps yields the stress as a function of the temperature, moisture and displacement increments

$$\{\sigma(t_n)\} = [A(\xi_n)][\bar{B}]\{U_o\} + \sum_{m=1}^{n} [A(\xi_n-\xi_m)][\bar{B}]\{\Delta U(t_m)\}$$

$$-3\alpha \sum_{m=1}^{n} [K(\xi_n-\xi_m)]\{\theta(t_n)\} - 3\beta \sum_{m=1}^{n} [K(\xi_n-\xi_m)]\{m(t_n)\} \qquad (4.96)$$

Note that the calculation performed in (4.96) has to be repeated for each element. Maximum shear stress for every element at every time step was also calculated from the relation

$$\tau_{max.}(r,t) = \frac{1}{2}|\sigma_{rr}(r,t) - \sigma_{\phi\phi}(r,t)| \qquad (4.97)$$

5. RESULTS AND DISCUSSION

Finite element formulation as it applies to the solution of thermo-hydro viscoelastic boundary value problems was presented in the previous chapter. De Baerdemaeker (1975) modified an existing finite element program for two-dimensional elasticity to accomodate the uniform temperature and moisture viscoelastic problems related to the loading of apples. The modification included a change to axially symmetric triangular elements, allocation of computer storage for the displacement increments calculated during each time step and the recalculation of the force vector on the right hand side of the equation (4.92) after each time step.

For stress analysis of soybean, however, due to some existing difficulties and exceptions, the above mentioned computer progrom had to be modified to accomodate the special case of the soybean model. These difficulties and exceptions were: (1) even though soybean is reported to behave viscoelastically (Saxena, 1972), due to lack of information on most of its material properties such as viscoelastic shear and bulk modulus as they vary with time, the computer program reduces to the one for elastic stress analysis. (2) from the reuslts of chapter 3, since the distribution of moisture and temperature was assumed radially

symmetric with respect to the geometrical center of the soybean model, every radius which extends from origin to the surface is representative of the whole two-dimensional model and so the formulation reduced to the one-dimensional case and this was also incorporated in the computer program. (3) the existing program was also modified to accomodate the effect of varying temperature and moisture on the nodal displacements, resulting force vector and the final outcome of the stresses.

The resulting computer program that was used to analyze the stresses in the soybean model (STRESS) as well as the program to determine the moisture and temperature distributions (SIMHMTR) are listed in Appendix A. The program STRESS has the option of having different material properties for the skin than the kernel itself. The stresses were simulated only for the first four hours of drying since it has been reported by several researchers such as Misra (1977) that most of the cracking occurs during the first few hours of drying. The kernel was assumed to have no initial stress and free expansion and contraction (skrinkage) of the kernel was allowed. Therefore all stresses within the kernel were due only to the temperature and moisture gradients occuring within the kernel.

The values of the material properties of the soybean which were used in analyzing the stresses are tabulated in Table 5.1.

Table 5.1 Rheological properties of the soybean used in stress analysis

Material Property	Value	Dimension
Poisson's Ratio (μ)	.4	-
Elastic Modulus (E)	100	MPa
Skin Elastic Modulus (E_s)	800	MPa
Elastic Bulk Modulus (K)	166.7	MPa
Elastic Shear Modulus (G)	35.7	MPa

5.1 Discussion on the Failure Criteria

Because of the unknown nature of cracking process and the small size and cellular structure of the soybean kernel, the conditions under which cracking occurs were studied rather than the mechanics of the cracking itself. Failure is characterized by exceeding a critical state of stress and since the stresses for the soybean model are available, it is necessary to apply the knowledge of the entire stress distribution to prevent the critical state of stress at which failure will occur. Basically there are four types of failure as determined from: normal stresses, shear stresses, energies, and normal strains (Dal Fabbro, 1979) which may exist for uniaxial, biaxial, or triaxial states of stress or strain.

It is reported by Miles and Rehkugler (1973) that shear stress is the most significant failure parameter for apples. Fridley et al. (1968)in conducting compression tests on peaches and pears, found that bruises occured in the area of maximum shear stress. Rao et al. (1975) reported that, although the numerical values of radial and tangential stresses will be greater than the shear stresses, the shear stress failure theory is probably suitable for many biological materials. In the latest study on failure of soybeans, Misra (1977) also assumed the maximum shear stress to be the criteria for failure.

Drying is a very different phenomenon than bruising, and grain materials may fail in tension. Studying the failure in a viscoelastic slab subjected to temperature and moisture gradients, Hammerle (1972) reported that since no shear exists it seemed reasonable to apply a tensile failure criterion instead of a shear criteria. Misra (1977) also reported that most stress cracking is expected at the surface of the soybean where tangential stress is twice that of the maximum shear stress if the soybean is a perfect sphere. Perry (1959) noted in examining the navy beans that the cracks "seemed to radiate from the hilum" creating a common check pattern. He further observed that under end loading conditions of the beans, the two cotyledones tended to separate, subjecting the seed coat to a tensile stress. Ultimately this led to failure of the coat in the form of cracking. Because of greater strength of the seed coat in the hilar region of the beans, the cracks tended to turn away from this region, producing the various check patterns often observed on damaged beans. Doing compression tests on soybeans, Saxena (1972) reported that the orientation of cracks depends on the test position of kernels. Soybeans in their most stable position (long axis horizontal and hilum on the side) did not split into two cotyledons, but the crack started from the surface at the hilum and oriented perpendicularly to the pre-existing failure plane of the specimen.

From the works of Hammerle (1972), Perry (1959), Saxena (1972), Misra (1977), and the results of this study (which will be discussed in the next section) it was concluded that, in the drying processes, tensile stress is the most significant factor to be studied in relation to the failure of grain materials. In this study, tangential stress was assumed to be the criteria for failure during drying of the soybean kernel. Principal stresses for this problem can easily be shown to be

$$
\begin{aligned}
\sigma_{I} &= \sigma_{\phi\phi}(r,t) = \sigma_{f}(t) \\
\sigma_{II} &= \sigma_{\theta\theta}(r,t) = \sigma_{\phi\phi}(r,t) = \sigma_{f}(t) \qquad (5.1) \\
\sigma_{III} &= \sigma_{rr}(r,t)
\end{aligned}
$$

where $\sigma_f(t)$ is the time dependent failure stress.

Because of the temperature and moisture loading conditions, the effects of the time-temperature and time-moisture shift factors must be included modifying equation (5.1) to

$$\sigma_{\phi\phi}(r,t,T,M) = \sigma_f(r,t,a_T(T),a_M(M)) \tag{5.2}$$

5.2 Analysis of the Results

Simulated maximum shear stresses at different radii inside the kernel and at the skin are plotted in Figures 5.1 and 5.2, for the first 4 hours of drying. As we see in Figure 5.1, maximum shear stress is always zero at the center of the kernel and increases as we approach the surface. In comparing Figures 5.1 and 5.2, a sudden jump in the magnitude of the maximum shear stress at the surface is very noticable. This is due to stiffer properties at the skin in compare to the rest of the kernel. At all different radii, maximum shear stress reaches a peak value in about an hour and then decays slowly. With the elastic solid assumption, the dried soybean will always have some stress, as was discussed by Misra (1977). With the viscoelastic assumption, the stresses reach a maximum and then relax slowly, approaching stress free conditions after a long period of time. This type of behavior is typical for a Maxwell model. The

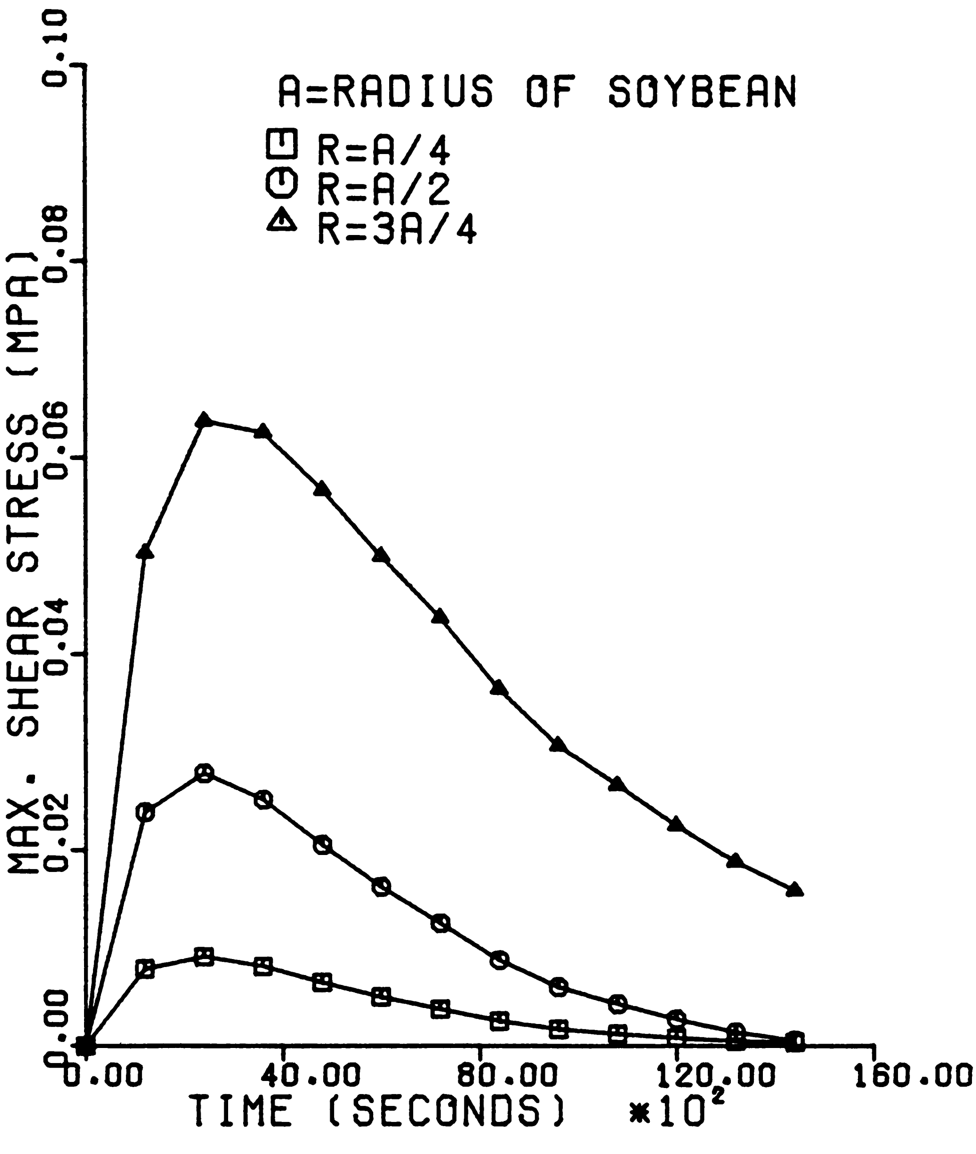

Figure 5.1. Simulated Maximum Shear Stress at Different Radii Inside the Soybean Model

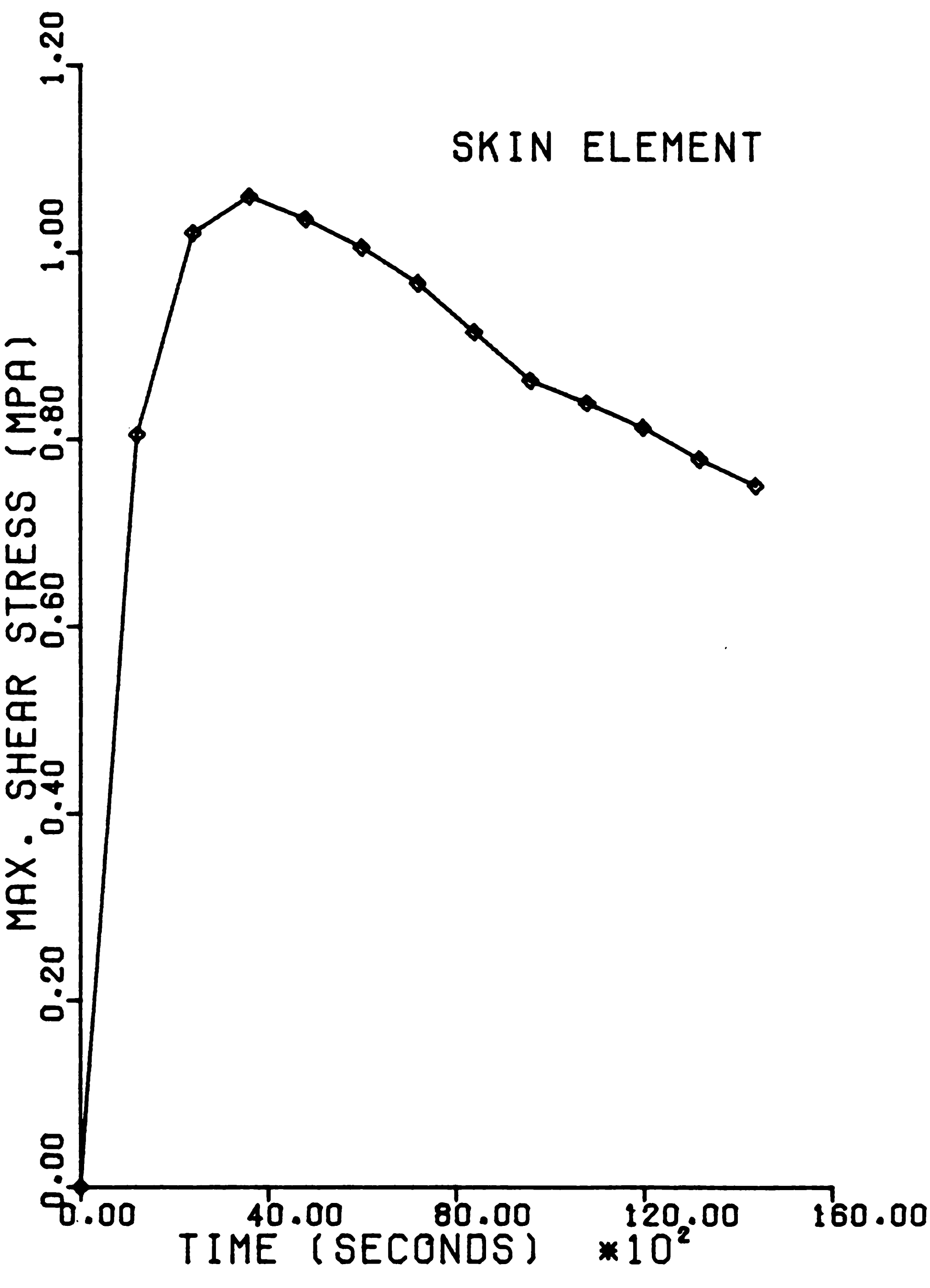

Figure 5.2. Simulated Maximum Shear Stress at the Surface

maximum shear stress in the skin element reached its peak value of 1.06 MPa in one hour.

The simulated radial and tangential stresses along the radius at the time the tangential stress reaches its maximum are plotted in Figure 5.3. The radius of the soybean was divided into 16 elements and all the stresses were evaluated at the center of the elements. It is clear from the figure that radial stress was negative or compressive all along the radius. It reached a maximum at about the mid-radius and approached zero at the skin element. Tangential stress on the other hand, was compressive in the first thirteen interior elements and became tensile between elements 13 and 14 and then experienced a sudden jump at the most outer element. It reached its peak value of 2.056 MPa at the skin element. The change of tangential stress from compressive stress to tensile stress indicates that the 3 outer layers were shrinking faster than the 13 inner layers as expected. The same trend of variation in radial and tangential stresses along the radius of soybean has also been reported by Misra (1977).

Since it was assumed that failure is due to tensile stresses and tangential stress is the only tensile stress which occured in the 3 outer layers of the soybean model, so it became necessary to monitor the variation of the tangential stress as a criteria for failure. Figure 5.4 shows the variation of the simulated tangential stress with time for the skin element where the big jump takes place in the

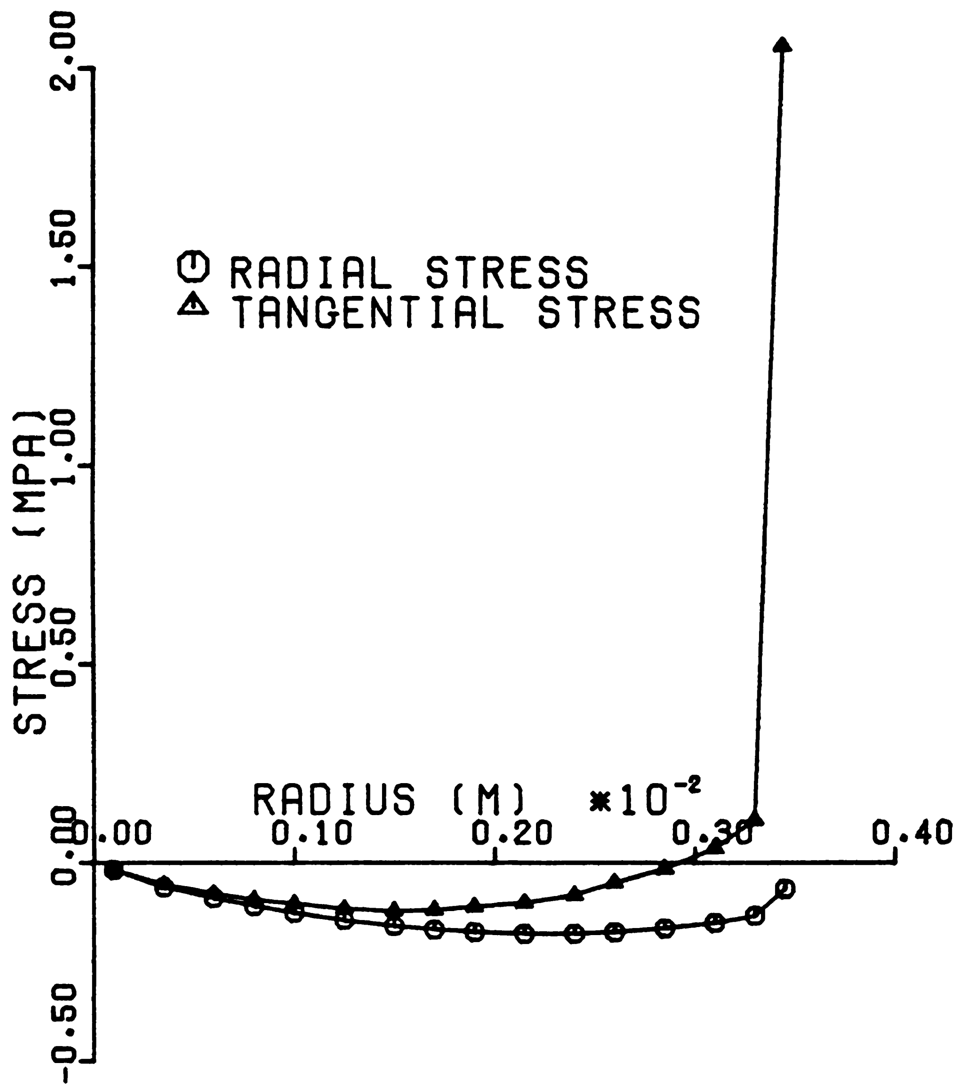

Figure 5.3. Simulated Radial and Tangential Stresses at the Time Tangential Stress Reaches its Maximum (One Hour)

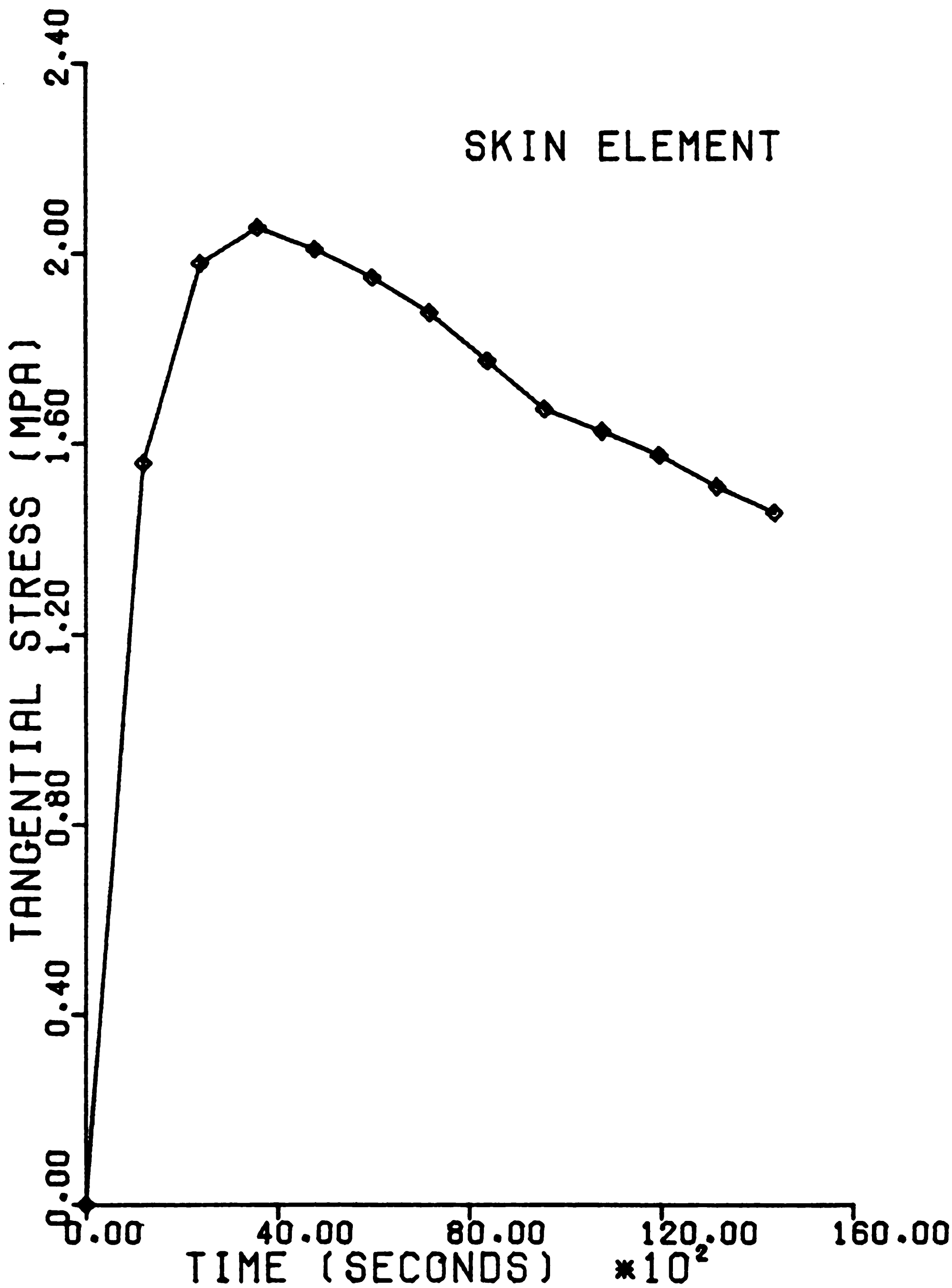

Figure 5.4. Simulated Tangential Stress at the Surface vs. Time

value of $\sigma_{\phi\phi}$. The shape of the curve is very similar to the one for maximum shear stress. Tangential stress is reaching its peak value of 2.056 MPa is one hour and then decays slowly. Again with the viscoelastic assumption, this stress should approach zero after a long period of time in order to make the dried soybean to reach a stress free condition. However, due to a lack of visco-elastic material properties, existing elastic propcrties were used and the solution actually reduced to an elastic one and, therefore, it is expected that the dried soybean will always have some stress.

Drying air temperature, relative humidity of the surrounding air and the equilibrium moisture content of the soybean used in the simulation of the stresses which are plotted in Figures 5.1 through 5.4 were 35°C, 65% (dry basis) and 11% (dry basis) respectively.

The effect of different drying conditions on simulated tangential stress at the surface was also studied and is shown in Figure 5.5. Two observations about the effect of increase in drying air temperature can be made from the model results. First the magnitude of peak tangential stress and the maximum temperature and moisture differnetials across the kernel are both directly proportional to the step increases in temperature. Second, the time to reach the peak tangential stress value is independent of the change in temperature. Gustafson et al. (1977) observed similar effects of temperature in studying the stresses in the corn kernel. It can be observed in Figure 5.5 that

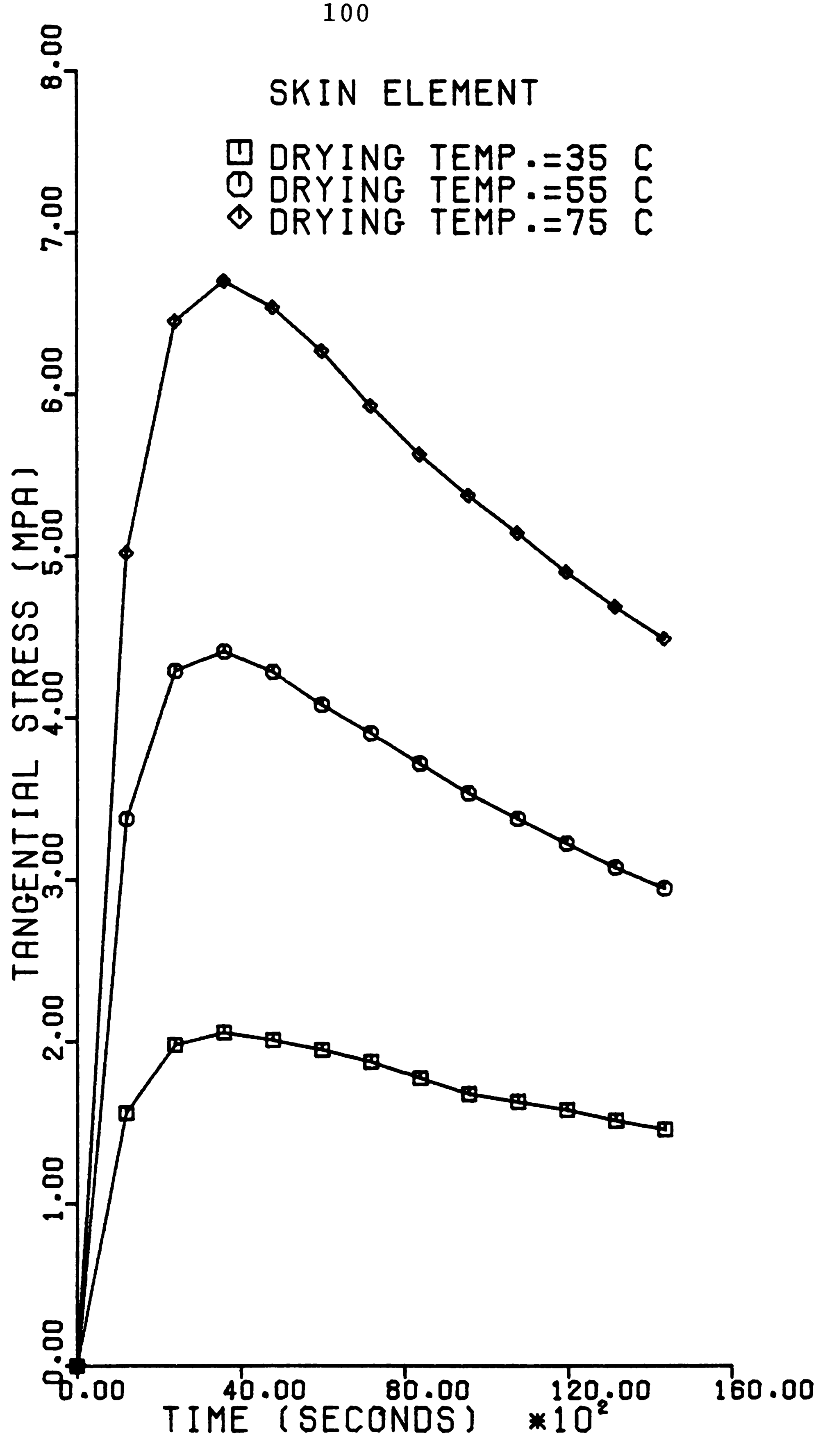

Figure 5.5. Simulated Tangential Stress at the Surface as Affected by Drying Temperature

the slope of the tangential stress curve increases with an increase in temperature. Based on his experimental results, Misra (1977) related this increase in the slope of the stress curve to the higher percentage of cracked soybeans. That is, there was less cracking at lower temperatures.

Soybeans fail (crack) if stresses due to thermal and hydro loading exceed the ultimate strength of the kernel. Even though the ultimate strength of the soybean is not available, for a given value of this property, it is apparent from Figure 5.5 that for higher drying temperatures the material will fail in shorter periods of time, if it fails in tension.

6. SUMMARY AND CONCLUSIONS

A numerical technique for the analysis of the stress crack formation in the soybean kernel resulting from temperature and moisture gradients during the drying process was developed by using finite element method. This technique first solves the simultaneous moisture and heat diffusion equations for the soybean model to obtain the distribution and gradients of moisture and temperature developed inside the kernel during the drying process. Then, the temperature and moisture gradients are used in a thermo-hydro viscoelastic finite element analysis to simulate the stresses in soybeans under thermo-hydro loads.

The following conclusions can be drawn from this study:

(1) The simulated drying curve agrees closely with the experimental results in the literature.

(2) Mass average temperature of the kernel reaches equilibrium in about one hour and then stays constant for the rest of the drying period.

(3) External layers reach the equilibrium moisture content much faster than the internal layers.

(4) Within the assumed model, the distribution of temperature and moisture are symmetric with respect to the center.

(5) The maximum shear stress is always zero at the center and reaches its peak value of 1.06 MPa at the surface in one hour.

(6) Tangential stress reaches its peak value of 2.056 MPa at the surface in one hour and then decays slowly.

(7) Radial stress is negative or compressive throughout the kernel and approaches zero at the surface after reaching its maximum value at about mid-radius.

(8) Tangential stress changes from compressive to tensile stress as it approaches the surface which means the outer layers are shrinking faster than the inner layers.

(9) The magnitude of peak tangential stress and the maximum temperature and moisture differentials across the kernel are directly proportional to the step increases in temperature.

(10) The time to reach the peak tangential stress value is independent of the change in temperature.

(11) For a given ultimate strength of the soybean, the material will fail in shorter periods of time for higher drying temperature if it fails in tension.

7. SUGGESTIONS FOR FUTURE RESEARCH

A specific recommendation for crack free drying can not be made from the results of this study. This was primarily due the lack of information on most of the material properties of the soybean kernel. In general this dissertation was able to introduce a new concept for attacking the stress cracking problem in grain drying. This study formulated the development of temperature and moisture gradients and the state of stress arising from them. With the required material properties in hand, some specific temperature and relative humidity guidelines could have been developed for crack free drying. This research has built a sound theoretical basis for such a study. Some of the important areas and material parameters related to stress cracking of the soybean which must be investigated are as follows:

(1) The dependence of parameters such as c, ρ, K' and D on temperature and moisture content was discussed in chapter two. In the drying process, any specific time corresponds to some specific levels of moisture content and temperature inside the kernel. For a finite element analysis of coupled heat and mass diffusion, the values of these parameters are needed at some specific increments of time. Therefore these

parameters should be represented either as functions of local temperature and moisture content or time. Amoung these parameters, the diffusion coefficient (D) needs additional study because this investigation showed that D is the most dominant factor in the diffusion process.

(2) Additional study is needed to determine whether a significant amount of moisture diffuses through the hilum region of the seed coat. This will help to improve the model and may eventually result in a nonsymmetric distribution of moisture within the kernel.

(3) Due to lack of information on viscoelastic properties of soybean, stress solutions were reduced to the one for elastic analysis. Two specific properties of soybean that are needed to obtain viscoelastic solutions are viscoelastic shear and bulk moduli.

Similar to the well-known relationships between the various moduli for isotropic elastic materials, there exist corresponding relationships between the various moduli for isotropic linear viscoelastic materials. That is to say, if any two of the seven characteristic functions of isotropic materials (Heer and Chen, 1969) are known from experiment, the others can be determined analytically. The interrelationships among four primary mechanical properties, bulk modulus (K), extension or tensile modulus (E), shear modulus (G) and Poisson's ratio (μ) are given by (Muki and

Sternberg, 1961)

$$E(t) = \frac{9G(t)K(t)}{3K(t)+G(t)} \quad , \quad K(t) = \frac{E(t)}{3[1-2\mu(t)]}$$

$$\mu(t) = \frac{3K(t)-2G(t)}{2[3K(t)+G(t)]} \quad , \quad G(t) = \frac{E(t)}{2[1+\mu(t)]}$$

Note that in the above relations, if the value for the required property is desired at a specific time, the two properties used in the calculation must be the values at that specified time.

Due to temperature and moisture content dependency of these viscoelastic properties, time-temperature and time-moisture shift factors, a_T and a_M, are needed to relate the behavior of these properties over the range of temperatures and moisture contents which would be encountered during the drying process. This is represented by master curves for different viscoelastic properties and its concept was discussed in chapter four.

For soybean, the parameters a_T and a_M are available (Herum, et al. 1973) but no attempt has been made for the determination of the four primary properties (E, μ, G and K). Saxena (1972) determined a "modified uniaxial compression modulus" (compressive force divided by constant deformation, kg/cm) for soybeans and presented the master curve for this "property", which has no use in this study.

It is clear that experimental determination of any two of the four primary properties is very essential for a successful study of this kind. With required properties in hand, their master curves could be obtained by using a_T and a_M. From these curves, specific values of the viscoelastic shear and bulk moduli corresponding to specific time increments could be calculated and used in the finite element analysis and the computer program STRESS to give the resulting state of stress.

(4) Because of a different cellular structure, soybean skin has different material properties than the cotyledons. The soybean model and the computer programs SIMHMTR and STRESS used in this study have the option of incorporating this factor, but again due to lack of information on the properties of skin, the same material properties were used as for cotyledons. More research is needed to evaluate the material parameters for the skin and this will help to improve the soybean model.

(5) Determination of the ultimate tensile strength of the seed coat is another subject for further research. Using elastic thin ring theory Hoki (1973) calculated the ultimate tensile strength of the navy bean's seed coat. The same method is applicable to soybeans, if the viscoelastic behavior of the skin is considered.

(6) The effect of initial moisture content, air flow rate and the relative humidity of the drying air on the drying process and the formation of cracks must be studied and incorporated in the model. Two recent studies by Ting et al. (1978) and White et al. (1978) indicated that drying damage is highly dependent on initial moisture content, relative humidity and air flow rate.

LIST OF REFERENCES

LIST OF REFERENCES

Alam, A., and G.C. Shove
1972 Hygroscopicity and thermal properties of soybeans. ASAE paper 72-320, St. Joseph, Michigan.

Alam, A., and G.C. Shove
1972 Conditioning soybeans - A review. ASAE paper 72-321, St. Joseph, Michigan.

Arora, V.K., S.M. Henderson and T.H. Burkhardt
1973 Rice drying and cracking versus thermal and mechanical properties. Tans. of the ASAE, 16(2):320-323.

Bacchus, N.N.
1971 Mechanical properties of soybeans. Unpublished M.S. thesis. Univerisity of Guelph, Ontario, Canada.

Becker, H.A. and H.R. Sallans
1955 A study of internal moisture movement in the drying of the wheat kernel. Cereal chemistry, 32(3):212-226.

Bellinger, P.L. ed.
1964 Thermal properties of grains. Agricultural Engineering Yearbook, American Society of Agricultural Engineers, St. Joseph, Michigan.

Bland, D.R.
1960 The theory of linear viscoelasticity. Pergamon Press, Oxford, England.

Brocci, R.A.
1969 Analysis of axisymmetric linear heat conduction problems by finite element method. An ASME paper presented for the winter meeting of ASME, November 20, 1969, L.A., California.

Byg, D.M. and W.H. Johnson
1970 Reducing soybean harvest losses. Ohio Report 55(1):17-18.

Chen, C.S. and W.H. Johnson
1969 Kinetics of moisture movement in hygroscopic material (I. Theoretical considerations of drying phenomena). Transactions of the ASAE, 12(1):109-113.

Chirife, J.
1971 Diffusional process in the drying of tapioca root. Journal of Food science, 36(2):327-330.

Chittenden, D.H. and A. Hustrulid
1966 Determining drying constants for shelled corn. Transactions of the ASAE, 9(1):52-55.

Chizhikov, A.
1960 The effect of drying conditions on the strength of maize kernels. Elevat. Prom., 26(9):15-16.

Christensen, R.M.
1971 Theory of viscoelasticity. An introduction. Academic Press, New York and London.

Crank, J.
1964 The mathematics of diffusion. Oxford University Press, New York, N.Y.

Dal Fabbro, I.M.
1979 Strain failure of apple material. Unpublished Ph.D. thesis, Michigan State University, East Lansing, Michigan.

De Baerdemaeker, J.G.
1975 Experimental and numerical techniques related to the stress analysis of apples under static loads. Unpublished Ph.D. thesis, Michigan State University, East Lansing, Michigan.

Ekstrom, G.A.
1965 Coefficient of cubical thermal expansion and some tensile properties of corn kernels and their relationship to stress crack formation. Ph.D. thesis, Purdue University Library.

Ekstrom, G.A., J.B. Liljedahl and R.M. Peart
1966 Thermal expansion and tensile properties of corn kernels and their relationship to cracking during drying. Transactions of the ASAE, 9(4):556-561.

Esau, K.
1960 Anatomy of seed plants. John Wiley, New York, New York.

Ferry, J.D.
1961 Viscoelastic properties of polymers. John Wiley and Sons, Inc., New York, New York.

Flügge, W.
1975 Viscoelasticity. Second editon, Springer - Verlag Publishing Co., Berlin/Heidelberg/ New York.

Fridley, R.B., R.A. Bradley, J.A. Rumsey and R.A. Adrian.
1968 Some aspects of elastic behavior of peaches and pears. Transactions of the ASAE, 11(46): 46-49.

Goncharova, Z.
1962 Investigation into the effect of hydrothermal treatment of grain on the changes in its structural and mechanical properties. Mukrom. Elevat. Prom., 28(9):8-10.

Gradowczyk, M.H. and F. Moavenzadeh
1969 Characterization of linear viscoelastic materials. Transaction of the Society of Rheology, 13(2):173-191.

Grosh, G.M. and M. Milner
1959 Water penetration and internal cracking in tempered wheat grains. Cereal Chemistry, 36:1-7.

Gupta, K.K. and E. Heer
1974 Viscoelastic structures. In structural mechanics computer programs. Edited by W. Pilkey, K. Saczalski and H. Schaeffer. University Press of Virginia, Charlotteville, Virginia.

Gustafson, R.J., D.R. Thompson and S. Sokhansanj
1977 Temperature and stress analysis of corn kernel - Finite element analysis. ASAE paper No. 77-5517 American Society of Agricultural Engineers, St. Joseph, Michigan.

Hall, C.W.
1961 Drying farm crops. Chapter 49, Agriculture Engineering Handbook, edited by C.B. Richey, McGraw Hill Book Co., Inc. New York, New York.

Hammerle, J.R.
1968 Failure in a thin viscoelastic slab subjected to temperature and moisture gradients. Ph.D. dissertation, Pennsylvania State University. University Microfilms International, Ann Arbor, Michigan.

Hammerle, J.R.
1970 The determination of transient temperature and moisture gradients in a slab. ASAE paper No.70-335, American Society of Agricultural Engineers, St. Joseph, Michigan.

Hammerle, J.R.
1972 Theoretical analysis of failure in a visco-elastic slab subjected to temperature and moisture gradients. Transactions of the ASAE, 5:960-965.

Hammerle, J.R. and N.N. Mohsenin
1970 Tensile relaxation modulus of corn horny endosperm as a function of time, temperature and moisture content. Transactions of the ASAE, 13(3):372-375.

Heer, E. And J.C. Chen
1969 Finite element formulation for linear thermo-viscoelastic material. Technical report 32-1381, Jet Propulsion Laboratory, Pasadina, California.

Henderson, S.M.
1954 The causes and characteristics of rice checking. Rice Journal, 57(5):16-18.

Henderson, S.M. and R.L. Perry
1967 Agricultural process engineering. Second edition. The AVI Publishing Company, Inc. Westport, Connecticut.

Herum, F.L., H.J. Barre, K. Majidzadeh and N.C. Saxena
1973 Viscoelastic behavior of soybeans due to temperature and moisture content. ASAE paper No. 73-319, American Society of Agricultural Engineers, St. Joseph, Michigan.

Hilton, H.H.
1954 Thermal stresses in thick walled cylinders exhibiting temperature dependent viscoelastic properties of the Kelvin type. Proc. of ASME, 2(3):547-553.

Hoki, M.O.
1973 Mechanical strength and damage analysis of navy beans. Ph.D. thesis, Michigan State University, East Lansing, Michigan.

Hustrulid, A. and A.M. Flikke
1959 Theoretical drying curve for shelled corn. Transaction of the ASAE, 2(1):112-114.

Hyde, E.O.C.
1954 The function of the hilum in some Papilionaceae in relation to the ripening of the seed and the permeability of the testa. Annals of Botany, 18:241-256.

Jasansky, A. and W.K. Bilanski
1973 Thermal conductivity of whole and ground soybeans. Transactions of ASAE, 16(1): 100-103.

Kunze, O.R. and C.W. Hall
1965 Relative humidity changes that causes brown rice to crack. Transactions of the ASAE, 8(3):396-399, 405.

Landau, H.G., J.H. Weiner and E.E. Zwicky
1960 Thermal stress in a viscoelastic plastic with temperature dependent yield stress. Journal of Applied Mech., Transactions of ASME, 82(3):297-300.

Leaderman, H.
1943 Elastic creep properties of filamentous materials and the other high polymers. p. 175. Textile foundation, Washington, DC.

Lee, E.H.
1964 Some recent developments in linear visco-elastic stress analysis. Proc. of the 11th International Congress of Applied Mechanics: 396-420.

Mannapperuma, J.D.
1975 Analysis of thermal and moisture stresses caused during drying of brown rice. Unpublished M.S. thesis, Louisiana State University.

Martin, C.R. and L.E. Stephens
1976 Broken cron and dust generated during repeated handling. ASAE paper 76-3026, American Society of Agricultural Engineers, St. Joseph, Michigan.

Miles, J.A., and G.E. Rehkugler
1971 The development of a failure criterion for apple flesh. ASAE paper no. 71-330, American Society of Agricultural Engineers, St. Joseph, Michigan.

Miller, M.K. and W.T. Guy, Jr.
1966 Numerical inversion of the Laplace transform by use of Jacobi Polynomials. SIAM Journal of Numerical Analysis, 3(4):624-635.

Milner, M.
1950 Biological processes in stored soybeans. Chapter 13, Soybeans and Soybean Products, Volume I, edited by K.S. Markley. Interscience Publishers, Inc., New York, New York.

Milner, M. and J.A. Shellenberger.
1953 Physical properties of weathered wheat in relation to internal fissuring detected radiographically. Cereal Chemistry, 30:202-212.

Misra, R.N.
1977 Failure and stress analysis in soybeans subjected to a temperature and moisture gradient. Unpublished Ph.D. thesis. North Carolina State University, Raleigh, North Carolina.

Misra, R.N. and J.H. Young
1978 Finite element analysis of simultaneous moisture diffusion and shrinkage of soybeans during drying. ASAE paper 78-3056, American Society of Agricultural Engineers, St. Joseph, Michigan.

Mohsenin, N.N.
1968 Physical properties of plant and animal materials: parts 1 and 2 of volume 1. The Pennsylvania State University, University Park, Pennsylvania.

Morland, L.W. and E.H. Lee
1960 Stress analysis for linear viscoelastic materials with temperature variation. Transacions of the Society of Rheology, 4:233-249.

Morrow, C.T.
1965 Viscoelasticity in a selected agricultural product. M.S. thesis. The Pennsylvania State University, University Park, Pennsylvania.

Muki, R. and E. Sternberg
1961 On transient thermal stresses in viscoelastic materials with temperature dependent properties. Journal of Applied Mechanics, 6:193-207.

Overhults, D.G., G.M. White, H.E. Hamilton and I.J. Ross
1973 Drying soybeans with heated air. Transactions of the ASAE, 16(1):112-113.

Paulsen, M.R., and G.H. Brusewitz
1976 Coefficient of cubical thermal expansion for spanish peanut kernels and skins. Transaction of ASAE, 19(3):592-600.

Perry, J.S.
1959 Mechanical damage to peabeans as affected by moisture, temperature and impact loading. Unpublished Ph.D. thesis, Michigan State University, East Lansing, Michigan.

Rao, V.N.M.
1971 Failure in a viscoelastic cylinder subjected to temperature and moisture graidents. M.S. thesis, North Carolina State University, Raleigh, North Carolina.

Rao, V.N.M., D.D. Hamann, and J.R. Hammerle
1975 Stress analysis of a viscoelastic sphere subjected to temperature and moisture gradients. Journal of Agricultural Engineering Research, 20:283-293.

Rosen, B.
1964 Fracture processes in polymeric solids. John Wiley and Sons, Inc., New York, New York.

Sabbah, M.A., G.E. Meyer, H.M. Keaner, and W.L. Roller
1976 Reversed-air drying for fixed bed of soybean seed. ASAE paper No. 76-3023, St. Joseph, Michigan.

Sarvacos, G.D. and S.E. Charm
1962 A study of mechanism of fruit and vegetable dehydration. Food Technology, 19:78-84.

Saxena, N.C.
1972 Viscoelastic characterizations of soybean grain under quasistatic loading. Ph.D. dissertation, The Ohio State University, University Microfilms International, Ann Arbor, Michigan.

Schwarzl, F., and A.J. Staverman
1952 Time-temperature dependence of linear viscoelastic behavior. Journal of Applied Physics, 23:858-843.

Segerlind, L.J.
1976 Applied finite element analysis. John Wiley and Sons., Inc., New York, New York.

Sharma, M.B.
1964 Viscoelasticity and mechanical properties of polymers. Summer institute of applied mechanics and material science. Department of Engineering Mech., Pennsylvania State University, University Park, Pennsylvania

Silberstein, D.A. and V.N.M. Rao
1976 Mechanical properties of peanuts at various temperatures and relative humidiites. Unpublished paper, Department of Food Science, University of Georgia, Athens, Georgia.

Singh, R., H.J. Barre, and M.Y. Hamdy
1972 Drying spherical porous bodies. Transactions of the ASAE, 15(2):338-341.

Smith, A.K. and S.J. Circle
1976 Soybeans: chemistry and technology. The AVI Publishing Company, Inc., Westport, Connecticut.

Stewart, B.R.
1964 Effect of moisture content and specific weight on the internal friction properties of sorghum grain. ASAE paper N. 64-804, American Society of Agricultural Engineers, St. Joseph, Michigan.

Taylor, R.L., K.S. Pister and G.L. Goudreau
1963 Thermomechanical analysis of viscoelastic solids. Int. Journal for Num. Meths. in Engineering, 2:45-59.

Thompson, R.A. and G.H. Foster
1963 Stress cracks and breakage in artificially dried corn. Market Research Report No. 631, USDA, in Cooperation with Agricultural Experiment Station, Purdue University.

Timbers, G.E.
1964 Some mechanical and rheological properties of Netted Gem. potato. Unpublished M.S. thesis, University of British Columbia.

Timoshenko, S.P. and J.N. Goodier
1970 Theory of elasticity. McGraw-Hill book Company, New York, New York.

Ting , K.C., G.M. White, I.J. Ross and O.J. Loewer
1978 Seed coat damage in deep-bed drying of soybeans. ASAE technical paper No. 78-3006, St. Joseph, Michigan.

Wang, J.K.
1956 Drying pea beans intermittently at 100°F. Unpublished M.S. thesis, Michigan State University, East Lansing, Michigan.

Wang, J.K. and C.W. Hall
1961 Moisture movement in hygroscopic materials. Transactions of the ASAE, 4(1):33-36.

Watts, K.C.
1967 Thermal properties of soybeans. M.S. thesis, University of Guelph, Guelph, Ontario, Canada.

Watts, K.C. and W.K. Bilanski
1970 Calorimetric determination of the specific heat of soybeans. Canadian Agr. Eng. 12(1):45-47.

Watts, K.C. and W.K. Bilanski
1973 Method for estimating the thermal diffusivity of whole soybeans. Transactions of ASAE, 16(6):1143-1145.

Whitaker, T.B., H.J. Barre and M.Y. Hamdy.
1969 Theoretical and experimental studies of diffusion in spherical bodies with a variable diffusion coefficient. Transactions of the ASAE, 12(5):668-672.

Whitaker, T.B. and J.H. Young
1972 Simulation of moisture movement in peanut kernels: Evaluation of diffusion equation. Transactions of the ASAE, 15(1):163-166.

White, G.M., T.C. Bridges, O.J. Loewer and I.J. Ross
1978 Seed coat damage in thin-layer drying of soybeans as affected by drying conditions. ASAE Technical paper No. 78-3052, St. Joseph, Michigan.

White, J.L.
1968 Finite element in linear viscoelasticity. Proceedings of the second conference in Matrix Methods in Structural Mechanics, AFFDL-TR-68-150:489-516.

Whitney, J.D. and J.G. Porterfield
1968 Moisture movement in porous, hygroscopic solid. Transactions of the ASAE, 11(5): 716-719.

Wilson, H.K.
1955 Grain crops. McGraw-Hill Book Company, New York, New York.

Young, J.H.
1969 Simultaneous heat and mass transfer in a porous, hygroscopic solid. Transactions of the ASAE 12(5):720-725.

Young, J.H. and T.B. Whitaker
1971 Evaluation of the diffusion equation for describing thin-layer drying of peanuts in the hull. Transactions of the ASAE, 14(2):309-312.

Zienkiewicz
1971 The finite element method in engineering science. McGraw-Hill, London.

Zoerb, G.C.
1958 Mechanical and rheological properties of grain. Ph.D. thesis, Michigan State University, East Lansing, Michgian.

Zoerb, G.C. and C.W. Hall
1960 Some mechanical and rheological properties of grains. Journal of Agri. Eng. Research 5(1):83-93.

APPENDIX A

COMPUTER PROGRAMS SIMHMTR AND STRESS

```
      PROGRAM SIMHMTR(INPUT,OUTPUT,TAPE60=INPUT,TAPE61=OUTPUT,
     1TAPE1,TAPE2,TAPE3,TAPE4=512,TAPE5=512,TAPE14)
      DIMENSION ISIDE(2),ESM(3,3),ECM(3,3)
      DIMENSION NS(3),R(3),Z(3),B(3),C(3),EF(3)
      DIMENSION BK(2900),F2(160),XMN(160),W(160)
      DIMENSION PI(160),QI(160)
      DIMENSION RI(160,24),SRI(160,24)
      COMMON/TLE/TITLE(20)
      COMMON A(1)
      REAL KR1,KR2,D,LG,LRHO,CRHO,MINF,MOISTMA,TEMPMA
      DATA IN/60/,IO/61/,NCL/1/,QG/0.0/
C   DEFINITION OF THE CONTROL PARAMETERS
C     NP-NUMBER OF GLOBAL TEMPERATURES OR MOISTURES, NE-NUMBER OF
C     ELEMENTS,KR1-CONDUCTIVITY WITHIN KERNEL,KR2-CONDUCTIVITY OF SKIN
C     D-MOISTURE DIFFUSIVITY
C
C   INPUT OF THE TITLE CARD AND THE CONTROL PARAMETERS
C
      REWIND 1
      REWIND 2
      REWIND 3
      NNN=0
      READ(IN,3) TITLE
    3 FORMAT(20A4)
  101 CONTINUE
      READ(IN,2) NP,NE,NBW,NIT,IWTR,DT,H,HM,TINF,MINF
    2 FORMAT(5I3,5F10.4)
      READ(IN,22) KR1,KR2,D,LRHO,CRHO,QG
   22 FORMAT(2F10.4,3E10.4,F10.4)
C
C   OUTPUT OF TITLE AND DATA HEADINGS
C
      WRITE(IO,4) TITLE,KR1,KR2,D,LRHO,CRHO,QG
    4 FORMAT(1H1////1X,20A4//1X,6HKR1   =,F10.4/1X,6HKR2   =,F10.4/1X,
     16HD     =,E12.4/1X,6HLRHO =,E12.4/1X,6HCRHO =,E12.4/1X,6HQG    =,
     1F10.4//1X85HNEL    NODE NUMBERS       R(1)          Z(1)          R(2)
     1          Z(2)          R(3)          Z(3)    )
C
C   CALCULATION OF THE POINTERS AND INITIALIZATION OF THE COLUMN VECTOR A( )
C
      JGF=NP*NCL
      JGCM=JGF+2*NP*NCL
      JGHM=JGCM+NP*NBW
      JEND=JGHM+NP*NBW
      CALL SETFL(A(JEND))
      DO13I=1,JEND
   13 A(I)=0.0
      DO70I=1,2900
   70 BK(I)=0.0
C*********
C   ASSEMBLYING OF THE GLOBAL STIFFNESS MATRIX AND GLOBAL FORCE MATRIX
C*********
C
C   INPUT AND ECHO PRINT OF ELEMENT DATA
C
      DO 7 NN=1,NE
      READ(IN,1) NEL,NS,ID,R(1),Z(1),R(2),Z(2),R(3),Z(3)
      R(1)=R(1)*.01 $ R(2)=R(2)*.01 $ R(3)=R(3)*.01
      Z(1)=Z(1)*.01 $ Z(2)=Z(2)*.01 $ Z(3)=Z(3)*.01
    1 FORMAT(5I3,6F10.4)
      WRITE(3,1) NEL,NS,ID,R(1),Z(1),R(2),Z(2),R(3),Z(3)
      WRITE(IO,23) NEL,NS,R(1),Z(1),R(2),Z(2),R(3),Z(3)
   23 FORMAT(1X,I3,2X,3I4,3X,6(2X,F8.4))
C
C   CALCULATION OF THE ELEMENT MATRICES
C
   21 RBAR=(R(1)+R(2)+R(3))/3.
      B(1)=Z(2)-Z(3)
      B(2)=Z(3)-Z(1)
      B(3)=Z(1)-Z(2)
      C(1)=R(3)-R(2)
      C(2)=R(1)-R(3)
      C(3)=R(2)-R(1)
      AREA2=R(2)*Z(3)+R(3)*Z(1)+R(1)*Z(2)-R(2)*Z(1)-R(3)*Z(2)-R(1)*Z(3)
      AR=RBAR/(2.*AREA2)
      DO5I=1,3
      EF(I)=QG*AREA2*(R(I)+3.*RBAR)/24.0
      DO5J=1,3
      IF(NNN.EQ.0) KR1=D
      IF(ID.EQ.1.OR.ID.EQ.3) KR2=KR1
      ESM(I,J)=(KR1*B(I)*B(J)+KR1*C(I)*C(J))*AR
```

```
      DEL=0.0
      IF(I.EQ.J) DEL=1.0
      IF(NNN.EQ.0) CRHO=1.0
    5 ECM(I,J)=AREA2*CRHO*DEL*(15.*RBAR+5.*R(I))/120.0
C
C     CALCULATION OF CONVECTION MATRIX
C
      IF(IO.LT.3) GOTO18
      READ(IN,9) NEL,ISIDE
    9 FCRMAT(3I3)
      DO10I=1,2
      IF(ISIDE(I).LE.0) GOTO18
      J=ISIDE(I)
      WRITE(IO,12) J,NEL
   12 FORMAT(5X,20HCONVECTION FROM SIDE,I4,11H OF ELEMENT,I4)
      K=J+1
      IF(J.EQ.3) K=1
      LG=SQRT((R(K)-R(J))**2+(Z(K)-Z(J))**2)
      IF(NNN.EQ.0) H=HM
      IF(NNN.EQ.0) TINF=MINF
      HL=LG*H*TINF/6.0
      EF(J)=EF(J)+(2.*R(J)+R(K))*HL
      EF(K)=EF(K)+(R(J)+2.*R(K))*HL
      HL=LG*H/12.0
      ESM(J,J)=ESM(J,J)+(3.*R(J)+R(K))*HL
      ESM(J,K)=ESM(J,K)+(R(J)+R(K))*HL
      ESM(K,J)=ESM(J,K)
   10 ESM(K,K)=ESM(K,K)+(R(J)+3.*R(K))*HL
C
C  INSERTION OF ELEMENT PROPERTIES INTO THE GLOBAL STIFFNESS MATRIX
C
   18 DO107I=1,3
      II=NS(I)
      J1=JGF+II
      A(J1)=A(J1)+EF(I)
      DO 108 J=1,3
      JJ=NS(J)
      JJ=JJ+1-II
      IF(JJ)109,109,6
    6 J1=JGCM+(JJ-1)*NP+II
      J2=JGHM+(JJ-1)*NP+II
      J3=(JJ-1)*NP+II
      A(J1)=A(J1)+ECM(I,J)+(DT/2.)*ESM(I,J)
      A(J2)=A(J2)+ECM(I,J)-(DT/2.)*ESM(I,J)
      BK(J3)=BK(J3)+ESM(I,J)
  109 CONTINUE
  108 CONTINUE
  107 CONTINUE
    7 CONTINUE
      CALL DCMPBD(A(JGCM+1),NP,NBW)
      J1=JGF+NP*NCL+1
      CALL TRANSNT(A(JGCM+1),A(JGHM+1),A(JGF+1),A(J1),A(1),BK(1),
     1NP,NBW,NCL,F2,XMN,W,DT,NIT,IWTR,NNN,LRHO,PI,QI,RI,SRI)
C*********
C  CALCULATION OF MOISTURE AND TEMPERATURE MASS AVERAGE
C*********
      REWIND 1
      CALL SETFL(A(NP))
      DO 111 J=1,NIT
      READ(1,601) (A(I),I=1,NP)
  601 FCRMAT(8F10.5)
      IF(J/IWTR*IWTR.NE.J)GOTO 111
      SUM1=0.0
      SUM2=0.0
      REWIND 3
      DO 86 KK=1,NE
      SUM=0.0
      READ(3,1) NEL,NS,ID,R(1),Z(1),R(2),Z(2),R(3),Z(3)
      IF(NEL.LE.0)STOP
      DO 87 I=1,3
      II=NS(I)
   87 EF(I)=A(II)
      AREA2=R(2)*Z(3)+R(3)*Z(1)+R(1)*Z(2)-R(2)*Z(1)-R(3)*Z(2)-R(1)*Z(3)
      RBAR=(R(1)+R(2)+R(3))/3.0
      SUM=SUM+(2.*R(1)+R(2)+R(3))*EF(1)+(R(1)+2.*R(2)+R(3))*EF(2) +
     1(R(1)+R(2)+2.*R(3))*EF(3)
      SUM1=SUM1+SUM*AREA2/12.
   86 SUM2=SUM2+AREA2*RBAR
      IF(NNN.EQ.1) GOTO501
      MOISTMA=SUM1/SUM2
      WRITE(IO,88) MOISTMA
```

```
   88 FORMAT (1X,23HMASS AVERAGE MOISTURE =,F10.4)
      GOTO 111
  501 TEMPMA=SUM1/SUM2
      WRITE(IO,98) TEMPMA
   98 FORMAT(1X,26HMASS AVERAGE TEMPERATURE =,F10.4)
  111 CONTINUE
      IF(NNN.EQ.1) STOP
      NNN=1
      GOTO 101
      END
      SUBROUTINE TRANSNT(GCM,GHM,P,TR,XI,BK,NP,NBW,NCL,F2,XMN,W,DT,
     1NIT,IWTR,NNN,LRHO,PI,QI,RI,SRI)
      COMMON/TLE/TITLE(20)
      COMMON A(1)
      DIMENSION GCM(NP,NBW),GHM(NP,NBW),P(NP,1),TR(NP,1),BK(NP,NBW)
      DIMENSION XI(NP,1),IB(25),BDYPHI(160),IPBV(160)
      DIMENSION PI(NP,1),QI(NP,1)
      DIMENSION RI(NP,NIT),SRI(NP,NIT)
      DIMENSION F2(NP,1),XMN(NP),W(NP)
      REAL LRHO
C
      IF(NNN.EQ.1) REWIND 2
      IO=1
      SDT=0.0
C   INPUT OF INITIAL CONDITIONS
C
   17 READ(60,5) (XI(I,1), I=1,NP)
    5 FORMAT(8F10.5)
      WRITE(61,6) TITLE
    6 FORMAT(1H1///1X,18HTRANSIENT ANALYSIS//1X,20A4)
      WRITE(61,7) SDT,(I,XI(I,1),I=1,NP)
    7 FORMAT(//1X,6HTIME =,E11.5/(1X,I3,3X,E17.6,5X,I3,3X,E17.6,5X,I3,3X
     1,E17.6,5X,I3,3X,E17.6))
      LCOUNT=NP/5+4
C
C   INPUTTING OF THE LOCATION OF PRESCRIBED BOUNDARY VALUES
C
      KN=0
   23 READ(60,3) IB
    3 FORMAT(25I3)
      DO18I=1,25
      IF(IB(I).LE.0) GO TO 22
      KN=KN+1
   18 IPBV(KN)=IB(I)
      GOTO23
C
C   SAVING OF PRESCRIBED BOUNDARY VALUES IN BDYPHI
C
   22 IF(KN.EQ.0) GOTO15
      DO14I=1,KN
      J=IPBV(I)
   14 BDYPHI(I)=XI(J,1)
C
C   CALCULATION OF PHI(I+1) FROM PHI(I)
C
   15 SDT=DT
      REWIND 1
      DO13KK=1,NIT
      CALL MULTBD(GHM,XI,TR,NP,NBW,NCL)
      IF(NNN.EQ.0)GOTO120
      READ(2,5) (XMN(I),I=1,NP)
  120 CONTINUE
      DO9I=1,NP
      IF(NNN.EQ.1)GOTO 201
      F2(I,1)=P(I,1)
      TR(I,1)=TR(I,1)+DT*F2(I,1)
      GOTO 9
  201 TR(I,1)=TR(I,1)+DT*(P(I,1)+(LRHO*F2(I,1))-XMN(I))
    9 CONTINUE
      CALL SLVBD(GCM,TR,XI,NP,NBW,NCL,ID)
C
C   RESETTING OF THE PRESCRIBED BOUNDARY VALUES
C
      IF(KN.EQ.0) GOTO21
      DO20I=1,KN
      J=IPBV(I)
   20 XI(J,1)=BDYPHI(I)
C
C   OUTPUT OF THE RESULTS
C
   21 WRITE(1,5) (XI(I,1),I=1,NP)
```

```
      IF(KK/IWTR*IWTR.NE.KK) GOTO16
      WRITE(61,7) SOT,(I,XI(I,1),I=1,NP)
      IF(NNN.EQ.1) GO TO 777
      DO 1001 I=136,NP
 1001 PI(I,1)=(XI(I,1)-.33)*.002657
      WRITE(4)PI
      IF(NNN.EQ.0) GO TO 16
  777 DO 1002 I=136,NP
 1002 QI(I,1)=(XI(I,1)-20.)*.0004
      WRITE(5)QI
   16 LCOUNT=LCOUNT+NP/5+3
   13 SOT=SOT+DT
      IF(NNN.EQ.0) GO TO 1300
C
C   CALCULATION OF THE NODAL FORCES
C   READING NODAL AND ELEMENT FORCES ON TAPE
C
      SOT=DT
      REWIND 5
      REWIND 4
      DO 1500 J=1,NIT
      READ(4)PI
      READ(5)QI
      DO 1400 I=136,NP
 1400 RI(I,J)=PI(I,1)+QI(I,1)
      RI(1,J)=RI(152,J)
      RI(2,J)=RI(150,J)
      RI(3,J)=RI(149,J)
      RI(4,J)=RI(148,J)
      RI(5,J)=RI(147,J)
      RI(6,J)=RI(146,J)
      RI(7,J)=RI(145,J)
      RI(8,J)=RI(144,J)
      RI(9,J)=RI(143,J)
      RI(10,J)=RI(142,J)
      RI(11,J)=RI(141,J)
      RI(12,J)=RI(140,J)
      RI(13,J)=RI(139,J)
      RI(14,J)=RI(138,J)
      RI(15,J)=RI(137,J)
      RI(16,J)=RI(136,J)
      RI(17,J)=RI(151,J)
      WRITE(61,7) SOT,(I,RI(I,J),I=1,17)
      WRITE(14,1100) (RI(I,J),RI((I+1),J),I=1,16)
 1100 FORMAT(2E17.6)
      DO 1450 I=1,16
 1450 SRI(I,J)=(RI(I,J)+RI((I+1),J))/2.
      WRITE(61,7) SOT,(I,SRI(I,J),I=1,16)
      WRITE(14,1200) (SRI(I,J),I=1,16)
 1200 FORMAT(E17.6)
 1500 SOT=SOT+DT
C
      IF(NNN.EQ.1) RETURN
 1300 REWIND 1
      NK=NIT*NP
      CALL SETFL(A(NK))
      DO155 I=1,NK
  155 A(I)=0.0
      READ(1,5) (A(I),I=1,NK)
      NITT=NIT-1
      DO52 KKT=1,NITT
      NL=(KKT-1)*NP
      DO100I=1,NP
      IJ=I+NL
  100 W(I)=(A(IJ)+A(IJ+NP))*LRHO/2.
      CALL MULTED(BK,W,XMN,NP,NBW,NCL)
      WRITE(2,5) (XMN(I),I=1,NP)
   52 CONTINUE
      RETURN
      END
```

```
      PROGRAM STRESS  (INPUT,OUTPUT,TAPE60=INPUT,TAPE61=OUTPUT,TAPE1,
     1TAPE17,TAPE19)
      COMMON/TLE/TITLE(20)
      DIMENSION GM(40),BM(40)
      COMMON A(1)
C
C  DEFINITION OF THE CONTROL PARAMETERS
C          NP - NUMBER OF GLOBAL DISPLACEMENTS,   NE - NUMBER OF
C             ELEMENTS,   NCL - NUMBER OF LOADING CONDITIONS
C          NBW - BANDWIDTH
C     DTI - SIZE OF THE TIME INTERVAL
C          IPR - PRINTING INDEX 0 = ONLY AXIAL FORCES   1 = ALL STRESSES
C          KP - TOTAL NR OF TIMES
C     SCALE = SCALE FACTOR FOR SPECIMEN DIMENSIONS
C     PAR - INDEX FOR SOLUTION   0 = VISCOELASTIC   1 = ELASTIC
C
C  INPUT OF THE TITLE CARD AND THE CONTROL PARAMETERS
C
      REWIND 17
      NCL=1
      READ(60,3)TITLE
    3 FORMAT(20A4)
      READ (60,1) NP,NE,NBW,KP,IPR,DTI,SCALE,PAR
    1 FORMAT (5I3,3F10.5)
      IF (SCALE.EQ.0.) SCALE=1.
      IPR1=1
      IF (IPR.EQ.1) IPR1=0
      JP=NP*(KP+1)
      JGSM =JP+NP
      JEND =JGSM+NP*NBW
      CALL SETFL (A(JEND))
      DO 100 I=1,JEND
  100 A(I)=0.0
C
      CALL  APREP (NE,KP,GM,BM,IPR,SCALE)
      REWIND1
      WRITE (61,222) NP,NE,NBW,KP,SCALE,PAR
  222 FORMAT (/,5X,I3,*=UNKNOWNS*,3X,I3,*=ELEMENTS*,3X,I3,*=BANDWIDTH*,
     13X,I3,*=TIME STEPS*,3X,F10.5,*=SCALE*,3X,F10.5,*=PARAMETER*,/)
      NTS=0
C
C  ASSEMBLYING OF THE GLOBAL MATRIX
C
      CALL BUILD (A(JGSM+1),NP,NBW,GM(1),BM(1),NE)
      REWIND1
      CALL EFMAX (A(JP+1),NP,NCL,NTS,IPR,KP,NE,PAR)
      REWIND 1
      CALL NODIS (A(JGSM+1),A(JP+1),NP,NBW,NCL,NTS,DTI,IPR)
      CALL DCMPBD (A(JGSM+1),NP,NBW)
      J1=1
      CALL SLVBD (A(JGSM+1),A(JP+1),A(J1),NP,NBW,NCL,IPR1)
      CALL SETFL (A(JGSM))
C
      DO9 I=1,NP
      J1=NP+I
    9 A(J1)=A(I)
      CALL ESTRAX2(A(1),NE,NP,KP,GM,BM,NTS,DTI,A(NP+1),IPR,LF,PAR)
      REWIND1
      DO 4 NTC=1,KP
      NTS=NTC
      DO 14 I=1,NP
   14 A(JP+I)=0.0
      CALL EFMAX (A(JP+1),NP,NCL,NTS,IPR,KP,NE,PAR)
      REWIND 1
      CALL SETFL(A(JEND))
C
      CALL BUILD (A(JGSM+1),NP,NBW,GM(1),BM(1),NE)
      REWIND1
      CALL NODIS (A(JGSM+1),A(JP+1),NP,NBW,NCL,NTS,DTI,IPR)
      CALL DCMPBD (A(JGSM+1),NP,NBW)
      J1=NP*NTC+1
      CALL SLVBD (A(JGSM+1),A(JP+1),A(J1),NP,NBW,NCL,IPR1)
      CALL SETFL (A(JGSM))
C
C  TOTAL DISPLACEMENT
C
      DO 10 I=1,NP
      J1=NP*NTC+I
   10 A(I)=A(I)+A(J1)
      CALL ESTRAX2(A(1),NE,NP,KP,GM,BM,NTS,DTI,A(NP+1),IPR,LF,PAR)
      REWIND 1
```

```
    4 CONTINUE
 1000 STOP
      END
      SUBROUTINE APREP(NE,KP,GM,BM,IPR,SCALE)
      DIMENSION GM(KP),BM(KP)
      COMMON/TLE/TITLE(20)
      DIMENSION NC(2)
C
C  OUTPUT OF TITLE AND DATA HEADINGS
C
      WRITE (61,924) TITLE
  924 FORMAT (1H1,///,10X,20A4,//)
      WRITE (61,25)
   25 FORMAT (//,10X,* MATERIAL PROPERTIES*,/,13X,*TIME*,11X,*BULK MODUL
     1US   SHEAR MODULUS*/)
      DO 26 I=1,KP
C
C  GM = SHEAR MODULUS       BM = BULK MODULUS
C
      READ (60,*) TIME,GM(I),BM(I)
      WRITE (61,28) TIME,BM(I),GM(I)
   28 FORMAT (8X,3(2X,E15.7))
   26 CONTINUE
      WRITE (61,24)
   24 FORMAT (//,10X,*RADIALLY SYMMETRIC BODY*//,10X,*NEL      NODE NUMBER
     1S*,10X,* R(1)          R(2)*,/)
C
C  INPUT AND ECHO PRINT OF ELEMENT DATA
C  STORAGE OF ELEMENT DATA ON SCRATCH TAPE
C  SCALING OF GEOMETRY
C
      REWIND1
      IF(SCALE.EQ.0.) SCALE=1.
      DO700 KK=1,NE
      READ  (60,2)  NEL,ND,ID,R1,R2
      R1=R1*SCALE
      R2=R2*SCALE
      WRITE (1,2)   NEL,ND,ID,R1,R2
    2 FORMAT (4I3,2F10.4)
      IF (IPR.NE.1) GO TO 700
      WRITE (61,23) NEL,ND,ID,R1,R2
   23 FORMAT (10X,I3,2X,3I3,3X,2(2X,F9.4))
  700 CONTINUE
      RETURN
      END
      SUBROUTINE BUILD (STFM,NP,NBW,GMM,BMM,NE)
      COMMON/TLE/TITLE(20)
      DIMENSION S(3,3),A(3,3)
      DIMENSION STFM(NP,NBW)
      COMMON/FETEL/NS(2),ELSTF(2,2)
C
C  GENERATION OF THE MATERIALS PROPERTY MATRIX S
C
      CALL MATPRP (S,GMM,BMM)
C
C INITALIZATION OF THE GLOBAL STIFFNESS MATRIX
C
      DO 13 I=1,NP
      DO13K=1,NBW
   13 STFM(I,K)=0.0
      A(1,1)=1714.27
      A(2,2)=A(1,1)
      A(1,2)=1142.87
      A(2,1)=A(1,2)
      A(3,1)=A(1,2)
      A(1,3)=A(1,2)
      A(3,3)=A(1,1)
      A(3,2)=A(1,2)
      A(2,3)=A(1,2)
C
      DO 700 KK=1,NE
C
C  GENERATION OF ELEMENT STIFFNESS MATRIX
C
      IF(KK.NE.16) CALL ESMAX(S)
      IF(KK.EQ.16) CALL ESMAX(A)
C
C  INSERTION OF ELEMENT PROPERTIES INTO THE GLOBAL STIFFNESS MAT
C
   15 DO 4 I=1,2
      II=NS(I)
```

```
      DO 4 J=1,2
      JJ=NS(J)
      JJ=JJ+1-II
      IF(JJ)4,4,7
    7 STFM(II,JJ)=STFM(II,JJ)+ELSTF(I,J)
    4 CONTINUE
  700 CONTINUE
      RETURN
      END
      SUBROUTINE MATPPP (S,GMM,BMM)
      DIMENSION S(3,3)
C
C  MATERIAL PROPERTIES MATRIX
C  RADIALLY SYMMETRIC STRESS ANALYSIS
C
      R=BMM+GMM*4./3.
      RR=BMM-GMM*2./3.
      S(1,1)=R
      S(2,2)=R
      S(1,2)=RR
      S(2,1)=RR
      S(3,1)=RR
      S(1,3)=RR
      S(3,3)=R
      S(3,2 )=RR
      S(2,3)=RR
      RETURN
      END
      SUBROUTINE ESMAX (S)
      COMMON/FE TEL/NS(2),ELSTF(2,2)
      DIMENSION NE(2)
      DIMENSION C(2,3),B(3,2),S(3,3)
      REAL LENGTH
      READ (1,2) NEL,NO,ID,R1,R2
    2 FORMAT (4I3,2F10.4)
C  CALCULATION OF THE SYSTEM DOF FROM THE NODE NUMBERS
C
      DO 18 I=1,2
   18 NS(I)=NE(I)
C
C  GENERATION OF THE B MATRIX AND THE INITIAL STRAIN MATRIX, ET
C
      LENGTH=R2-R1
      RBAR=(R1+R2)/2.
      DO 20 I=1,3
      DO 20 J=1,2
   20 B(I,J)=0.0
      B(1,1 )=-1.0
      B(1,2)=1.0
      B(2,1)=(R2/RBAR)-B(1,2)
      B(2,2)=B(1,2)-(R1/RBAR)
      B(3,1)=B(2,1)
      B(3,2)=B(2,2)
C
C  MATRIX MULTIPLICATION TO OBTAIN C=(BT)(S)
C
      DO 22 I=1,2
      DO 22 J=1,3
      SUM=0.0
      DO 25 K=1,3
   25 SUM=SUM+B(K,I)*S(K,J)
   22 C(I,J)=SUM
C
C  MATRIX MULTIPLICATION TO OBTAIN ELSTF AND TF
C        ELSTF=(BT)(S)(B)
C
      DO 27 I=1,2
      DO 27 J=1,2
      SUM=0.0
      DO 28 K=1,3
   28 SUM=SUM+C(I,K)*B(K,J)
      ELSTF(I,J)=SUM*2.0*3.14159265*RBAR/LENGTH
   27 CONTINUE
      RETURN
      END
      SUBROUTINE EFMAX (GF,NP,NCL,NTS,IPR,KP,NE,PAR)
      DIMENSION GF(NP,NCL),BV(2)
      DIMENSION C(2,2),G(2,1),H(1,2)
      DIMENSION ND(2)
      COMMON/TLE/TITLE(20)
      COMMON/FFT/NS(2),EFMAT(2,1)
```

```
      REAL LENGTH
C
C   INITIALIZATION OF THE GLOBAL FORCE MATRIX
C
      DO 12 J=1,NP
      DO 12 JM=1,NCL
   12 GF(J,JM)=0.0
      NT=1
      IF(PAR.EQ.1) NT=NTS
      DO 26 I=NT,NTS
      REWIND 1
      DO 27 KK=1,NE
      DO 29 JM=1,NCL
      READ(1,3) NEL,ND,ID,R1,R2
    3 FORMAT (4I3,2F10.4)
C
C   GENERATION OF G AND H MATRICES
C
      LENGTH=R2-R1
      RBAR=(R1+R2)/2.
      G(1,1)=2.0*R2/RBAR-3.0
      G(2,1)=3.0-2.0*R1/RBAR
      H(1,1)=R2**3.0-3.0*R2*R1**2.0+2.0*R1**3.0
      H(1,2)=2.0*R2**3.0-3.0*R2**2.0*R1+R1**3.0
C
C   MATRIX MULTIPLICATION TO OBTAIN C=(G)(H)
C
      DO 22 JK=1,2
      DO 22 J=1,2
      K=1
   22 C(JK,J)=G(JK,K)*H(K,J)
C
C   READ THERMAL AND HYDRO NODAL LOADS (ALPHA*THETA+BETH*M)
C
      IF(NTS.EQ.0) GO TO 8
      READ(17,6) BV
    6 FORMAT(2E17.6)
      IF(NTS.GT.0) GO TO 9
    8 BV(1)=BV(2)=0.0
    9 CONTINUE
C
C   MATRIX MULTIPLICATION TO OBTAIN EFMAT
C
      IF(KK.EQ.16) GO TO 36
      EFMAT(1)=(3.14159265*166.7/(LENGTH**2.0))*(C(1,1)*BV(1)
     1+C(1,2)*BV(2))
      EFMAT(2)=(3.14159265*166.7/(LENGTH**2.0))*(C(2,1)*BV(1)
     1+C(2,2)*BV(2))
      IF(KK.NE.16) GO TO 37
   36 EFMAT(1)=(3.14159265*1333.34/(LENGTH**2.0))*(C(1,1)
     1*BV(1)+C(1,2)*BV(2))
      EFMAT(2)=(3.14159265*1333.34/(LENGTH**2.0))*(C(2,1)
     1*BV(1)+C(2,2)*BV(2))
   37 CONTINUE
C
C   INPUT OF THE NODAL FORCE VALUES IN THE GLOBAL FORCE VECTOR
C
      DO 19 JK=1,2
   19 NS(JK)=ND(JK)
      II=NS(1)
      JJ=NS(2)
      GF(II,JM)=GF(II,JM)+EFMAT(1)
      GF(JJ,JM)=GF(JJ,JM)+EFMAT(2)
   29 CONTINUE
   27 CONTINUE
   26 CONTINUE
      RETURN
      END
      SUBROUTINE NODIS (GSM,GF,NP,NBW,NCL,NTS,DT,IPR)
      DIMENSION GSM(NP,NBW) ,GF(NP,NCL),IB(2),BV(2),IBD(40),BVD(40)
C ****************
C   INPUT OF THE CONSTANT BOUNDARY DISPLACEMENTS
C *******************
      IN=60
      IF(NTS.GT.0) GO TO 11
      IC=0
C
C   INPUT OF NODAL DISPLACEMENT INCREMENTS
C   INCREMENTS ARE IMPOSED AT EACH TIME STEP
C
   13 READ (IN,203)IB,NEXTD,BV
```

```
  203 FCRMAT(2I3,I2,2F10.3)
      CO 1 L=1,2
      IF (IB(L).LE.0) GOTO2
      IO=IO+1
      IBO(IO)=IB(L)
    1 BVO(IO)=BV(L)
      GOTO13
    2 IOF=IO+1
    7 IO=IOF
C
C     INPUT OF NODAL DISPLACEMENTS THAT REMAIN CONSTANT
C     INCREMENTS ARE EQUAL TO ZERO AFTER FIRST TIME STEP
C
   14 READ (IN,203) IB,NEXTD,BV
      CO 5 L=1,2
      IF (IB(L).LE.0) GOTO 3
      IBO(IO)=IB(L)
      BVO(IO)=BV(L)
    5 IO =IO+1
      GOTO14
    3 IOC=IO -1
      IBO(IO)=0
      IF (NTS.LE.1) GO TO 6
   11 CO 12 I=IOF,IOC
      BVO(I)=0.
   12 CONTINUE
C
C     INSERT KNOWN DISPLACEMENTS IN SYSTEM OF EQUATIONS
C
    6 CALL VBODIS (GSM,GF,NP,NBW,NCL,IBO,BVO,IPR)
   10 CONTINUE
      RETURN
      END
      SUBROUTINE VBODIS (GSM,GF,NP,NBW,NCL,IB,BV,IPR)
      DIMENSION GSM(NP,NBW),GF(NP,NCL),IB(40),BV(40)
      IO=61
      IF (IPR.NE.1) GO TO 100
      WRITE(IO,206)
  206 FCRMAT(////,1X,* PRESCIBED NODAL DISPLACEMENT INCREMENTS*/)
  100 CONTINUE
      ID=0
      CO 221 L=1,40
      IF(IB(L).LE.0) GO TO 215
      ID=ID+1
      I=IB(L)
      BC=BV(L)
C**************
C     INPUT CF THE PRESCRIBED NOCAL VALUES
C
C     MOCIFICATICN OF THE GLOBAL STIFFNESS MATRIX AND THE
C                   GLOBAL FORCE MATRIX USING THE METHOD OF
C                   DELETICN OF ROWS AND COLUMNS
C**************
      K=I-1
      CO211J=2,NBW
      M=I+J-1
      IF(M.GT.NP) GO TO 210
      CO218 JM=1,NCL
  218 GF(M,JM)=GF(M,JM)-GSM(I,J)*BC
      GSM(I,J)=0.0
  210 IF(K.LE.0) GO TO 211
      CO 219 JM=1,NCL
  219 GF(K,JM)=GF(K,JM)-GSM(K,J)*BC
      GSM(K,J)=0.0
      K=K-1
  211 CCNTINUE
  212 CO 220 JM=1,NCL
  220 GF(I,JM)=GSM(I,1)*BC
  221 CONTINUE
C
C     OUTPUT OF THE BOUNDARY VALUES, (BV)
C
  215 IF(ID.EQ.0) RETURN
      IF(IPR.NE.1) GO TO 101
      WRITE(IO,207) (IB(L),BV(L),L=1,ID)
  207 FCRMAT(1X,2(I3,E14.5,2X))
  101 CONTINUE
      RETURN
      END
      SUBROUTINE ESTRAX2(X,NE,NP,KP,GP,BM,NTS,DT,DU,IPRI,EF,PAR)
      COMMON/TLE/TITLE(20)
```

```
      DIMENSION X(NP),DL(NP,NTS)
      DIMENSION STRA(3),STRE(3),DSTR(3),U(2)
      DIMENSION NS(2),B(3,2),NC(2)
      DIMENSION S(3,3)
      DIMENSION ES(3), SS(3)
      DIMENSION GM(KP),EM(KP)
      DIMENSION EF(1)
      COMMON/NODC/NNC(100)
      REAL LENGTH
C
C   ADVANCE PAGE AND PRINT TITLES
C
      IPR=1
      DUMMY=0.
      IF (IPRI.NE.1) IPR=0
      IF (IPR.EQ.0) GO TO 83
      WRITE(61,80) TITLE
   80 FORMAT(1H1,///////,10X,20A4)
      WRITE(61,81)
   81 FORMAT(/10X,*ELEMENT STRESSES AND STRAINS*//)
   83 CONTINUE
      DO 86 IJ=1,NE
C
C   INPUT OF THE ELEMENT DATA
C
      READ (1,2) NEL,ND,ID,R1,R2
    2 FORMAT  (4I3,2F10.4)
C
C  GENERATION OF THE B MATRIX
C
      LENGTH=R2-R1
      RBAR=(R1+R2)/2.
      DO 90 I=1,3
      DO 90 J=1,2
   90 B(I,J)=0.0
      B(1,1)=-1.0
      B(1,2)=1.0
      B(2,1)=(R2/RBAR)-B(1,2)
      B(2,2)=B(1,2)-(R1/RBAR)
      B(3,1)=B(2,1)
      B(3,2)=B(2,2)
C
C   CALCULATION OF THE GLOBAL DOF FROM THE NODE NUMBERS
C
   59 DO 52 I=1,2
   52 NS(I)=ND(I)
C
C   CALCULATION OF THE ELEMENT DISPLACEMENTS
C
      I=1
      NS1=NS(I)
      NS2=NS(I+1)
      U(I)=X(NS1)
      U(I+1)=X(NS2)
C
C   CALCULATION OF THE STRAIN MATRIX,  (STRAIN)=(B)(U)
C
   54 DO 55 I=1,3
      SUM=0.0
      DO 82 K=1,2
   82 SUM=SUM+B(I,K)*U(K)
   55 STRA(I)=SUM/LENGTH
C
C   CALCULATION OF THE STRESS  MATRIX  ***  TIME INCREMENT PROCEDURE
C
      DO 105 I=1,3
  105 STRE(I)=0.
      NT=1
      IF(PAR.EQ.1) NT=NTS
      DO 200 J=NT,NTS
      IF(NTS.EQ.0) GO TO 8
      READ(17,7) EF
    7 FORMAT(E17.6)
      IF(NTS.GT.0) GO TO 9
    8 EF(1)=0.0
    9 CONTINUE
      IF(NTS.EQ.0) NNTS=NTS+1
      IF(NTS.GT.0) NNTS=NTS
      I=1
      NS1 =NS(I)
      NS2=NS(I+1)
```

```
      U(I)= DU(NS1,J)
      U(I+1)=DU(NS2,J)
      DO 102 I=1,3
      SUM =0.
      DO 103 K=1,2
  103 SUM=SUM + B(I,K)* U(K)
  102 DSTR(I)=SUM/LENGTH
C
C   MATERIALS PROPERTIES
C
      CALL MATPRP (S,GM(NNTS),BM(NNTS))
      IF(IJ.EQ.16) GO TO 206
C
      DO 106 I=1,3
      SUM=0.
      DO 107 K=1,3
  107 SUM=SUM+S(I,K)*DSTR(K)
  106 STRE(I)=STRE(I)+SUM-3.0*166.7*EF(1)
      IF(IJ.NE.16) GO TO 203
  206 CONTINUE
      S(1,1)=1714.27
      S(2,2)=S(1,1)
      S(1,2)=1142.87
      S(2,1)=S(1,2)
      S(3,1)=S(1,2)
      S(1,3)=S(1,2)
      S(3,3)=S(1,1)
      S(3,2)=S(1,2)
      S(2,3)=S(1,2)
      DO 207 I=1,3
      SUM=0.0
      DO 208 K=1,3
  208 SUM=SUM+S(I,K)*DSTR(K)
  207 STRE(I)=STRE(I)+SUM-3.0*1333.34*EF(1)
  203 CONTINUE
      NNTS=NNTS-1
  200 CONTINUE
C
C   STRAIN RATES
C
      DO 109 I=1,3
  109 DSTR(I)=DSTR(I)/DT
      XNTS=NTS
      TIME=XNTS*DT
C
      IF (IPR.EQ.0) GO TO 431
      WRITE(61,17) NEL,NS
   17 FORMAT( /10X,*ELEMENT*I4,5X,*SYS DOF*,4X,2I5)
C
C   CALCULATION OF THE PRINCIPAL STRESSES
C   NOT CALCULATED WHEN NO PRINT REQUEST
C
      IF(STRE(1).LT.STRE(2)) GO TO 790
      SS(1)=STRE(1)
      SS(2)=STRE(2)
      SS(3)=STRE(3)
      GO TO 791
  790 SS(1)=STRE(2)
      SS(2)=STRE(3)
      SS(3)=STRE(1)
  791 CONTINUE
      SMAX=SS(1)
      SMIN=SS(3)
      TM=(SMAX-SMIN)/2.
      CONTINUE
C
C   CALCULATION OF THE PRINCIPAL  STRAINS
C
      IF(STRA(1).LT.STRA(2)) GO TO 890
      ES(1)=STRA(1)
      ES(2)=STRA(2)
      ES(3)=STRA(3)
      GO TO 891
  890 ES(1)=STRA( 2)
      ES(2)=STRA(3)
      ES(3)=STRA(1)
  891 CONTINUE
      EMAX=ES(1)
      EMIN=ES(3)
      SM=(EMAX-EMIN)/2.
      CONTINUE
```

```
C
C  PRINTING OF THE RESULTS
C
      IF (IPR.EQ.0) GO TO 420
C
      WRITE (61,95) RBAR,TIME
   95 FORMAT(10X,*RBAR= *,F10.4,10X,*TIME=*,F10.4)
      IF (IPRI.EQ.2) GO TO 510
      WRITE (61,110) STRA
  110 FORMAT (5X,*STRAINS*,  17X,*ERR  = *,E12.5,5X,*EFF  = *,E12.5,
     15X,*ETT  = *,E12.5)
      WRITE (61,111)DSTR
  111 FORMAT ( 5X,*STRAIN RATES*,  12X,*DERR = *,E12.5,5X,*DEFF = *,
     1E12.5,5X,*DETT = *,E12.5)
      WRITE (61,113) ES,SM
  113 FORMAT ( 5X,*PRINCIPAL STRAINS*,   8X,*E1   = *,E12.5,5X,*E2   = *
     1,E12.5,5X,*E3   = *,E12.5,5X,*SMAX = *,E12.5)
  510 CONTINUE
      WRITE (61,112) STRE
  112 FORMAT ( 5X,*STRESSES*,  16X,*SRR  = *,E12.5,5X,*SFF  = *,E12.5,
     15X,*STT  = *,E12.5)
      WRITE (61,115) SS,TM
  115 FORMAT ( 5X,*PRINCIPAL STRESSES*,   6X,*S1   = *,E12.5,5X,*S2   =
     1*,E12.5,5X,*S3   = *,E12.5,5X,*TMAX = *,E12.5)
  511 CONTINUE
  420 CONTINUE
  431 CONTINUE
C
C     PUTTING STRESS DATA ON TAPE 19 FOR PLOTTING
C
      IF(AMOD(TIME,1200.).NE.0) GO TO 800
      WRITE(19,787) TIME,RBAR,STRE(1),STRE(2),TM
  787 FORMAT(5E12.5)
  800 CONTINUE
   86 CONTINUE
      RETURN
      END
```

```
      PROGRAM KPLOT (INPUT,OUTPUT,TAPE15)
      DIMENSION IBUF(1027)
      DIMENSION XX(4),YY(4)
      DIMENSION SRR(400),SFF(400),TMAX(400),TIME(400),RBAR(400)
      CALL PLOTS(IBUF,1027,2)
      CALL PLIMIT(300.)
      CALL PLOT(2.0,2.5,-3)
      XX(1)=0.0
      XX(2)=.004
      YY(1)=-.5
      YY(2)=2.0
      REWIND 15
      CALL SCALE(XX,4.0,2,1)
      CALL SCALE(YY,5.0,2,1)
    2 CONTINUE
      NP=0
      DO 4 I=1,16
      READ(15,3)TIME(I),RBAR(I),SRR(I),SFF(I),TMAX(I)
      IF(EOF(15).NE.0) GO TO 222
    3 FORMAT(5E12.5)
      NP=NP+1
    4 CONTINUE
      RBAR(NP+1)=XX(3)
      RBAR(NP+2)=XX(4)
      SRR(NP+1)=YY(3)
      SRR(NP+2)=YY(4)
      SFF(NP+1)=YY(3)
      SFF(NP+2)=YY(4)
      CALL AXIS(0.,1.,10HRADIUS (M),10,4.,0.,XX(3),XX(4))
      CALL AXIS(0.,0.,12HSTRESS (MPA),12,5.0,90.,YY(3),YY(4))
      CALL LINE(RBAR,SRR,NP,1,1,1)
      CALL LINE(RBAR,SFF,NP,1,1,2)
      CALL SYMBOL(.5,4.0,.14,1,0.,-1)
      CALL SYMBOL(0.5,3.8,.14,2,0.,-1)
      CALL SYMBOL(0.7,3.9,.14,13HRADIAL STRESS,0.,13)
      CALL SYMBOL(0.7,3.7,.14,17HTANGENTIAL STRESS,0.,17)
      CALL PLOT(10.0,0.0,-3)
      GO TO 2
  222 CONTINUE
      CALL PLOT(13.,0.,999)
      END
```

```
      PROGRAM KPLOT (INPUT,OUTPUT,TAPE15)
      DIMENSION IBUF(1027)
      DIMENSION XX(4),YY(4)
      DIMENSION TIME(400),TMAX(400)
      CALL PLOTS(IBUF,1027,2)
      CALL PLIMIT(300.)
      CALL PLOT(2.0,2.5,-3)
      REWIND 15
      XX(1)=0.0
      XX(2)=15000.
      YY(1)=0.0
      YY(2)=.1
      CALL SCALE(XX,4.0,2,1)
      CALL SCALE(YY,5.0,2,1)
      CALL AXIS(0.,0.,14HTIME (SECONDS),-14,4.,0.,XX(3),XX(4))
      CALL AXIS(0.,0.,23HMAX. SHEAR STRESS (MPA),23,5.,90.,
     1YY(3),YY(4))
      DO 8 J=3,11,4
      REWIND 15
      DO 11 I=1,J
   11 READ(15,100)
  100 FORMAT(1X)
      DO 14 N=1,13
      READ(15,10)TIME(N),TMAX(N)
   10 FORMAT(E12.5,36X,E12.5)
      IF(N.EQ.13) GO TO 14
      DO 13 ICARD=1,15
   13 READ(15,100)
   14 CONTINUE
      NP=13
      TIME(NP+1)=XX(3)
      TIME(NP+2)=XX(4)
      TMAX(NP+1)=YY(3)
      TMAX(NP+2)=YY(4)
      IF(J.EQ.3) GO TO 75
      IF(J.EQ.7) GO TO 76
      IF(J.EQ.11) GO TO 77
   75 CALL LINE(TIME,TMAX,NP,1,1,0)
      CALL SYMBOL(1.,4.9,.14,19HA=RADIUS OF SOYBEAN,0.,19)
      CALL SYMBOL(1.,4.6,.14,0,0.,-1)
      CALL SYMBOL(1.2,4.5,.14,5HR=A/4,0.,5)
      GO TO 8
   76 CALL LINE(TIME,TMAX,NP,1,1,1)
      CALL SYMBOL(1.,4.4,.14,1,0.,-1)
      CALL SYMBOL(1.2,4.3,.14,5HR=A/2,0.,5)
      GO TO 8
   77 CALL LINE(TIME,TMAX,NP,1,1,2)
      CALL SYMBOL(1.,4.2,.14,2,0.,-1)
      CALL SYMBOL(1.2,4.1,.14,6HR=3A/4,0.,6)
    8 CONTINUE
      CALL PLOT(10.,0.,-3)
      REWIND 15
      XX(1)=0.0
      XX(2)=15000.
      YY(1)=0.0
      YY(2)=1.2
      CALL SCALE(XX,4.0,2,1)
      CALL SCALE(YY,6.0,2,1)
      CALL AXIS(0.,0.,14HTIME (SECONDS),-14,4.,0.,XX(3),XX(4))
      CALL AXIS(0.,0.,23HMAX. SHEAR STRESS (MPA),23,6.,90.,
     1YY(3),YY(4))
      DO 12 I=1,15
   12 READ(15,100)
      DO 15 N=1,13
      READ(15,10)TIME(N),TMAX(N)
      IF(N.EQ.13) GO TO 15
      DO 16 ICARD=1,15
   16 READ(15,100)
   15 CONTINUE
      NP=13
      TIME(NP+1)=XX(3)
      TIME(NP+2)=XX(4)
      TMAX(NP+1)=YY(3)
      TMAX(NP+2)=YY(4)
      CALL LINE(TIME,TMAX,NP,1,1,5)
      CALL SYMBOL(2.0,5.5,.14,12HSKIN ELEMENT,0.,12)
      CALL PLOT(13.,0.,999)
      END
```

```
      PROGRAM KPLOT (INPUT,OUTPUT,TAPE15,TAPE18,TAPE19)
      DIMENSION IBUF(1027)
      DIMENSION XX(4),YY(4)
      DIMENSION TIME(400),SFF(400)
      ITAPE=15
      CALL PLOTS(IBUF,1027,2)
      CALL PLIMIT(30.)
      CALL PLOT(2.0,2.5,-3)
      CALL FACTOR(.9)
      XX(1)=0.0
      XX(2)=15000.
      YY(1)=0.0
      YY(2)=7.0
      CALL SCALE(XX,4.0,2,1)
      CALL SCALE(YY,8.0,2,1)
      CALL AXIS(0.,0.,14HTIME (SECONDS),-14,4.,0.,XX(3),XX(4))
      CALL AXIS(0.,0.,23HTANGENTIAL STRESS (MPA),23,8.,90.,
     1YY(3),YY(4))
    1 CONTINUE
      REWIND ITAPE
      DO 12 I=1,15
   12 READ(ITAPE,100)
  100 FORMAT(1X)
      DO 15 N=1,13
      READ(ITAPE,20) TIME(N),SFF(N)
   20 FORMAT(E12.5,24X,E12.5,12X)
      IF(N.EQ.13) GO TO 15
      DO 16 ICARD=1,15
   16 READ(ITAPE,100)
   15 CONTINUE
      NP=13
      TIME(NP+1)=XX(3)
      TIME(NP+2)=XX(4)
      SFF(NP+1)=YY(3)
      SFF(NP+2)=YY(4)
      IF(ITAPE.EQ.15) GO TO 50
      IF(ITAPE.EQ.18) GO TO 60
      IF(ITAPE.EQ.19) GO TO 70
   50 CALL LINE(TIME,SFF,NP,1,1,0)
      CALL SYMBOL(1.2,7.8,.14,12HSKIN ELEMENT,0.,12)
      CALL SYMBOL(1.,7.5,.14,0,0.,-1)
      CALL SYMBOL(1.2,7.4,.14,17HDRYING TEMP.=35 C,0.,17)
      GO TO 80
   60 CALL LINE(TIME,SFF,NP,1,1,1)
      CALL SYMBOL(1.,7.3,.14,1,0.,-1)
      CALL SYMBOL(1.2,7.2,.14,17HDRYING TEMP.=55 C,0.,17)
      GO TO 80
   70 CALL LINE(TIME,SFF,NP,1,1,5)
      CALL SYMBOL(1.,7.1,.14,5,0.,-1)
      CALL SYMBOL(1.2,7.,.14,17HDRYING TEMP.=75 C,0.,17)
   80 CONTINUE
      IF(ITAPE.EQ.19) GO TO 800
      IF(ITAPE.EQ.18) ITAPE=19
      IF(ITAPE.EQ.15) ITAPE=18
      GO TO 1
  800 CONTINUE
      CALL PLOT(13.,0.,999)
      END
```

```
      PROGRAM FEPLOT(INPUT,OUTPUT,TAPE60=INPUT,TAPE61=OUTPUT)
      DIMENSION IBUF(1000),X(3000),Y(3000),XX(6),YY(6),TITLE(8)
C
C     INPUT AND OUTPUT OF TITLE AND PARAMETER VALUES
C
      READ(60,5) TITLE
    5 FORMAT(8A10)
      READ(60,6) NE,XYR
    6 FORMAT(I3,2F10.4)
      WRITE(61,7) TITLE
    7 FORMAT(1H1,////5X,8A10)
      WRITE(61,9) NE,XYR
    9 FORMAT(/5X,20HNUMBER OF ELEMENTS =,I5/5X,10HXY RATIO =,F10.4)
      WRITE(61,8)
    8 FORMAT(//5X,7HELEMENT,5X,2HXI,8X,2HYI,8X,2HXJ,8X,2HYJ,8X,2HXK,8X,2
     $HYK)
C
C     BASIC CALCULATIONS
C
      NN=NE*4
      YAXIS=5.0
      XAXIS=YAXIS*XYR
C
C     INPUT OF ELEMENT DATA
C
      DO 1J=1,NE
      JI=(J-1)*4+1
      JE=JI+2
      READ(60,25) X(JI),Y(JI),X(JI+1),Y(JI+1),X(JI+2),Y(JI+2)
   25 FORMAT(15X,6F10.4)
      X(JE+1)=X(JI)
      Y(JE+1)=Y(JI)
      WRITE(61,26) J,X(JI),Y(JI),X(JI+1),Y(JI+1),X(JI+2),Y(JI+2)
   26 FORMAT(5X,I5,6F10.4)
    1 CONTINUE
C
C     START OF THE PLOT  STATEMENTS
C
      CALL PLOTS(IBUF,1000,2)
      CALL PLOT(2.5,1.75,-3)
      CALL SCALE (X,XAXIS,NN,1)
      XX(5)=X(NN+1)
      XX( 6)=X(NN+2)
      CALL SCALE (Y,YAXIS,NN,1)
      YY(5)=Y(NN+1)
      YY( 6)=Y(NN+2)
      CALL AXIS (0.0,0.0,9HZ-AXIS CM,9,YAXIS,90.0,Y(NN+1),Y(NN+2))
      CALL AXIS (0.0,0.0,9HR-AXIS CM,-9,XAXIS,00.0,X(NN+1),X(NN+2))
      DO 10 J=1,NN,4
      DO 88 L=1,4
      K=L-1
      XX(L)=X(J+K)
   88 YY(L)=Y(J+K)
   10 CALL LINE (XX,YY,4,1,0,0)
      CALL SYMBOL(2.,4.8,.14,19HFINITE ELEMENT GRID,0.,19)
      CALL SYMBOL(2.4,4.6,.14,12H255 ELEMENTS,0.,12)
      CALL SYMBOL(2.4,4.4,.14,9H152 NODES,0.,9)
      CALL PLOT(12.0,0.0,999)
      END
```